Symmetry and Topology in Disordered Systems

by

Ruochen Ma

A thesis
presented to the University of Waterloo
in fulfillment of the
thesis requirement for the degree of
Doctor of Philosophy
in
Physics

Waterloo, Ontario, Canada, 2023

Examining Committee Membership

The following served on the Examining Committee for this thesis. The decision of the Examining Committee is by majority vote.

External Examiner:	Chao-Ming Jian Assistant Professor, Dept. of Physics, Cornell University
Supervisor(s):	Yin-Chen He Adjunct Faculty Dept. of Physics and Astronomy, University of Waterloo Roger Melko Professor Dept. of Physics and Astronomy, University of Waterloo
Internal Member(s):	Chong Wang Adjunct Faculty Dept. of Physics and Astronomy, University of Waterloo Anton Burkov Professor Dept. of Physics and Astronomy, University of Waterloo
Internal-External Member:	Ben Webster Associate Professor Dept. of Mathematics, University of Waterloo

Author's Declaration

This thesis consists of material all of which I authored or co-authored: see Statement of Contributions included in the thesis. This is a true copy of the thesis, including any required final revisions, as accepted by my examiners.

I understand that my thesis may be made electronically available to the public.

Statement of Contributions

Ruochen Ma was the sole author for Chapter. 1 which was not written for publication. This thesis consists in part of three manuscripts written for publication. Ruochen Ma was the first author for the three manuscripts.

Chapter. 2 of this thesis consists mostly of material published in Ref. [115]. This work was done under the supervision of Chong Wang.

Chapter. 3 of this thesis consists mostly of material in published in Ref. [116]. This work was done in collaboration with Jian-Hao Zhang, Zhen Bi, Meng Cheng and Chong Wang. All authors shared the work of performing the research and preparing the manuscript draft.

Chapter. 4 of this thesis consists mostly of material published in Ref. [114]. This research was conducted solely by Ruochen Ma.

Abstract

Symmetry-protected topological (SPT) phases are many-body quantum states that are topologically nontrivial as long as the relevant symmetries are unbroken. In this thesis I show that SPT phases are also well defined for *average* symmetries, where quenched disorders locally break the symmetries, but restore the symmetries upon disorder averaging. An example would be crystalline SPT phases with imperfect lattices. Specifically, I define the notion of average SPT for disordered ensembles of quantum states. We then classify and characterize a large class of average SPT phases using a decorated domain wall approach, in which domain walls (and more general defects) of the average symmetries are decorated with lower dimensional topological states. We then show that if the decorated domain walls have dimension higher than $(0 + 1)d$, then the boundary states of such average SPT will almost certainly be long-range entangled, with probability approaching 1 as the system size approaches infinity. This generalizes the notion of t'Hooft anomaly to average symmetries, which we dub "average anomaly". The average anomaly can also manifest as constraints on lattice systems similar to the Lieb-Schultz-Mattis (LSM) theorems, but with only average lattice symmetries. We also generalize our problem to "quantum disorders", which describe an environment that can form quantum entanglement with the system of interest, ultimately leading to a mixed state upon tracing out the environment. We present a theory of such generalized average SPTs for mixed states purely based on density matrices and quantum channels. We further explore SPT phases that exist only in disordered systems. Our results indicate that topological quantum phenomena associated with average symmetries can be at least as rich as those with ordinary exact symmetries.

Then the focus of our investigation shifts towards the study of open quantum systems governed by non-unitary dynamics. Specifically, I investigate the effects of measurements and decoherence on long distance behaviors of quantum critical systems. We demonstrate that measurements and decoherence can be viewed as dynamic generalizations of the two aforementioned types of disorders in equilibrium. We classify different measurements and decoherence based on their timescales and symmetry properties, and show that they can be described by replicated Keldysh field theories with distinct physical and replica symmetries. Low energy effective theories for various scenarios are then derived using the symmetry and

fundamental consistency conditions of the Keldysh formalism. As an example, we apply this framework to study the critical Ising model in both one and two spatial dimensions. Our results demonstrate that non-unitary dynamics of open systems can be systematically studied based on simple symmetry constraints.

Acknowledgements

First and foremost, I would like to express my gratitude to my advisors, Dr. Chong Wang and Dr. Yin-Chen He, without whom the completion of this thesis would not have been possible. Conversations with Chong were undoubtedly the most enlightening part of my PhD study at Perimeter. As a mentor, he taught me how to grasp the essence of a problem and construct a physical picture that connects seemingly disparate topics. I have always been awestruck by his creativity and clarity of thought. While I may never achieve the same level of depth as him, his guidance has enabled me to think independently and critically. Yin-Chen patiently guided me through the early, awkward stage of my PhD study. During my first two years, our whole afternoon discussions in his office established my way of understanding fundamental topics in condensed matter physics. In just an hour-long discussion with him, I often learned more than I would in an entire week spent reading papers.

I would also like to thank the other members of the condensed matter theory group at Perimeter, who created an inspiring environment that greatly benefited me. I would like to extend a special thanks to Liujun Zou, who has always been a role model for me with his broad knowledge of various topics in physics and his persistent questioning. I am grateful to my officemate Matthew Yu, a master of mathematics, for patiently answering my numerous questions. Additionally, I am grateful to Anton Burkov and Roger Melko for taking the time to join my advisory committee, and to Chao-Ming Jian and Ben Webster for serving as members of my thesis defense committee.

I would like to express my appreciation to the entire staff at Perimeter Institute for their incredible support and dedication, particularly during the challenging times of the pandemic. I would also like to extend my thanks to my friends in Waterloo and around the world.

Finally, I would like to express my gratitude to my parents for their unwavering love. When I write of my parents, my words appear wan and pallid. My PhD journey was full of ups and downs (and downs and downs), and without their support, I would not have been able to overcome these struggles.

Dedication

To my parents.

月明闻杜宇，南北总关心。

Wheresoever I roam, though far apart we be,

Parents' hearts still hold me close, their love I see.

Table of Contents

List of Figures

List of Tables

Chapter 1

Introduction

The classification of matter is intimately linked to the concept of symmetry, which holds a central place in contemporary physics [119, 103]. Landau's paradigm of phases of matter has played a significant role in shaping this understanding. Specifically, this paradigm posits that (1) phases of matter can be classified based on the symmetries of their corresponding Hamiltonians at the microscopic level, as well as how these symmetries are broken or preserved at macroscopic scales. Moreover, (2) transitions between distinct phases are described by the fluctuations of a local order parameter that transforms non-trivially under the symmetry being broken. The combination of this paradigm and the idea of renormalization group (RG) has been successful in unifying a large range of phases, both in and out of equilibrium.

Since the discovery of the Quantum Hall effect [97, 159], the focus has shifted towards characterizing topological phenomena that extend beyond the well-established Landau paradigm. A prominent example is the fractional quantum Hall states that emerge in two-dimensional electronic systems subjected to a magnetic field, characterized by a filling fraction

$$\nu = p/q, \tag{1.1}$$

where p and q are integers with no common factors, and q is typically odd. These states exhibit quasi-particle excitations that obey fractional statistics, rendering them non-creatable by any local operators. Another striking aspect of a fractional quantum Hall state is that

its ground state degeneracy is dependent on the spatial manifold's topology. In general, a quantum matter (with a finite energy gap in the thermodynamical limit) exhibiting such non-local quasi-particle excitations and topology-dependent ground state degeneracy is deemed to be in a topologically ordered phase. These phases are described by various topological quantum field theories (TQFT) that govern their low-energy properties.

Physically, topological phases are characterized by quantized topological invariants, such as the ground state degeneracy, which cannot vary continuously within the phase. As a result, two states with distinct invariants must be separated by a phase transition. A contemporary formulation of this notion is through the pattern of quantum entanglement in the ground state wave function. In particular, topologically ordered phases exhibit long-range quantum entanglement in their ground state wave function, and their ground state cannot be produced from a trivial product state, such as an atomic insulator, using a finite-depth local unitary circuit.

The presence of symmetry can numerously enrich the story of the classification of matters based on the entanglement pattern of the ground state. Symmetry quantum numbers associated with quasi-particle excitations and properties of symmetry defects provide additional topological invariants to differentiate between different phases of matter. Again, the fractional quantum Hall states offer a straightforward example of such an enriched topological phase, where quasi-particle excitations carry fractional electric charge. For instance, a quasi-particle excitation (anyon) at the filling fraction $\nu = 1/3$ carries charge $1/3$ in units of electron charge, with the symmetry (U(1) charge conservation) acting projectively on the quasi-particles. The topological orders with distinct projective symmetry realizations on quasi-particles are referred to as symmetry-enriched topological (SET) phases.

In terms of the entanglement pattern in the ground state, the classification of phases are enhanced by the symmetry properties of the quantum circuit. It is possible that some states which belong to the same phase in the absence of symmetry, and hence can be connected by a finite depth local circuit, will be placed into distinct phases if the gates in the circuit necessarily break the symmetry. Thus, symmetry can even enrich the classification of short-range entangled (SRE) phases, which are those that can be adiabatically connected to a product state using a finite depth local circuit. These phases are referred to as Symmetry-Protected Topological (SPT) phases. A well-known example is the Topological Insulator

[100]. Since SPT phases are the primary focus of this thesis, we provide a more detailed definition of this concept in the next subsection.

1.1 SPT phases and t 'Hooft anomalies

An SPT state is short range entangled, in the sense that it can be adiabatically connected to a trivial un-entangled product state. However, in the case of a non-trivial SPT state, the adiabatic paths are prohibited by the presence of a certain symmetry, known as the "protecting symmetry". In another word, a non-trivial SPT state can only be distinguished from a product state when the protecting symmetry is preserved. An example of such a protecting symmetry is the $U(1)$ charge conservation and time-reversal symmetry in band topological insulators (TIs) [72, 136], where these symmetries must be preserved to distinguish topological and trivial atomic insulators. It should be noted that, in the bulk or on a compact spatial manifold without a boundary, an SPT phase is almost trivial, meaning that all excitations are gapped, with all correlation functions of local operators decaying exponentially, and the ground state is unique.

However, interesting things happen when we go to the boundary. For instance, in the case of a band TI, the gapless surface modes emerge as long as the $U(1)$ charge conservation and time reversal symmetry are preserved [136]. The Haldane-AKLT chain [2] in one spatial dimension is an example of an interacting system that hosts an SPT state. On each lattice site, we have a spin-1 degree of freedom, with a Hamiltonian

$$H = \sum_i P_2(\mathbf{S}_i + \mathbf{S}_{i+1}), \tag{1.2}$$

where P_2 is a projection operator onto the spin-2 subspace. In the ground state, the total spin of each nearest neighbouring pair cannot be 2 due to the energetic reason. Although in the bulk there is a unique gapped ground state with exponentially decaying correlation functions, a dangling spin-1/2 moment emerges at the end of the chain, which gives a two-fold degeneracy at each end. A physical understanding of these boundary excitations is that, as the bulk of the system cannot be adiabatically dis-entangled while preserving

Figure 1.1: A pictorial demonstration of the ground state wave function of the Haldane-AKLT chain. Each solid point represents a spin-1/2 degree of freedom. Two spin-1/2's connected by a line form a singlet. The ovals denote projection operators onto the spin-1 Hilbert space. Note that there is a dangling spin-1/2 moment at the end of the chain.

the symmetry, at the interface between the SPT and the vacuum, we are guaranteed to encounter a singularity.

This idea is formulated in quantum field theory by the notion of 't Hooft quantum anomaly. The crucial point is that boundaries of SPT phases necessarily realize the protecting symmetries in an anomalous way: the boundary state of a d-dimensional SPT cannot be realized as a $(d-1)$-dimensional local lattice system with the same symmetry. In the example of the Haldane-AKLT chain, the dangling spin-1/2 moment associated with each end realizes the spin rotation symmetry projectively, which cannot be realized alone in a strictly zero dimensional system (a point) with spin-1 degrees of freedom. In general, the consequence of a 't Hooft anomaly is that the boundary of an SPT must be non-trivial in one of three ways: (1) breaking the protecting symmetry spontaneously, (2) being gapless, or (3) developing topological order when the boundary is in a spatial dimension greater than or equal to 2.

It is worth noting that the anomalies need not necessarily manifest only at the boundary of a system, but it can also arise due to the specific structure of the Hilbert space. Lattice systems constrained by the Lieb-Schultz-Mattis (LSM) condition provide a prominent example of such systems [111, 124, 74]. The canonical illustration of such a system is a translationally invariant lattice spin system possessing $SO(3)$ spin rotation symmetry and a spin-1/2 moment per unit cell. It is well-known that such a system exhibits a mixed t'Hooft anomaly between the discrete lattice translation and spin rotation symmetries [37]. Consequently, a unique gapped ground state cannot be realized in the presence of the t'Hooft anomaly.

Thus far, in the discussion of SPT phases and quantum anomalies, it has been crucial that the relevant protecting symmetry is preserved exactly.

1.2 Average SPT phases

A natural question is, how exact does the protecting symmetry has to be? Specifically, if we have some *quenched disorders* that locally break the protecting symmetry, but on average still respect the symmetry (such as magnetic impurities in TI), could the state still be in some topologically nontrivial phase? In other words, could *average symmetry* protect nontrivial topological phases?

Previous studies have shown that some features of SPT phases in clean systems survive "statistically-symmetric" disorder present on the boundary, which lead to the concept of "statistical topological insulator" [59, 120]. One example is the three dimensional (3D) weak TI, made by stacking layers of a 2D TI. The surface state of the 3D weak TI is protected against Anderson localization even with strong disorder, if the translation symmetry along the stacking direction is restored by disorder averaging[137, 121]. A similar delocalization appears on the surface of a 3D strong TI subject to a random magnetic field with zero mean[56], and an even richer set of phenomena were discussed in the presence of interactions[92].

Key questions, however, remain unanswered. Previous studies focused on the effects of disorders on the boundary. It is then natural to ask: are the bulk topological phases sharply defined with average symmetries? If so, what are their signatures in the bulk, and how could we classify such phases? This question is particularly relevant for SPT phases protected by crystalline symmetries [55, 153, 156], since impurities and lattice defects are ubiquitous in crystalline solids and the symmetry of an ideal lattice in reality is respected at best only on average. Of course when the material sample is of high quality, one can treat the ideal lattice as a good approximation. However, if the disorders become non-negligible, does the entire notion of crystalline SPT lose its meaning?

Even for the boundary physics, the problems were tackled on a case-by-case basis in existing literature. Given a symmetry group $\mathcal{G}$ that contains an average symmetry G,

how do we systematically decide whether the boundary has to be nontrivial in some way? For free fermion states this issue was discussed in Ref. [59], but for interacting systems the question is largely open. In the standard theory of clean SPT, the non-triviality of the boundary is ultimately guaranteed by the aforementioned t 'Hooft quantum anomaly, which is decided by the bulk topological invariant. Familiar examples include the $(3+1)d$ TI surface protected by parity anomaly, and the integer quantum Hall edge protected by chiral anomaly. So the question about boundary properties can be rephrases as: does the notion of quantum anomaly exist for average symmetry? If anomaly can indeed be defined, how does such "average anomaly" constrain the infrared (IR) dynamics of the boundary theory?

As mentioned in the last subsection, t'Hooft anomaly also appear in lattice systems with LSM constraints. As a consequence, the low energy dynamics of these lattice systems cannot be completely trivial: either the symmetry will be spontaneously broken, or the system will form some long-range entangled ground state that is either topologically ordered or gapless. Besides a translation invariant lattice spin-1/2 system with $SO(3)$ spin rotation symmetry, similar t'Hooft anomalies also arise for other internal symmetries as long as they admit projective representations, and for other lattice symmetries such as rotation and reflection[129]. Recently, it was shown in Ref. [93] that, at least for $(1+1)d$ spin chains with $SO(3)$ symmetry, the LSM constraint holds even if the translation symmetry becomes only an average symmetry. Even though the argument in Ref. [93] does not make explicit connection to anomaly, it does suggest that the LSM anomaly should exist for arbitrary dimensions and for more general symmetries (such as time-reversal). Making this connection more explicit, precise and general is an open direction of great importance.

In this thesis we will address all of the above issues in Chapter. 2. As an appetizer, the key to these questions is to realize that

1. SPTs, whether in the bulk or on the boundary, are characterized by the properties of symmetry defects. The symmetry defects, e.g. twisted boundary conditions and gauge fluxes, may carry quantized invariants that can be used to define different phases. A well-known example is that in the bulk of a 3D TI, a unit magnetic monopole carries half-integral electric charge [135, 139, 176].

2. For an average symmetry G in a disordered ensemble, even though the ground state in each disorder realization is not a G-eigenstate, we can still define defects associated with G for the entire ensemble – all we need is to modify the disorder potential accordingly.

Therefore by characterizing the defects, or equivalently domain walls of the average symmetries, we obtain an understanding of average SPT phases. Essentially, lower-dimensional states can be decorated onto the domain walls, similar to the case of clean SPTs. This "decorated domain wall"[34] picture turns out to be powerful both in the bulk and on the boundary.

1.3 Topological phases with average symmetries

In this thesis, I will also extend the discussion to a general framework for topological phases with average symmetries. As discussed in preceding subsections, an SPT phase is described by a series of topological invariants ("topological response"), characterizing the properties of symmetry defects. The decorated domain wall construction provides a mathematical framework for this idea. Specifically, starting from a phase in $(d+1)$-dimensional spacetime in which the symmetry G is spontaneously broken, a symmetric state can be obtained by condensing G-domain walls. Non-trivial SPT phases can be produced by decorating codimension p topological defects of G with $(d-p+1)$-dimensional SPT phases protected by unbroken symmetries in the system, before the domain wall proliferation. In order for the condensation of G-domain walls to give rise to a unique gapped ground-state in the bulk, certain consistency conditions for the defect decoration must be satisfied [172].

When we introduce quenched disorders that break the G-symmetry to the system, the condensation of domain walls associated with the G symmetry is not allowed. Specifically, the domain wall configurations can no longer form a coherent quantum superposition, instead becoming classical objects whose positions are determined by the symmetry-violating disorder. However, the entire ensemble of disorder still preserves the G symmetry upon averaging, ensuring that configurations with domain walls of arbitrarily large sizes are

present within the disorder ensemble. As a result, domain walls must proliferate through classical probability to restore the G symmetry at the ensemble level.

As elaborated in Chapter 3, this proliferation of domain walls through "classical probability" has a profound impact on the consistency conditions imposed on the decorated domain wall construction. Namely, the set of consistency conditions that a decoration pattern must satisfy is reduced. This reduction in consistency conditions paves the way for the possibility of *intrinsically* disordered average Symmetry-Protected Topological (ASPT) phases. These phases have no counterparts in clean SPT phases. The study of intrinsically disordered ASPT phases is one of the focuses of this thesis. I will present a unified mathematical framework for the classification of SPT phases with average symmetry – the spectral sequence.

The notion of SET phases can also be extended to ensembles with quenched disorders. In a system without symmetry-violating disorders, symmetry can enrich a topological order in three ways: (1) A symmetry may permute anyon excitations while leaving the fusion and braiding data invariant. (2) Symmetry can act projectively on anyons, leading to "symmetry fractionalization". (3) One has to specify the fusion and brading properties of symmetry defects. These data must satisfy a set of consistency conditions known as Unitary Modular Tensor Categories (UMTC), which has been extensively studied in the literature [12]. This thesis will demonstrate that the proliferation of average symmetry defects through classical probability leads to modifications of the UMTC consistency conditions. In particular, some SET phases in clean systems are trivialized, while the possibility of phases that only exist in disordered ensembles is opened.

It is necessary to differentiate between two distinct concepts of a "disordered ensemble". Specifically, when we refer to "quenched disorder", we consider an ensemble of disordered Hamiltonians that correspond to specific disorder configurations. In this case, the disorder can be viewed as a classical random potential, and our interest lies in the topological properties of the ensemble of ground states, each of which is a pure state. SPT phases in such disordered ensembles will be referred to as disordered SPT phases. Superficially, the ensemble gives a density matrix $\rho = \sum_I P_I |\Psi_I\rangle\langle\Psi_I|$, with $|\Psi_I\rangle$ the ground state for the Ith disorder realization and P_I the corresponding probability. However, a crucial point is that the states $\{|\Psi_I\rangle\}$ form a fixed basis for the ensemble. Another scenario covered in

this thesis is referred to as "decohered" or quantum disorder. Here, the system can form quantum entanglement with its environment (the "quantum disorder"). Nonetheless, the observables of interest are confined to the "dynamical" Hilbert space that does not include the disorder degrees of freedom. In other words, the disorders are traced out, leaving a mixed state. In this scenario, the ensemble representation of the density matrix is subject to basis choice, due to the purification theorem [133]. SPT phases in mixed states will be referred to as decohered SPT phases.

In the thesis, it will be demonstrated that the classification of ASPT phases differs depending on whether we consider quenched disorders, or decohered or quantum disorders. In fact, similar distinction also appears in the context of dynamics of open quantum systems, which include dynamics with measurements or decoherence. In this thesis I will also present a theory that systematically studies the impact of measurements and decoherence on the long-distance behaviors of quantum critical states from a symmetry perspective. As will be explained shortly, a non-unitary dynamics with stochastic state update induced by measurements is characterized by an ensemble of state trajectories, which are labeled by the measurement outcomes. Decoherence, on the other hand, can be interpreted in terms of the coupling to a bath. In this sense, non-unitary dynamics is inherently related to "quenched" or "quantum" disorders.

1.4 Non-unitary dynamics: A symmetry perspective

The recent advancements in quantum devices [134, 7] have led to a renewed interest in the study of open quantum systems, where the dynamics is not solely governed by the Hamiltonian. Of particular interest is the class of monitored quantum systems, which experience both a deterministic unitary time evolution and stochastic state updates from measurements. The study of such systems has revealed the existence of a measurement-induced phase transition [151, 110, 28, 67, 85, 9], which causes a qualitative change in the entanglement properties of the system. More recently, the impact of decoherence has become a focal point of research due to the unavoidable interaction of realistic quantum devices with their surrounding environments, leading to noise-induced effects [11, 48, 106,

184].

From a physical perspective, the three aforementioned types of dynamics, namely Hamiltonian, measurement, and decoherence, have rather distinct effects on many-body quantum states:

1. A Hamiltonian, or a general unitary time evolution, typically results in the generation of quantum entanglement among microscopic degrees of freedom in the system. For instance, a local Hamiltonian usually produces entanglement in its ground-state within a correlation length. This correlation length can be as large as the entire system size near a quantum criticality.

2. Local measurements with post-selection, on the other hand, project the state onto an eigenstate of a local observable, leading to a decrease in the entanglement between the measured microscopic component and the rest of the system, as well as between the system and its environment. It is important to note that, despite the stochastic nature of the state update following measurement, an initial pure state of the system remains pure throughout the time evolution. At the end of the evolution, we obtain an ensemble of state trajectories that are each labeled by a particular sequence of measurement outcomes.

3. Decoherence arises from the interaction between a quantum system and its surrounding environment, which generates quantum entanglement between the two. Because all observables are associated with the system and not the environment, the latter is effectively traced out. Therefore, generic decoherence processes increase the mixedness of a quantum system.

Previous investigations have revealed that the interplay between these dynamics can lead to a diverse range of collective phenomena and phase transitions. However, the majority of these studies have been focused on particular lattice models and specific types of measurements or decoherence.

In Chapter. 4 of the thesis, I will provide a description of the universal features of an open system characterized by a large correlation length, which can arise from any of the

three aforementioned dynamics or their competition. For the sake of simplicity, we focus on the impact of local measurements or decoherence ("perturbations"), on the ground-state of a quantum Hamiltonian at criticality. Specifically, we examine two timescales of the perturbations: a finite time perturbation that is independent of the system size, and a perturbation over a period of time that is comparable to the system size. These two time scales are motivated by the following two questions respectively: (1) What is the nature of the quantum state resulting from measurements or decoherence on a critical ground-state? (2) What properties of the critical ground-state survive in the stationary state, when a critical Hamiltonian is in an environment with measurements or decoherence? In order to approach the long wavelength physics, in particular the ensemble-averaged correlation functions and entanglement entropy, we use a replicated Keldysh field theory [149, 86] to describe the effect of measurements or decoherence. This part can be regarded as a continuation of the previous study on quenched disorders and quantum disorders – in fact, we will see that they share very similar mathematical structures, respectively.

1.5 Plan of the thesis

The rest of the thesis is structured as follows: Chapter 2 presents a theory of average symmetry-protected topological (ASPT) phases in disordered ensembles, where the quenched disorders break part of the protecting symmetries while restoring the symmetry upon disorder averaging. Section 2.6 provides a theory for symmetry-protected topological (SPT) phases in mixed states, also known as decohered SPTs. Chapter 3 extends the discussion to a general framework of topological phases with average symmetries, including those intrinsically disordered/decohered ASPT phases and average symmetry-enriched topological (SET) orders. Finally, Chapter 4 presents a study of the effects of measurements and decoherence on long-distance behaviors of quantum critical states from a symmetry perspective. There are many important open questions in the directions that I cover in this thesis, which will be elaborated upon in the concluding sections of each chapter.

Chapter 2

Average Symmetry-Protected Topological Phases

2.1 Summary of results

This Chapter is largely based on Ref. [115]. We highlight the main results of this chapter below. This part will also serve as a map for the rest of this chapter.

1. In Sec. 2.2, we carefully define some basic notions such as average symmetry and average SPT phases in a disordered ensemble. In particular, even though we do not assume the disorders to be weak, we do assume that the ground states in different disorder realizations to be adiabatically connected to each other. This, together with other physically intuitive assumptions, allow us to make controlled arguments throughout this thesis.

2. In Sec. 2.3 we develop the picture of decorated domain walls (or defects in general). In particular, we argue that topologically nontrivial phases arise when the average-symmetry domain walls are decorated with nontrivial states protected by exact symmetries. For example, if the total symmetry $\mathcal{G} = K \times G$, where K is an exact symmetry and G is an average symmetry, then within the group-cohomology

formalism, bosonic SPT phases are classified by (Theorem. 1)

$$\sum_{p=1}^{d+1} H^{d+1-p}(G, H^p(K, U(1))). \tag{2.1}$$

In particular, group-cohomology states protected solely by G (classified by $H^{d+1}(G, U(1))$ becomes trivial as G becomes an average symmetry. This result also applies when G is the average lattice symmetry, appropriate for realistic crystalline systems, and K is the exact internal symmetry. The result can also be extended to states beyond group-cohomology. In Table 2.1 we list the classification of bosonic SPT phases for several simple symmetry classes, in space dimensions $1, 2, 3$, including those beyond group-cohomology.

3. In Sec. 2.4 we show using a modified flux-insertion argument that, when nontrivial states are decorated on domain walls with dimensions higher than $(0+1)d$ (e.g. $p > 1$ in Eq. (2.1)), the boundary state is almost certainly long-range entangled (or long-range correlated) – the probability for realizing such long-range entangled ground state approaches 1 as the system size $L \to \infty$ (Theorem 2). In contrast, if states are decorated on $(0+1)d$ domain walls (e.g. $p = 1$ in Eq. (2.1)), then the boundary state for all disorder realizations can be short-range entangled – the only nontrivial feature in this case is that different disorder realizations may not be adiabatically connected in the presence of such mildly anomalous boundary. In Table 2.1 we list, in parenthesis, those states that do (almost certainly) have long-range entangled boundary states.

4. The above result on average anomaly is used in Sec. 2.4.3 to show a Lieb-Schultz-Mattis (LSM) constraint for systems with average translation symmetry, where each lattice unit cell contains a projective representation of the exact on-site symmetry (such as spin-1/2 moment for $SO(3)$ or Kramers' doublet for time-reversal). We argue that in such systems the ground state will almost certainly be long-range entangled (or long-range correlated), with probability approaching 1 as the system size $L \to \infty$.

5. In Sec. 2.5 we consider $(3+1)d$ fermion systems in two symmetry class: AII class ($U(1) \rtimes \mathcal{T}$ with Kramers' doublet fermions) and AIII class ($U(1) \times \mathcal{T}$). In both cases

we consider average time-reversal symmetries. The AII class is relevant for electronic solids with spin-orbit interactions, with magnetic impurities that locally break time-reversal; the AIII class is relevant for quantum Hall plateaux transitions with average particle-hole symmetry. We show that for the AII case, the classification is reduced from $\mathbb{Z}_2^3$ in the clean case to $\mathbb{Z}_2^2$; for the AIII case, the classification is reduced from $\mathbb{Z}_8 \times \mathbb{Z}_2$ to $\mathbb{Z}_4 \times \mathbb{Z}_2$. All these nontrivial states have long-range entangled surface states with probability one, except for the $n = 2$ state in the $\mathbb{Z}_4$ factor of AIII, in which the surface state can be short-range correlated for each individual disorder realization. The anomaly structure for the AIII case is consistent with numerical simulations on multi-component quantum Hall plateau transitions.

6. In Sec. 2.6 we further generalize our problem to quantum disorders, where disorders are described by quantum mechanical degrees of freedom that can form nontrivial (but still invertible) many-body entanglement within themselves. This converts our problem to the study of SPT phases in mixed states – a problem that has been recently studied[42] in the context of open quantum systems. We find that

   - States protected solely by the average symmetry, including invertible states that do not need any symmetry, become trivial.
   - Time-reversal symmetry always behave as an average symmetry.
   - Bosonic SPTs described by elements in Eq. (2.1) are still nontrivial. For this statement, we give a careful justification in $(1+1)d$ in terms of the string order parameters, and give a plausibility argument in the more general cases.

We end with some discussions in Sec. 2.7.

2.2 Generalities

Let us begin by introducing some useful concepts and physically defining our questions more precisely. To start, we consider a fixed lattice Hilbert space with a local tensor product structure $\mathcal{H} = \otimes_i \mathcal{H}_i$ (i labeling lattice sites), and an ensemble of *local* Hamiltonians $\{H_I\}$

Symmetry	$(1+1)d$	$(2+1)d$	$(3+1)d$
$\mathbb{Z}_2^{(ave)}$	0	0	0
$(\mathbb{Z}_2^T)^{(ave)}$	0	0	$\mathbb{Z}_2$ $(\mathbb{Z}_2)$
$\mathbb{Z}_2 \times \mathbb{Z}_2^{(ave)}$	$\mathbb{Z}_2$ (0)	$\mathbb{Z}_2^2$ $(\mathbb{Z}_2)$	$\mathbb{Z}_2^2$ $(\mathbb{Z}_2)$
$\mathbb{Z}_2 \times (\mathbb{Z}_2^T)^{(ave)}$	$\mathbb{Z}_2$ (0)	$\mathbb{Z}_2^2$ $(\mathbb{Z}_2)$	$\mathbb{Z}_2^3$ $(\mathbb{Z}_2^2)$
$\mathbb{Z}_2^T \times \mathbb{Z}_2^{(ave)}$	$\mathbb{Z}_2$ $(\mathbb{Z}_2)$	$\mathbb{Z}_2$ $(\mathbb{Z}_2)$	$\mathbb{Z}_2^3$ $(\mathbb{Z}_2^3)$

Table 2.1: Classification of bosonic average SPT phases in some symmetry classes, in space dimension $d = 1, 2, 3$. The classification in parenthesis are those with long-range entangled boundary states.

and their ground states $\{|\Psi_I\rangle\}$, with probability $\{P_I\}$. For concreteness the Hamiltonian takes the form

$$H_I = H_0 + \sum_i (v_i^I \mathcal{O}_i + h.c.), \tag{2.2}$$

where v_i^I is a quenched disorder potential (I labeling a particular realization and i labeling a lattice site), $\mathcal{O}$ is a local operator, and H_0 is the disorder-free part of the Hamiltonian. We require the disorder to be at most short-range correlated, namely $\overline{v_i^* v_j}$ should decay exponentially with $|i-j|$.

We now consider two types of global symmetries. The **exact symmetry** K commutes with both the disorder-free part and the disordered part of the Hamiltonian, for any individual realization of the disorder. The **average symmetry** (or statistical symmetry)[59, 56, 93, 92] G only commutes with H_0 and is broken by each realization of the disorder potential, so effectively the disorder potential v transforms non-trivially under G. We then require that the probability distribution $P[v]$ to be invariant under a G transform, so the entire statistical ensemble stays invariant, hence the name average (or statistical) symmetry. For simplicity we will often focus on cases where the full symmetry of the ensemble $\mathcal{G}$ is given by $K \times G$. But we note that in general, $\mathcal{G}$ is given by the group extension,

$$1 \longrightarrow K \longrightarrow \mathcal{G} \longrightarrow G \longrightarrow 1, \tag{2.3}$$

where $K \subset \mathcal{G}$ is a normal subgroup. $\mathcal{G}$ may or may not contain an anti-unitary (time reversal) element. We shall also assume that both K and G acts locally (namely their

actions within each lattice unit cell are unentangled), so they do not suffer from any t'Hooft anomaly – we shall come back to this issue later when discussing boundary properties.

We now proceed to define the analogue of symmetric short-range entangled (SRE) states, but for the entire statistical ensemble $\{H_I, |\Psi_I\rangle, P_I\}$. It is natural to consider cases in which each individual $|\Psi_I\rangle$ is SRE (and symmetric under K), namely each H_I is gapped with a unique symmetric ground state. However for our purpose this is not enough: we would like to forbid the ensemble from containing states in different SRE phases (possibly protected by K) separated by topological phase transitions[1]. We therefore have

Definition 1. *A K-**symmetric SRE ensemble** is one that only contains K-symmetric SRE ground states $\{H_I, |\Psi_I\rangle\}$, with any pair of states being adiabatically connected to each other while preserving K.*

Notice that we impose the symmetric SRE condition on *all* states in the ensemble, including those rare states with vanishing probability in thermodynamic limit. This is to avoid potential subtleties from Griffiths-like singularities. We expect this no-rare-region restriction to be physically reasonable far away from quantum phase transitions. The interplay between rare region effects and topological phase transitions is a fascinating subject that we leave to future studies.

To study symmetric SRE states, we further demand that the ensemble of states $\{|\Psi_I\rangle\}$ does not break the symmetries spontaneously. For exact symmetries this simply means that each individual state $|\Psi_I\rangle$ does not break the symmetries (i.e. is not a cat state), which is anyway guaranteed by the symmetric SRE condition. The question is slightly subtler for average symmetries. One could, for example, detect spontaneous breaking of an average symmetry G by measuring the average magnitude of the integrated order parameter

$$M \equiv \overline{|\sum_i \langle \phi_i \rangle|}, \tag{2.4}$$

where ϕ_i is some local order parameter (defined near site i) that transforms nontrivially under G, $\langle ... \rangle$ denotes the expectation value with respect to a particular quantum state,

[1] If the disorder potential v takes continuous values in a connected space, this would be automatically forbidden by imposing symmetric SRE on each individual state. However in more general cases, the condition has to be imposed separately.

and the overline denotes the disorder (ensemble) averaging (we shall use this notation throughout this Chapter). If the ensemble spontaneously breaks G, we expect M to be proportional to the volume L^d. For symmetric ensembles we expect a smaller scaling – for example, a trivial paramagnetic state will have $M \sim O(L^{d/2})$.

The above way of detecting spontaneous breaking of average symmetries, however, is not very convenient for our purpose. In this thesis, instead, we will guarantee the absence of spontaneous G-breaking primarily through proliferation of domain walls (or other defects such as vortices). Essentially, we demand that at sufficiently large length scale (larger than the correlation length), domain walls (or other appropriate defects) will always appear to restore the statistical G symmetry. At low enough dimensions ($2d$ for discrete symmetries), such domain wall proliferation is always guaranteed by the Imry-Ma theorem[81].

Next we shall define the notion of **continuous symmetric deformation** – the analogue of symmetric adiabatic evolution – for our SRE ensembles. This task is relatively straightforward: we continuously deform both the Hamiltonians (H_0 and $\mathcal{O}_i$ in Eq. (3.11)) and the probability distribution of the disorder $P[v]$, such that (1) both the Hamiltonians and the disorder correlations remain short-ranged, and (2) the ensemble of states remains symmetric and SRE throughout.

We are now ready to define the notion of average SPT phases:

Definition 2. *Two SRE ensembles, with exact symmetry K and average symmetry G, belong to the same* ***average SPT phase*** *iff there is a path of continuous symmetric deformation connecting the two.*

As in most other topology problems, it is impractical to check all continuous paths between two states. Instead it is much more useful to construct topological invariants to distinguish different phases. This will be the task of next Section.

2.3 Decorated domain wall approach

In this section we will generalize the decorated domain wall approach[34], a powerful construction for standard SPT phases, to the study of average SPT phases. Let us first

review the idea of constructing standard SPT phases by the decorated domain wall (more generally, symmetry defect) construction in clean systems[34], where all symmetries are exact. Starting from a phase in $(d+1)$-dimensional space-time, in which G is broken spontaneously, a symmetric state can be obtained from condensation of G-domain walls. Non-trivial SPT phases are produced by decorating codimension p (with respect to the space-time) topological defects of G with $(d-p+1)$-dimensional SPT phases protected by the unbroken symmetry K before the domain wall proliferation. In order for the condensation of G-domain walls to be gapped with a unique ground-state in the bulk, there is a set of consistency conditions for the defect decoration [172], such that G-defect of each codimension is free of K-anomaly. In this scheme the protected surface states appear naturally: topological defects that end at the surface carry the non-trivial boundary modes of the lower dimensional SPT phases protected by the symmetry K.

For simplicity let us tentatively assume G to be discrete and unitary – the more general cases are similar in conclusions but more subtle in details. The decorated domain wall approach can be equivalently formulated as follows: consider the SPT state $|\Psi\rangle$, and act on it with the symmetry element $g \in G$, but only in a (large enough) subregion A (say with a disk geometry): $U_g^A \equiv \prod_{i\in A} U_g^i$ (U_g^i is the local g-generator). The symmetric SRE nature of $|\Psi\rangle$ implies that acting with U_g^A has nontrivial effect only near the boundary of A [132, 161, 49], namely $U_g^A|\Psi\rangle = V_g^{\partial A}|\Psi\rangle$, where $V_g^{\partial A}$ is a unitary operator that is nontrivial (non-identity) only near the boundary ∂A. In this case a decorated domain wall simply means that $V_g^{\partial A}$ creates a nontrivial phase in one dimension lower. Similar considerations can be carried out for defects with higher codimensions[172] and for anti-unitary symmetries[146].

Now we add quenched disorder that breaks the G-symmetry to the system. One can imagine that now the system consists of patches with different symmetry breaking patterns, which are pinned by the symmetry-violating disorder. In two adjacent patches, the states are related by an action of the broken symmetry. As a result, the interface between two adjacent patches naturally realizes a G-domain wall. The idea is that, similar to the case in clean systems, we can decorate the domain walls with nontrivial lower dimensional invertible phases, such as SPT phases protected by the exact symmetry. When the disorder has a random distribution so that the G-symmetry is restored on average, one again gets

a G-defect network, extending over the entire system.

The above picture is very similar to the standard (exact symmetry) SPT, but with one important difference: for standard SPT the domain walls proliferate as coherent quantum superpositions, with well defined phase factor associated with each domain wall configuration – for example, the bosonic $\mathbb{Z}_2$ Levin-Gu state[109] has a (-1) factor for each Ising domain wall; for average SPT, however, the domain walls proliferate through classical probability, with no analogue of quantum phase factors. Therefore SPT states that are nontrivial due to such phase factors in the domain wall superpositions have no analogue in average SPT.

Let us try to make the decorated domain wall picture for average SPT more precise. Consider a particular realization, say, $\{v_i\}$ in Eq. (3.11), with the ground state $|\Psi\rangle$. Now consider a different realization, with $\tilde{v}_i = v_i$ for i outside of a region A, and $\tilde{v}_i = g v_i g^{-1}$ inside the region A (for example for Ising symmetry $\tilde{v}_i = -v_i$ for $i \in A$), and denote the corresponding ground state as $|\tilde{\Psi}\rangle$. These two disorder realizations have essentially identical probability. The absence of spontaneous G-breaking, together with the SRE nature of the ensemble, implies that for large enough A, the two should look identical deep inside $\bar{A}$, and should differ only by a g-action deep inside A – the only potential nontrivial difference can only happen near the boundary ∂A. Formally,

$$U_g^A |\Psi\rangle = V_g^{\partial A} |\tilde{\Psi}\rangle, \tag{2.5}$$

with $V_g^{\partial A}$ defined nontrivially only on ∂A. If we choose a different disorder realization, say v_i' with ground state $|\Psi'\rangle$, we can similarly define $\tilde{v}_i'$ and $|\tilde{\Psi}'\rangle$. By assumption (Def. 1), all these states are connected through some K-symmetric adiabatic evolutions (or K-symmetric finite depth unitary circuit). Moreover, the evolution connecting $|\Psi\rangle$ to $|\Psi'\rangle$ (call it W) and that connecting $|\tilde{\Psi}\rangle$ to $|\tilde{\Psi}'\rangle$ (call it W') must be identical deep inside $\bar{A}$ and differ only by conjugating g deep inside A. These facts are enough to show that

$$U_g^A |\Psi'\rangle = (V_g^{\partial A})' |\tilde{\Psi}'\rangle, \tag{2.6}$$

where $(V_g^{\partial A})'$ and $V_g^{\partial A}$ only differ by an adiabatic evolution on ∂A. In other words, the topological nature of $V_g^{\partial A}$ does not depend on the choice of disorder realization, even though non-universal properties of $V_g^{\partial A}$ certainly does depend on details of the disorder

potential. Similarly, one can show that the topological nature of $V_g^{\partial A}$ also does not depend on the choice of the region A, as long as A is large enough – essentially, Def. 1 requires different domain wall configurations to be adiabatically connected to each other, which in turn requires the decorating phases on the domain walls to remain the same no matter where the domain walls move to. The only way to change the topological property of $V_g^{\partial A}$ is to go through a phase transition – at least for some of the states in the ensemble.

The above arguments establishes the (topological part of) $V_g^{\partial A}$, the "decoration" on the domain walls, as a robust property describing the corresponding average SPT phases.

2.3.1 Topological response from replica field theory

Similar to the standard SPT theory, the decorated domain wall construction can be rephrased as a topological response theory for background gauge fields. For this purpose, we work with the path integral and use the replica trick: we replicate the Lagrangian N_r times to obtain the action

$$S = \int dt d^d x \sum_{\alpha=1}^{N_r} \mathcal{L}[\phi_\alpha(x,t), v(x)] + \int d^d x V[v(x)], \tag{2.7}$$

where ϕ represent all the dynamical degrees of freedom, α is the replica index, v is the disorder potential. The first term represents the dynamics of ϕ's and their interactions with v, and the second term generates the classical probability of the disorder potential. Note that while the dynamical fields $\phi(x,t)$ depend on both space and time, the disorder potential $v(x)$ only varies in space and is constant in time.

The replicated action Eq. (2.7) is, by definition, invariant under the full symmetry group $\mathcal{G}$. The disorder potential v is invariant under the exact symmetry K, but transforms non-trivially under the average symmetry G. There is no obstruction in coupling the theory in Eq. (2.7) to a background gauge field in $\mathcal{G}$, call it $A^{\mathcal{G}}$. The only subtlety is that since v is constant in time, any gauge transformation associated with G must be constant in time. This then requires the G gauge field, denoted as A^G, to be trivial along the time direction. Since the time component of a gauge field couples to the symmetry charge, the constraint on G gauge field is simply a reflection of the fact that G-charge is not conserved

for our system, and one cannot use G-charges to distinguish different phases of matter. The spacial components of A_G, on the other hand, are not constrained. In fact, the average symmetry defects, discussed in the decorated domain wall construction, can be precisely described using the spacial components of A_G following standard procedures. For example, a nontrivial holonomy of A^G along a spacial cycle represents a twisted boundary condition for both the dynamical fields and the disorder potential.

We can now formally integrate out the dynamical fields ϕ, and obtain the partition function that depends on the background gauge field $A^{\mathcal{G}}$ and the spacetime $(d+1)$-manifold X. For an invertible phase (such as SPT) in a clean setup, the global properties are included in a topological quantum field theory (TQFT) as the imaginary phase of the Euclidean partition function[90],

$$\ln(Z[X,\, A]) \sim iS_{\text{top}}[X,\, A] + \cdots, \tag{2.8}$$

in which the terms omitted are irrelevant below the bulk energy gap. In the presence of quenched randomness, the disorder-averaged effective action can be obtained from the replica limit [6]

$$\begin{aligned} S[X, A^{\mathcal{G}}] &= \overline{\ln Z[X, A^{\mathcal{G}}]} \\ &= \lim_{N_r \to 0} \frac{1}{N_r} \overline{(Z[X, A^{\mathcal{G}}]^{N_r} - 1)}, \end{aligned} \tag{2.9}$$

where the overbar denotes the disorder average. Analogous to clean systems, the topological term that survives the replica limit $N_r \to 0$ in Eq. (2.9) encodes the topological properties of the disorder system.

Here we make a side remark. The maximal symmetry group (let us denote it by $\tilde{\mathcal{G}}$) of the actions in Eq. (2.7) is not the "full symmetry group" $\mathcal{G}$ that acts diagonally on all replicas. For example, if $\mathcal{G} = K \times G$, then $\tilde{\mathcal{G}} = K^{N_r} \times G$, since each replica can transform under K independently while leaving the Lagrangian invariant. More generally, $\tilde{\mathcal{G}}$ is defined by the following morphism of short exact sequences:

$$\begin{array}{ccccccccc} 1 & \longrightarrow & K^{N_r} & \longrightarrow & \mathcal{G}^{N_r} & \longrightarrow & G^{N_r} & \longrightarrow & 1 \\ & & \cong\uparrow & & f\uparrow & & F\uparrow & & \\ 1 & \longrightarrow & K^{N_r} & \longrightarrow & \tilde{\mathcal{G}} & \longrightarrow & G & \longrightarrow & 1 \end{array} \tag{2.10}$$

Here F is the diagonal map, and we ignore the (in general discrete) rotation symmetry among the replicas. Coupling the overall $\tilde{\mathcal{G}}$ symmetry to backgrounds enables us to calculate quantities such as

$$\lim_{N_r \to 0} \overline{\langle O_1^\alpha O_2^\beta \rangle} - \overline{\langle O_1^\alpha \rangle \langle O_2^\beta \rangle}, \tag{2.11}$$

where $\alpha \neq \beta$ and O_1, O_2 are arbitrary operators. Physically these quantities encode nontrivial sample-to-sample fluctuations in the disordered ensemble. Since we have assumed (Def. 1) that different disorder realizations are adiabatically connected, we do not expect such sample-to-sample fluctuations to play an important role in our discussions. One can, however, ask whether by relaxing our assumptions, we can discover nontrivial topological properties associated with sample-to-sample fluctuations (such as a topological analogue of the universal conductance fluctuation[108]), as may be captured by coupling to $\tilde{\mathcal{G}}$ gauge field. We leave this intriguing possibility for future study.

We are now ready to classify and characterize a large class of ASPT phases. For SRE phases for which the ground-state is unique and gapped on any closed spatial manifold, this problem is equivalent to the classification of associated invertible TQFTs (see Eq. (2.8) and Eq. (2.9)), studied by the cobordism theory [91, 90, 89, 54]. The static disorder modifies the classification by constraining the space-time configurations of the background fields of average symmetries, i.e. it quenches the holonomy of A^G along the time cycle. For example, a clean topological phase remains nontrivial if and only if the corresponding TQFT remains non-trivial given this constraint. Next, with some simple examples, we illustrate how the topological response theory naturally leads to the decorated domain wall construction.

2.3.2 Simple examples: group cohomology states with $\mathcal{G} = K \times G$

Let us consider bosonic SPT phase described by group cohomology[31]. For simplicity we also assume $\mathcal{G} = K \times G$, namely the group extension Eq. (2.3) is trivial. In this case the group cohomology classification in $(d+1)$-dimensional space-time can be rewritten by the

Künneth formula,

$$H^{d+1}(\mathcal{G}, U(1)) = \sum_{p=0}^{d+1} H^{d+1-p}(G, H^p(K, U(1))), \tag{2.12}$$

in which the corresponding coefficient group is twisted if G or K contains time reversal [89]. This mathematical formula can be understood from the perspective of topological effective actions. For a bosonic system, the topological action in Eq. (2.8) can be expressed as an integral of a local Lagrangian $\mathcal{L}$ over space-time,

$$S_{\text{top}} = 2\pi \int_X \mathcal{L}, \tag{2.13}$$

where $\mathcal{L}$ is a $(d+1)$-dimensional cocycle, built out of flat background gauge fields (and $w_1(TX)$, the first Stiefel-Whitney class of the space-time, which can be viewed as the time reversal gauge field). In particular, $\mathcal{L}$ may be written as a cup-product $\mathcal{L} = \mathcal{L}_1 \cup \mathcal{L}_2$, where $\mathcal{L}_1$ and $\mathcal{L}_2$ are two cocycles constructed from the background gauge fields in the theory, whose degrees sum to $(d+1)$. As the effective action of an SRE phase, we require $\mathcal{L}$ to be gauge invariant on any closed space-time. For a compact X, the Poincare duality $H^p(X) \cong H_{d+1-p}(X)$ (with the coefficient in any ring) enables us to rewrite the action as

$$S_{\text{top}} = 2\pi \int_{\hat{\mathcal{L}}_2} \mathcal{L}_1, \tag{2.14}$$

where $\hat{\mathcal{L}}_2$ is the Poincare dual (with respect to X) of the cocycle $\mathcal{L}_2$.

To make connections between current discussion and the decorated domain wall picture, note that if the cocycle $\mathcal{L}_2$ is taken to be the background gauge field A^G of a symmetry G, the Poincare dual surface $\hat{\mathcal{L}}_2$ is simply a G-domain wall. The action in Eq. (2.14) hence describes an effective $(d-1+1)$-spacetime-dimensional topological phase, living on the wall. This precisely corresponds to the SPT phase decorated on the codimension-1 G-domain wall. Gauge invariance of $\mathcal{L}$ ensures the consistency between the decoration and the fusion rules of the domain walls. The same argument also holds for defects of higher codimensions, where $\mathcal{L}_2$ are cocycles of higher degrees built out of A^G. Therefore a physical interpretation of an element of $H^{d+1-p}(G, H^p(K, U(1)))$ in Eq. (2.12) is a consistent decoration of a p-dimensional G-defect by a K-SPT phase in p-dimensional space-time.

When static randomness turns G into an average symmetry, A^G can have non-trivial holonomies only around spatial cycles. Equivalently, this means the symmetry defect $\hat{\mathcal{L}}_2$ extends along time, while its spatial position is pinned. A straightforward observation is that the topological action of the $p = 0$ element (i.e. the group cohomology $H^{d+1}[G, U(1)]$, with twisted coefficient if G contains time reversal) in Eq. (2.12) becomes trivial if the holonomy of A^G around time cycle is quenched, i.e. $\int_\tau A^G = 0$. For example, the Levin-Gu state[109] has partition function $S = \pi \int a \cup a \cup a$ ($a \in H^1(X, \mathbb{Z}_2)$ being the background $\mathbb{Z}_2$ gauge field), and is trivial if a along the time direction is set to zero. This confirms our physical expectation based on the domain wall proliferation picture at the begining of Sec. 2.3.

In contrast, the effective actions of elements in Eq. (2.12) with $p > 0$ remain non-trivial. The physical picture is precisely the decorated domain walls discussed at the beginning of Sec. (2.3). We therefore conclude

Theorem 1. *Bosonic SPT phases with symmetry $\mathcal{G} = K \times G$ (K being exact and G being average) described within group cohomology are classified by*

$$\sum_{p=1}^{d+1} H^{d+1-p}(G, H^p(K, U(1))). \tag{2.15}$$

Namely, only mixed topological response between G and K (or pure response for K alone) remain nontrivial as G becomes average symmetry.

Going beyond group-cohomology classification, at least for bosonic systems with $\mathcal{G} = K \times G$, is not too complicated. The only new ingredient is that on the domain walls we can also decorate nontrivial invertible topological phases, resulting in mixed "gauge-gravity" topological response[169] – essentially the cocycles in Eq. (2.14) can also involve characteristic classes of the spacetime itself. Such response will remain nontrivial as G becomes average symmetry. For example, decorating the chiral E_8 state[95] on the average time-reversal domain walls results in the so-called $efmf$ state[163, 166, 20] in $(3 + 1)d$ protected by the average time-reversal symmetry. So we conclude that as G becomes average symmetry, a nontrivial $K \times G$ boson SPT in the clean limit becomes trivial iff the SPT is characterized by a pure G-gauge response (no K gauge field or gravity involved).

In Table 2.1 we list the classification of bosonic SPT phases for some simple symmetry classes, in space dimensions $1, 2, 3$, including states beyond group-cohomology.

So far we have analyzed clean SPT phases and showed many of those remain nontrivial as G becomes average symmetry. From a different perspective, however, in our analysis we have exhausted all the possible ways to decorate the domains walls. Therefore what we obtained is also a complete classification of average SPT phases, at least within the decorated domain wall picture. We note that, once we go beyond the simple case of $\mathcal{G} = K \times G$, the completeness of this classification is no longer guaranteed, and we shall explore this extremely intriguing possibility in future study.

2.3.3 Application: crystalline SPT

For the purpose of classifying SPT phases, crystalline symmetries can be treated with internal symmetries on the same footing. This fact, known as the "crystalline equivalence principle"[156], allows us to apply results in this section to crystalline SPT phases in realistic crystals, where the lattice symmetries are only preserved on average.

Many physically relevant examples can be described as $\mathcal{G} = K \times G$, where K is an exact internal symmetry (e.g. time-reversal, spin $SO(3)$ etc.), and G represents the lattice symmetries such as translation, rotation and reflection. For boson (or spin) systems, Eq. (2.15) then gives the group-cohomology classifications. States beyond group-cohomology are classified similarly, with nontrivial invertible states decorated on domain walls.

We can also give a simple example of crystalline SPT phase that is nontrivial in the clean limit, but becomes trivial once the crystal symmetry becomes average symmetry: consider a $(2+1)d$ SPT state with C_2-rotation (inversion) symmetry. The only nontrivial state, which is the crystalline counterpart of the Levin-Gu state[109], can be constructed by putting a nontrivial C_2 charge at the C_2 rotation center. When the C_2 symmetry becomes average, the notion of "nontrivial C_2 charge" no longer makes sense, therefore the state becomes trivial.

It is illuminating to compare the decorated defect pictures in three differnt types of SPTs:

- In the standard internal symmetry SPTs, the defects condense into quantum superpositions. In other words, the defects proliferate quantum mechanically.
- In crystalline SPTs, the crystalline defects, such as crystalline unit cells, rotation axes and reflection planes, are static[153, 80, 154, 46, 183].
- In average SPTs, the average symmetry defects are static in each disorder realization, but they proliferate probabilistically in the ensemble of states.

In this sense, the average SPTs are somewhat in between internal and crystalline SPTs. As we have discussed in this Section, although subtle distinctions between average and standard SPTs do exist, the overall pictures are quite similar in terms of decorated and proliferated defects (domain walls).

2.3.4 Brief comments on general cases

If the exact and average symmetries form nontrivial group extensions Eq. (2.3), then we do not have Künneth formula and the decorated domain wall construction will in general become more complicated.

Let us first review the idea of decorated domain walls in clean systems in the general cases (with possibly nontrivial group extensions). In D-spatial dimensions, the construction starts with a phase in which the G symmetry is broken spontaneously. Such a phase admits domain wall excitations, such that a domain wall labeled by an element $g \in G$ interpolates between two symmetry breaking patterns related by a g action. A G-symmetric state can be obtained by quantum disordering the symmetry breaking phase, i.e. condensing G-domain walls. It is known that the domain wall condensation may give rise to a non-trivial $\mathcal{G}$-SPT phase, if one decorates a G-defect in the symmetry breaking phase, i.e. a domain wall or a (multi-)domain wall junction, of codimension p with a $(D-p)$-dimensional SPT phase protected by the unbroken K symmetry [34]. Crucially, in order for the condensation of G-defects to be SRE, the following consistency conditions must be satisfied:

1. G-defects of each codimension should be free of K-anomaly. Namely, the defects can be gapped without breaking K;

2. K is preserved during a continuous deformation of the G-defect network;

3. There is no Berry phase accumulated after a closed path of continuous deformation.

Physically, the third condition is required since the many-body wavefunction is single-valued; the G-domain walls can be condensed without breaking K once the second consistency condition is respected; and the first condition guarantees the resulting state to be gapped with a unique ground-state. The wave-function of the gapped $\mathcal{G}$ SPT produced is a superposition of all domain wall patterns. These consistency conditions may be formulated mathematically by the Atiyah-Hirzebruch spectral sequence (AHSS). We refer the reader to [172, 60] for details. In the decorated domain wall scheme the protected surface states appear naturally: topological defects that end at the surface carry the non-trivial boundary modes of the lower dimensional SPT phases protected by the symmetry K.

Now we make G an average symmetry and decorate nontrivial invertible states on G domain walls. The first two conditions above should still be satisfied, since we are interested in SRE ensembles (Def. 1). The third condition, however, does not seem to be necessary, since the domain walls no longer form coherent superpositions. This leaves the possibility of *intrinsically disordered* average SPTs that have no counter parts in clean systems. This intriguing possibility will be reported in the next chapter.

2.4 Average anomalies and boundary properties

For ordinary SPT, it is well known that a nontrivial bulk leads to nontrivial boundaries. Specifically, the boundary theory will have t'Hooft anomaly that matches the bulk topological response. The t'Hooft anomaly imposes powerful constraints on the IR boundary dynamics. For example, the anomalous boundary cannot be symmetrically gapped with a unique ground state. A natural question is: how does a nontrivial bulk average SPT phase constrain its boundary dynamics? Or equivalently, what are the consequences of an "average anomaly"?

As we will see below, the answer to the above question depend on the dimensions of the decorated states on the proliferated domain walls. There are two different categories

that we shall discuss separately.

2.4.1 The trivial case: $(0+1)d$ decoration

Let us illustrate the physics with a simple example. We start from the $(1+1)d$ cluster model [155, 152]:

$$H_{\text{cluster}} = -\sum_n Z_{n-1} X_n Z_{n+1}, \tag{2.16}$$

in which X and Z are Pauli matrices. The cluster chain is in an SPT phase protected by a $\mathbb{Z}_2 \times \mathbb{Z}_2$ symmetry, which is generated by

$$K = \prod_n X_{2n+1}, \quad G = \prod_n X_{2n}. \tag{2.17}$$

We then add to the Hamiltonian in Eq. (2.16) disorder that violates one of the $\mathbb{Z}_2$ symmetries, say G, but restores it on average. For example, we add the following term

$$H_{\text{dis}} = -\sum_n h_{2n} Z_{2n}, \tag{2.18}$$

where h_{2n}'s are onsite potentials distributed uniformly in $[-\delta, \delta]$. The disorder Hamiltonian is symmetric under K, while respects G only on average.

The cluster chain Eq. (2.16) can be interpreted as decorating a nontrivial K charge at each G domain wall, and then condense the domain walls to get a $\mathbb{Z}_2 \times \mathbb{Z}_2$ symmetric topological phase. Once the random field is turned on, the G domain walls no longer condense as the G symmetry is explicitly broken for each disorder realization. However, for each realization, there will in general be many G domain walls, and each domain wall still traps a nontrivial K charge. The resulting state is therefore a nontrivial $\mathbb{Z}_2 \times \mathbb{Z}_2^{(ave)}$ SPT.

We can in fact push our model to strong disorder regime, and obtain a much simpler effective model:

$$H = -\sum_n \left(Z_{2n} X_{2n+1} Z_{2n+2} + h_{2n} Z_{2n} \right), \tag{2.19}$$

where $h_{2n} \in \{\pm 1\}$ are independent binary random variables defined on each even-integer site. The ground state of each individual Hamiltonian is simply an un-entangled product state, with each even site in $|Z_{2n} = h_{2n}\rangle$ and odd site in $|X_{2n+1} = h_{2n}h_{2n+2}\rangle$. This ensemble has the same domain wall decoration pattern as the previous model (as can be checked explicitly using Eq. (2.5)), and is therefore an equally valide (but much simpler) representation of the $\mathbb{Z}_2 \times \mathbb{Z}_2^{(ave)}$ SPT.

The fact that each disorder realization simply gives an un-entangled product state is true even when the system has boundaries. This immediately means that our "average cluster chain" does not have nontrivial boundary state – unlike the clean cluster model which has a robust ground state degeneracy once put on an open chain. This can also be understood directly from the edge state: each end of the clean cluster chain forms a two-dimensional projective representation of $\mathbb{Z}_2 \times \mathbb{Z}_2$, in which the generators of G and K act as anti-commuting Pauli matrices σ_x and σ_z, respectively. Now adding, even only on the boundary, a random G-breaking field $h\sigma_z$ will lift the edge degeneracy completely.

We have demonstrated that the $\mathbb{Z}_2 \times \mathbb{Z}_2^{(ave)}$ cluster chain does not have nontrivial boundary dynamics. The boundary, however, does have a notable feature: the K-charge is fixed by $\mathrm{sgn}(h)$ which fluctuates from sample to sample. This means that different samples will not be symmetrically and adiabatically connected to each other, violating one of the key assumptions of our SRE ensemble (Def. 1). So our SPT is similar to the standard SPTs, in the sence that when the system has boundaries the state cannot stay SRE – although in the above example it violates the SRE condition in a rather trivial way.

It is straightforward to generalize the above observations to all the average SPT states, in any dimensions, in which only $(0+1)d$ states are decorated on average-symmetry domain walls. Such states can be continuously deformed to a limit where each disorder realizations simply gives a product state, without any interesting boundary dynamics. This aspect is in fact familiar in crystalline SPT phases[80, 58]: if we decorate $(0+1)d$ states (for example, some integer $U(1)$ charges) on crystalline defects (such as in each unit cell of translation symmetries), we obtain crystalline SPT phases without nontrivial boundary dynamics – instead we obtain a variety of atomic-like insulators that are not symmetrically and adiabatically connected to each other.

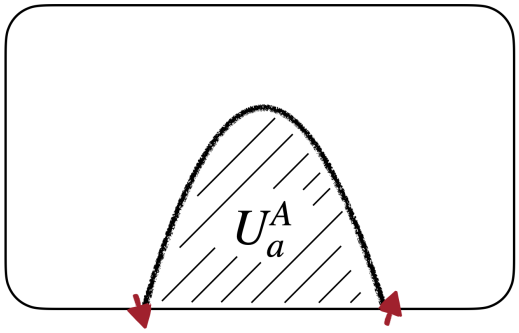

Figure 2.1: The decorated domain wall picture in the presence of a physical edge.

2.4.2 Nontrivial cases: higher-dimensional decoration

We now move on to the much more interesting cases with higher dimensional domain wall decorations. We shall employ a modified version of flux-insertion argument commonly used in the study of topological phases. Let us again illustrate with a simple example.

Consider a $(2+1)d$ boson SPT, with the exact symmetry$K = SO(3)$, average symmetry $G = \mathbb{Z}_2$ and full symmetry $\mathcal{G} = SO(3) \times \mathbb{Z}_2$. The only non-trivial element in $H^1[G, H^2(K, U(1))]$ has a topological action

$$S_{\text{top}} = \pi \int_X a \cup w_2^{SO(3)}, \tag{2.20}$$

where a is the background $\mathbb{Z}_2$ field and $w_2^{SO(3)}$ is the Second Stiefel-Whitney class of the $SO(3)$ probe field. This state has a simple physical picture in terms of decorated domain walls: on each $\mathbb{Z}_2$ domain wall there is a Haldane chain protected by the $SO(3)$ symmetry.

Let us now put the system on a space manifold with boundary, and ask how likely it is for the ground state $|\Psi\rangle$, for one realization of the disorder potential v, to be short-range entangled. We argue below that such "uninteresting" ground state must be very rare as the system size becomes large. The trick is to use the partial symmetry transform to create domain walls, similar to the argument used in Sec. 2.3, but now with a spacial boundary.

Let us start by assuming that $|\Psi\rangle$ (under a particular $\mathbb{Z}_2$-breaking disorder realization v) is short range entangled, with exponentially decaying connected correlation functions

and a nonzero energy gap. Now take a large enough sub-region A that includes a segment on the physical edge (Fig. 2.1), and flip all the random $\mathbb{Z}_2$-breaking fields v inside A, so that we are now considering a different disorder realization with

$$\tilde{v}(x \in A) = -v(x \in A), \;\; \tilde{v}(x \in \bar{A}) = v(x \in \bar{A}). \tag{2.21}$$

We denote the ground state under $\tilde{v}$ as $|\tilde{\Psi}\rangle$. Similar to the bulk argument (Eq. (2.5)), we expect that

$$U_a^A |\Psi\rangle = V_a^{\partial A} |\tilde{\Psi}\rangle, \tag{2.22}$$

with $V_a^{\partial A}$ creating an $SO(3)$-protected Haldane chain on domain wall ∂A (not including the segment on the physical edge). But contrary to the bulk argument in Sec. 2.3, the domain wall ∂A itself has boundaries – it terminates on the physical edge at two points. If $|\tilde{\Psi}\rangle$ is also short-range entangled (with correlation length much shorter than the edge segment), then $V_a^{\partial A}$ will create a pair of half-integer spins at the two ends of ∂A. Since we assume $SO(3)$ to be exactly preserved, the two spins should be locked into a singlet, which leads to a nontrivial correlation at large distance – the state effectively becomes long-range entangled. But this should not happen, as the left hand side of Eq. (2.22) is clearly short-range entangled: it is just a depth-1 unitary, U_a^A, acting on a short-range entangled state $|\Psi\rangle$. Therefore the assumption that $|\tilde{\Psi}\rangle$ is short-range entangled must be wrong. To make Eq. (2.22) valid, $|\tilde{\Psi}\rangle$ must already have a singlet pair distributed at the two ends of ∂A, so that acting on it with the Haldane chain creation operator $V_a^{\partial A}$ removes the singlet pair and recovers a short-range correlated state.

Once we understand the long-range correlated (or entangled) nature of $|\tilde{\Psi}\rangle$, it is obvious that such states can be created in many other ways: we can change the region A so that ∂A end at different point on the physical edge, we can also have multiple such regions that lead to many long-range singlets on the edge. Crucially, all such states appear with same probability as $|\Psi\rangle$, since, by definition of the average $\mathbb{Z}_2$ symmetry, flipping the sign of the random potential v in a region larger than correlation length should not change its realization probability. Therefore as the system size goes to infinity, there are infinitely many ways to create long-range entanglement out of a short-range entangled state, with essentially equal probability. This in turn means that a short-range entangled state $|\Psi\rangle$ can appear at most with a vanishing probability.

The above argument generalizes to other average SPT phases, as long as the nontrivial invertible states being decorated on the domain walls (defects) are higher than $(0+1)d$. In other words,

Theorem 2. *An average SPT with decoration dimension $p > (0+1)$ will have long-range entangled boundary state with probability approaching 1 in the thermodynamic limit.*

In Table 2.1 we list, in parenthesis, those states that do have long-range entangled boundary states (with probability approaching unity).

2.4.3 Application: Lieb-Schultz-Mattis constraints with average lattice symmetries

Readers familiar with random spin chains will recognize the long-range entangled state constructed in Sec. 2.4.2 as essentially the random singlet state[117, 41, 51]. Indeed, without any change in the argument, we can replace the average $\mathbb{Z}_2$ symmetry in the example of Sec. 2.4.2 with a $\mathbb{Z}$ symmetry. By the spirit of "crystalline equivalence principle"[156] we can interpret this $\mathbb{Z}$ as lattice translation. The corresponding bulk system is a stack of $SO(3)$ Haldane chains with an average translation symmetry perpendicular to the chains. On the boundary we obtain a disordered spin-1/2 chain with average translation symmetry. The result of Sec. 2.4.2 then becomes a disordered version[93] of the Lieb-Schultz-Mattis (LSM) theorem[111], which states that a disordered spin-1/2 chain with average translation symmetry must stay long-range entangled with probability one. The random singlet state with arbitrarily long-ranged singlet pairs is a classic example of such states.

Using the crystalline equivalence principle[156], we can conclude that all the generalized LSM anomalies for other lattice symmetries[129, 179] (rotation, reflection etc.) still imply long-range entanglement (with probability 1) when the lattice symmetry becomes average.

Let us provide a more direct and detailed argument for the simple case of $(1+1)d$ systems with average lattice translation symmetry. Consider a spin chain with exact on-site symmetry K, with the Hilbert space for each lattice unit cell forming a projective representation $\omega_{uc} \in H^2(K, U(1))$. For concreteness we can think of $K = SO(3)$ and the system being a spin-1/2 chain, although this will not be necessary.

Now assume that for some disorder realization (with a local Hamiltonian $H = \sum_i H_i$), the ground state $|\Psi\rangle$ is short-range entangled with a finite correlation length ξ. Let us then consider a different Hamiltonian $\tilde{H} = \sum_i \tilde{H}_i$, defined with a large subregion (a long segment) A, such that

1. for i far outside A, $\tilde{H}_i = H_i$,
2. for i deep inside A, $\tilde{H}_i = H_{i-1}$,
3. for i near the boundary ∂A, $\tilde{H}_i$ can take any value in the ensemble.

Essentially we have translated the Hamiltonian inside region A by one unit cell, which is the translation analogue of the partial symmetry operation in Sec. 2.4.2. This disorder realization will have a different probability with H, but crucially the two probabilities only differ by a constant factor, depending on details at ∂A but independent of either the size or location of region A (as long as A is large enough).

Since we have assumed the original state $|\Psi\rangle$ to be short-range correlated with a clear energy gap, the change in a local Hamiltonian term (say at i) should only affect properties near i. So the new ground state $|\tilde{\Psi}\rangle$ should be identical to $|\Psi\rangle$ far out of A, and be identical to the translated version $T_x|\Psi\rangle$ deep inside A. However, these two conditions imply that at each boundary ∂A there is an extra half-integer spin (or projective representation in general). In order to form a symmetric state, these two half-integer spins have no choice but to form a singlet with each other (since regions deep inside and far outside of A are determined already). This creates a long-range correlation across the large region A.

Let us make the above argument more explicit in terms of reduced density matrices. We denote a sub-segment deep inside A as A_-, the region far outside A as $\overline{A_+}$, and the remaining two regions (the left and right boundaries) as ∂A_L and ∂A_R. We further denote $\widetilde{A_-}$ as A_- translated to the right by one unit cell, $\widetilde{\partial A_L}$ as ∂A_L plus one unit cell right to it, and $\widetilde{\partial A_R}$ as ∂A_R minus its leftmost unit cell. We now consider reduced density matrices from the state $|\Psi\rangle$ (denoted as ρ) and from the state $|\tilde{\Psi}\rangle$ (denoted as $\tilde{\rho}$. For an SRE state, at each of the four entanglement cuts (let us denote as a, b, c, d from left to right) we can extract an element of $\omega \in H^2(K, U(1))$ from the entanglement spectrum[132]

(for $K = SO(3)$ this $\mathbb{Z}_2$ number is just measuring the parity of singlet bonds across each cut). Since we have a nontrivial $\omega_{uc} \in H^2(K, SO(3))$ per unit cell, we have the relations $\omega_a - \omega_b = \omega_{uc} \times |\partial A_L|$ and $\omega_c - \omega_d = \omega_{uc} \times |\partial A_R|$. Now the SRE nature of $|\Psi\rangle$ and the relation between $\tilde{H}$ and H imply that $\rho(\overline{A_+}) = \tilde{\rho}(\overline{A_+})$ and $\rho(A_-) = \tilde{\rho}(\widetilde{A_-})$. Therefore at each of the four entanglement cuts we should have $\omega = \tilde{\omega}$ (now $\tilde{b}$ and $\tilde{c}$ are translated from b and c by one unit cell). However, this means that for the two boundary regions, $\tilde{\omega}_a - \tilde{\omega}_b = \omega_{uc} \times (|\widetilde{\partial A}_L| - 1)$ and $\tilde{\omega}_c - \tilde{\omega}_d = \omega_{uc} \times (|\widetilde{\partial A}_R| + 1)$. Therefore the two regions $\widetilde{\partial A}_L \cup \widetilde{\partial A}_R$ cannot be short-range entangled – the only way to have a symmetric state is for the two regions, separated by $\widetilde{A_-}$, to entangle with each other.

We can now make the above argument for any large region A, even multiple of them. Since the probability to create such long-range correlation does not depend on the size and location of A, we again conclude that for such systems, short-range entangled ground state must be extremely rare, with at most vanishing probability as system size $L \to \infty$.

We note that for $K = SO(3)$, a similar average LSM theorem have been shown in Ref. [93]. Our argument here is more general, although the conclusion is not as strong – for example, we make not direct statement about averaged correlation functions or energy gaps.

2.5 Fermionic examples

In this section, we discuss two particularly interesting examples of fermionic ASPT phases. They are 3D fermionic TIs in symmetry class AII and AIII. We study the former using a systematic decorated domain wall construction similar to that in Ref. [153], and the latter by examining the reduction of the clean classification. One will see the insight we obtained in Sec. 2.3 works equally well for systems with fermions and/or beyond the group cohomology classification.

2.5.1 Class AII

Let us first consider 3D TIs protected by $U(1) \rtimes \mathcal{T}$ symmetry (class AII), in which $U(1)$ is the electron charge conservation and $\mathcal{T}$ is time reversal, with $\mathcal{T}^2 = -1$ when acting on fermionic operators. Importantly, $\mathcal{T}$ preserves the $U(1)$ charge. We consider the case where $\mathcal{T}$ becomes an average symmetry, while charge conservation remains exact. As illustrated in Sec. 2.3, the ASPT phases in our symmetry setting can be constructed by decorating a $(3-p)$D fermionic $U(1)$ SPT on each codimension-p (with respect to the 3D space) $\mathcal{T}$-symmetry defect. The first two consistency conditions listed in Sec. 2.3.4 need to be satisfied. In the disorder setting, the first condition ensures each state in the mixed ensemble is $U(1)$-symmetric and SRE, while the second guarantees any pair of states can be adiabatically connected without breaking $U(1)$ – this is precisely our definition for a $U(1)$ symmetric SRE ensemble. Specifically, the construction follows the guideline below:

- One starts from the top codimension $p = 0$, and decorates $\mathcal{T}$-defects of increasing p successively;
- The quantum anomalies must cancel out on codimension p defects, given all previous decorations with codimensions $p' < p$;
- After the $p = 3$ decoration, the second consistency condition in Sec. 2.3, i.e. the constraints on continuous deformations of domain walls, must be satisfied.

In this section we present the decorated defect construction in a physical way. A rigorous AHSS calculation can be found in Appendix. A.1.

Let us start with codimension-0 defects, namely, the 3D patches in which $\mathcal{T}$ is broken by the disorder. It is known that fermionic SPT phases protected by $U(1)$ symmetry are classified by the spin^c cobordism group of a point, $\Omega^{\bullet}_{\text{spin}^c}(\text{pt})$ [91, 54, 68, 62]. In particular, there is no 3D non-trivial phase protected by $U(1)$ alone. Therefore, all 3D patches are in the trivial $U(1)$ symmetric SRE phase.

We then move on to codimension-1 $\mathcal{T}-$domain walls between the patches. Since two adjacent patches are both in the same (trivial) phase, the wall in between traps no anomalous surface mode and can thus be gapped without breaking the $U(1)$ symmetry. One now

decorates the $\mathcal{T}$-domain wall with 2D $U(1)$ SPT phases. There are two non-trivial choices: the integer quantum Hall (IQH) state and the Kitaev E_8 state [96], each of which has a $\mathbb{Z}$ classification. We label the two integers by n_I and n_E for the IQH state and the E_8 state respectively. The elementary E_8 state with $n_E = 1$ has 8 chiral bosons at the edge, which can be thought of as protected by a gravitational anomaly, whose "probe field" is the background space-time geometry.

Naively, one may expect decorating 2D layers labeled by different integers leads to different 3D SPT phases. However, this is not the case. The easiest way to see this is to consider decorating an IQH state with $n_I = 2$ on the $\mathcal{T}$-domain wall. When a domain wall is cut open at the surface of the system, a helical edge state with chiral central charge $c = 2$ appears. We can deposit $n_I = \pm 1$ IQH states on the surfaces of the domains, such that at the surface $\mathcal{T}$-domain wall boundary there arises chiral modes with $c = -2$. The two counter-propagating modes can be trivialized by turning on a coupling, resulting in a unique gapped ground-state both in the bulk and on the surface[2]. The same argument also applies to the E_8 decoration, which implies that the indices n_I and n_E are only defined modulo 2. This argument resembles the operation of adjoining layers in Ref. [153]. In summary, for $p = 1$ we have two possible decorations, each of which is labeled by $\mathbb{Z}_2$.[3] One more comment is hereafter we require any two defects that can be smoothly deformed into each other to be decorated by the same lower dimensional phase. This is due to the assumption that states in different disorder realizations should be adiabatically connected (Def. 1).

Next we proceed to codimension-2 $\mathcal{T}$-defects, i.e. the 1D intersections of $\mathcal{T}$-domain walls. We should first examine whether the possible decorations in lower codimensions lead to any quantum anomaly. A 1D domain wall intersection is shown in Fig. **??**, with an IQH/E_8 decorated on each domain wall. (Remember that the edge chirality is defined only mod 2.) The intersection has no net chirality and can thus be gapped without $U(1)$

[2]As argued in Sec. 2.4, if the surface can be made SRE in the presence of a bulk decoration with dimension $p > (0+1)$, this decoration is guaranteed to be trivial.

[3]Mathematically, each of the two decorations is described by the cohomology $H^1(\mathbb{Z}_2^{\mathcal{T}}, \mathbb{Z}^{\mathcal{T}}) = \mathbb{Z}_2$, where $\mathbb{Z}^{\mathcal{T}}$ denotes the twisted coefficient, reflecting the fact that time reversal acts non-trivially on the IQH and E_8 states.

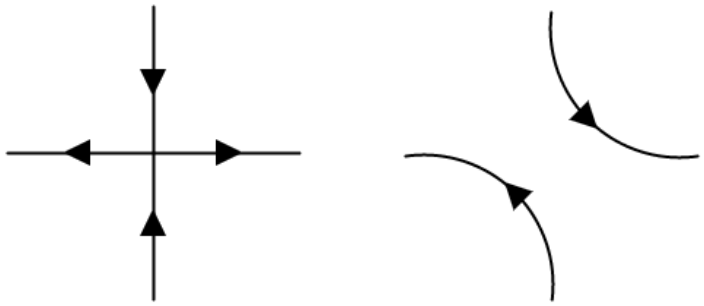

Figure 2.2: (a) Left: An intersection of two $\mathcal{T}$-domain walls, which is decorated by an IQH/E_8 state, viewed from the top. Solid lines represent an IQH/E_8 state on each half plane, with chiralities of edge modes indicated by the arrows. (b) Right: To see there is no gapless chiral mode at the intersection, note that it can be smoothly deformed into two disjoint walls.

symmetry breaking.[4] We then consider decorating a domain wall intersection with 1D fermionic SPT phases protected by the exact $U(1)$ symmetry. However, there is no non-trivial 1D SPT protected by $U(1)$ alone. Therefore we do not have any new decoration at codimension 2.

One can repeat the same procedure for codimension-3 $\mathcal{T}$-defects, namely, 0D points, each of which is an intersection of three domain walls. It is straightforward to see that a 0D defect can always be gapped without breaking the exact $U(1)$ symmetry, given all the previous decorations. The reason is simply that there is no non-trivial $U(1)$ SPT in 1D, whose anomaly inflow can protect a zero mode in 0D as a boundary state. As a result, for each *quenched* realization of disorder pattern, $\mathcal{T}$-symmetry defects in all codimensions can be trivially gapped out.

By assumption in Def. 1, we demand that the $U(1)$ charge must be conserved when the

[4] An intersection of $\mathcal{T}$-domain walls is trivial, in the sense that it can be deformed locally to the configuration in Fig. **??**. The two configurations differ at most by a 1D SRE state. This observation leads to the same result that the domain wall intersection traps no 1D gapless mode.

$\mathcal{T}$ domain walls are deformed continuously. The decorations by the IQH and the E_8 state are consistent with this constraint, as shown by an explicit spectral sequence calculation in Appendix. A.1. On the other hand, one may decorate each 0D $\mathcal{T}$-defect point using 0D $U(1)$ SPT states. These $U(1)$ SPT states have a $\mathbb{Z}$ classification, whose physical meaning is the $U(1)$ charge quantum number carried by the 0D ground-state. For symmetry class AII, a $\mathcal{T}$ transformation preserves the $U(1)$ charge. The only decoration consistent with the fusion rule of 0D $\mathcal{T}$-defects is the trivial one (Note that 0D point-like $\mathcal{T}$-defects can annihilate in pairs, thus decorating charges on them is forbidden since it breaks the $U(1)$ charge conservation during the deformation of $\mathcal{T}$ defects.), which is described by the cohomology $H^3(\mathbb{Z}_2, \mathbb{Z}) = 0$.[5] As a result, there is no new possible decoration at 0D (codimension 3).

At this point, we have exhausted all possible decorations on $\mathcal{T}-$defects of all codimensions, and have also ensured the consistency, i.e. the domain wall condensation has a unique gapped ground-state with the decorations described. We thus reach our final result: when $\mathcal{T}$ is restored on average, 3D TIs in symmetry class AII are classified by $\mathbb{Z}_2^2$, generated by placing an IQH state or an E_8 state on the $\mathcal{T}$ domain wall, respectively. Moreover, since both decorations are extended in space (2D), from Theorem 2 we conclude that all the non-trivial ASPTs in this symmetry class have long range entanglement on the surface with probability one in the thermodynamic limit.

The classification of clean $3D$ TIs in class AII is $\mathbb{Z}_2^3$[165, 167, 54]. In comparison, our $\mathbb{Z}_2^2$ classification for the ASPT in this symmetry class misses one nontrivial state. The missing state, known as $eTmT$ state, can be obtained from the domain wall condensation approach with some nontrivial phase factors in the domain wall condensate. As we explained in Sec. 2.3, such state is no longer nontrivial when the symmetry becomes average, as coherent superpositions are replaced by classical probabilities, and the notion of superposition phase factors is no longer well defined. From the topological response point of view, the topological effective action of the $eTmT$ state reads [89]

$$S_{\text{top}} = \pi \int_X w_1^4, \tag{2.23}$$

where w_1 is the first Stiefel-Whitney class ("time reversal gauge field") of the worldvolume

[5] Here the coefficient is untwisted, as $\mathcal{T}$ preserves the $U(1)$ charge in class AII.

of the $(3+1)d$ bulk. The average nature of time-reversal gives the constraint

$$\int_\tau w_1 = 0, \tag{2.24}$$

under which the TQFT in Eq. (2.23) vanishes identically.

2.5.2 Class AIII

We now study the disorder classification of 3D TIs with symmetry group $U(1) \times \mathcal{T}$ (class AIII), with $\mathcal{T}$, sometimes also called "particle-hole symmetry" as in quantum Hall context, being an average symmetry. Unlike the electric charge, now the $U(1)$ charge is odd under time reversal.

For simplicity, here we explicitly focus on the clean SPT phases, classified by $\mathbb{Z}_8 \times \mathbb{Z}_2$ [167], and ask which of these phases remain nontrivial as $\mathcal{T}$ becomes an average symmetry. The $\mathbb{Z}_2$ factor corresponds to the $e_f m_f$ state, which as we showed in Sec. 2.5.1 remains nontrivial in the presence of disorder. Similarly, the $n = 1$ state in the $\mathbb{Z}_8$ can be understood as decorating an IQHE on the $\mathcal{T}$-domain walls, which remains nontrivial as argued also in Sec. 2.5.1. The $n = 4$ state in the $\mathbb{Z}_8$ factor is known to be equivalent to the bosonic $eTmT$ state, so from our argument in Sec. 2.5.1 it should become trivial once $\mathcal{T}$ becomes average. The only nontrivial question now is what happens to the $n = 2$ state.

In the clean setup, this state can be constructed by decorating a unit $U(1)$ charge at each $0D$ intersection of three $\mathcal{T}$-domain walls[6]. This is a nontrivial decoration pattern, as the $U(1)$ charge decorated at each $0D$ $\mathcal{T}$-defect can not be removed as long as $U(1)$ remains exact.[7] So we conclude that the bulk state should remain nontrivial as $\mathcal{T}$ becomes

[6] This is only allowed by the defect fusion rule when $\mathcal{T}$ reverses the $U(1)$ charge, which is the case for class AIII.

[7] Mathematically, 3D TIs in class AIII is classified by the cobordism group $\Omega^4_{\text{pin}^c}(\text{pt}) = \mathbb{Z}_8 \times \mathbb{Z}_2$, which is an iterated extension of

$$H^1(\mathbb{Z}_2^{\mathcal{T}}, \mathbb{Z}^{\mathcal{T}} \oplus \mathbb{Z}^{\mathcal{T}}) = \mathbb{Z}_2 \times \mathbb{Z}_2 \tag{2.25}$$

$$\text{by } H^3(\mathbb{Z}_2^{\mathcal{T}}, \mathbb{Z}^{\mathcal{T}}) = \mathbb{Z}_2 \tag{2.26}$$

$$\text{by } H^5(\mathbb{Z}_2^{\mathcal{T}}, \mathbb{Z}^{\mathcal{T}}) = \mathbb{Z}_2. \tag{2.27}$$

average symmetry. However, since the $U(1)$ SPT phase decorated on the $\mathcal{T}$ defect is in $0D$ (a charge), there is no protected surface state for the $n = 2$ state based on the discussion in Sec. 2.4.1.

To summarize, the final classification for 3D TIs in class AIII with average time reversal symmetry is $\mathbb{Z}_4 \times \mathbb{Z}_2$, in which the $n = 2$ state in the $\mathbb{Z}_4$ factor has no symmetry protected long range entanglement on the surface.

We make a comment in connection to the (disordered) integer quantum Hall plateau transition. The average particle-hole symmetry, relating filled and empty Landau levels, emerges naturally at the plateau transition. The resulting $U(1) \times \mathcal{T}^{(ave)}$ has the same anomaly as the $n = 1$ state in the $\mathbb{Z}_8$ factor (in clean limit). Our result shows that the plateau transition in two-layer systems ($n = 2$ in $\mathbb{Z}_8$), even though being technically "anomalous", is not protected to be long-range entangled. This is consistent, in a nontrivial manner, with the numerical fact that such transition can indeed be Anderson localized.

2.6 Generalized quantum disorder: a quantum channel approach

So far we have treated disorder as purely classical degrees of freedom. However, real disorders, such as impurities in solids, are quantum mechanical, and in principle can develop interesting quantum entanglement within themselves (even though these may not be energetically favorable in typical conditions). In this section, we generalize our considerations to disorders that can develop invertible quantum many-body entanglements. This is a minimal quantum mechanical generalization of disorder, as the disorder potential still remain short-range correlated. We dub such disorders **invertible quantum disorders**. The observables of our interest, however, will still only live in the "dynamical" Hilbert space that does not involve the disorder degrees of freedom. In other words, the disorders are traced out, leaving behind a mixed state. This motivates us, in this section, to develop an

The physical meaning is that $n = 2$ mod 4 elements in the $\mathbb{Z}_8$ factor have a $U(1)$ charge decorated on each codimension 3 ($0D$) time reversal defect.

SPT theory for such mixed state based purely on the density matrix $\rho = \sum_I P_I |\Psi_I\rangle\langle\Psi_I|$ (I labeling each "disorder realization" in the generalized sense), without referring to any parent Hamiltonian. For this purpose, we will first need to modify some notions in Sec. 2.2, including SRE ensembles, exact and average symmetries, so that these notions are defined purely in terms of the density matrix ρ.

2.6.1 Symmetries and short-range entanglement

As mentioned in the Introduction, in clean systems an SPT has a symmetric SRE ground-state, yet which can not be deformed to a trivial product state using a finite depth quantum circuit if certain symmetries are imposed. To be clear on what states one should consider in the presence of invertible disorder, we need a mixed state generalization of SRE state and the symmetry conditions to which it is subject.

Let us consider a discrete lattice Λ in d dimensional space. The total Hilbert space $\mathcal{H}$ is a tensor product of local Hilbert spaces placed at each lattice site, $\mathcal{H} = \otimes_{i\in\Lambda}\mathcal{H}_i$. One can define the notion of SRE mixed state, purely based on the density matrix, following Hastings [77]:

Definition 3. *Let ρ be the density operator of a mixed state, acting on the Hilbert space $\mathcal{H}$. ρ is SRE if it has a SRE purification. Specifically, there exist the following:*

- *An enlarged Hilbert space $\mathcal{H}' = \mathcal{H}\otimes\mathcal{D}$, constructed by tensoring in additional degrees of freedom on each site;*
- *A SRE pure state $|\psi\rangle$ defined in the Hilbert space $\mathcal{H}'$, such that*

$$||\rho - \mathrm{tr}_{\mathcal{D}}(|\psi\rangle\langle\psi|)||_1 < \epsilon, \tag{2.28}$$

with vanishing ϵ in the thermodynamic limit (the system size $L \to \infty$). Here the $||...||_1$ denotes the trace norm, which for a Hermitian operator is the sum of the absolute values of its eigenvalues.

Physically, an SRE mixed state is one that can be obtained from an SRE pure state by tracing out ancillas defined locally on each site. In disorder systems, it is instructive

to think of the ancillary space $\mathcal{D}$ as describing the disorder and the partial trace of $\mathcal{D}$ as encoding how the system of interest (in the Hilbert space $\mathcal{H}$) is affected by the interaction with disorder. For this Section, we will focus on disorder ensembles that are SRE in the sense of Definition. 3. We should emphasize that such purification is in general not unique, and we will not focus on properties that are sensitive to details of the SRE purification – its mere existence is enough for our purpose.

Analogous to the clean case, the density operator ρ and quantum circuits implemented on ρ are subject to some symmetry conditions. For a moment, let us focus on onsite *unitary* symmetries. As before, we consider two distinct types of symmetries in this Chapter. The first is the exact symmetry, intuitively, the symmetry respected by all possible realizations of disorder. We denote the exact symmetry group by K. For each element $k \in K$, there is a corresponding unitary operator $U(k)$ acting on $\mathcal{H}$, which forms a linear representation of K:

$$U(k) = \otimes_{i\in\Lambda} u_i(k), \tag{2.29}$$

where $u_i(k)$ is the (linear) representation of K on a single site $i \in \Lambda$. We generalize the concept of symmetric quantum state to mixed ensembles as following.

Definition 4. *An SRE mixed state ρ has an exact unitary symmetry K, if there exist*

- *an enlarged Hilbert space $\mathcal{H}'$ with symmetry action*

$$\tilde{S}(k) = U(k) \otimes \mathbf{1}^{\mathcal{D}}; \tag{2.30}$$

- *a SRE purification $|\psi\rangle$ of ρ, defined in the enlarged space $\mathcal{H}'$, such that $|\psi\rangle$ is an eigenstate of $S(k)$ for each $k \in K$.*

Note that the ancillary Hilbert space $\mathcal{D}$ is in a trivial representation of K. It is not difficult to show that, if an SRE ρ has an exact symmetry K, it can be decomposed into an incoherent sum of pure states, which are all eigenstates of $U(k)$ with the *same* eigenvalue.

We now define average symmetry G for our mixed state. The hallmark of an average symmetry is that disorders also transform nontrivially. This motivates the following definition:

Definition 5. *An SRE mixed state described by a density operator ρ has an average unitary symmetry G if*

- *there exists a SRE purification $|\psi\rangle$ of ρ, defined in an enlarged space $\mathcal{H}'$ with symmetry action*
$$\tilde{S}(g) = U(g) \otimes U(g)^{\mathcal{D}}, \tag{2.31}$$
such that $|\psi\rangle$ is an eigenstate of $S(g)$ for each element g in group G.

We emphasize that the ancillary space $\mathcal{D}$ is in a *non-trivial* representation of G. With this definition, a density matrix ρ with average symmetry G commutes with the operator $U(g)$ (both viewed as operators acting on the Hilbert space of interest $\mathcal{H}$):

$$\begin{aligned} U(g)\rho =& \mathrm{tr}_{\mathcal{D}}[(U(g)^{\mathcal{D}})^\dagger U(g) \otimes U(g)^{\mathcal{D}} |\psi\rangle\langle\psi|] \\ =& \mathrm{tr}_{\mathcal{D}}[(U(g)^{\mathcal{D}})^\dagger |\psi\rangle\langle\psi| U(g) \otimes U(g)^{\mathcal{D}}] = \rho U(g), \end{aligned} \tag{2.32}$$

which is consistent with our expectation for a "statistical symmetry" that is respected on average. A key difference from an exact symmetry is that, when we simultaneously diagonalize the density operator ρ and $U(g)$, ρ is written as an incoherent sum of pure states, with in general different charges under G.

We are now ready to discuss *relations* between SRE ensembles. In the standard theory of SPT, quantum states are divided into equivalence classes, where two states are in the same phase iff they can be connected by a symmetric finite-depth local unitary. Naturally, for mixed ensembles, the state equivalence relation can be defined using "symmetric finite-depth" quantum channels[42]. In general, a quantum channel, which is a completely positive trace-preserving map between density operators, can be realized by a unitary acting on an extended system [133]. We therefore define symmetric finite-depth local quantum channels as following.

Definition 6. *A quantum channel $\mathcal{E}$ on a system with Hilbert space $\mathcal{H}$ is a symmetric finite-depth local quantum channel if it has a purification to a unitary W on a space $\mathcal{H}'' = \mathcal{H} \otimes \mathcal{A}$, such that for some ancilla state $|a\rangle \in \mathcal{A}$,*

$$\mathcal{E}(\rho) = \mathrm{tr}_{\mathcal{A}}[W(\rho \otimes |a\rangle\langle a|)W^\dagger]. \tag{2.33}$$

Specifically, we have

- *The ancillary space $\mathcal{A}$, which is a tensor product of local degrees of freedom at each site, should* not *be confused with the space $\mathcal{D}$ that is used to purify the density operator ρ. However, $\mathcal{A}$ carries the* same *symmetry representation as the disorder (and the space $\mathcal{D}$);*

- *W is a finite-depth local unitary on $\mathcal{H}''$;*

- *W is composed of gates that commute with $S(k) = U(k) \otimes \mathbf{1}^{\mathcal{A}}$ and $S(g) = U(g) \otimes U(g)^{\mathcal{A}}$, but do not commute with $U(g)$ that acts on $\mathcal{H}$ alone;*

- *The ancilla state $|a\rangle$ is a product state symmetric under $U(g)^{\mathcal{A}}$.*

One can easily check that a symmetric quantum channel preserves exact and average unitary symmetries of an ensemble. Physically, this means that when we apply the quantum channel, the mixed ensemble does not exchange K charge with the ancillas in $\mathcal{A}$. On the other hand, the total G charge of $\mathcal{H}$ and $\mathcal{A}$ is conserved, though there can be charge exchange between them.

We now comment on time reversal symmetry $\mathcal{T}$. As time reversal is anti-unitary, there is no way for the ancillary Hilbert space $\mathcal{D}$ to transform trivially like Eq. (2.30). Meanwhile, one cannot tell whether a mixed state is an exact or average eigenstate by the $\mathcal{T}$-"charges" when written as an incoherent sum, since time-reversal eigenvalue is anyway a basis-dependent quantity. At best we can define a mixed state ρ to be time-reversal invariant when

$$\mathcal{T}\rho\mathcal{T}^{-1} = \rho. \tag{2.34}$$

An equivalent statement is that ρ has a purification $|\psi\rangle$ defined in an enlarged Hilbert space $\mathcal{H}'$, such that $|\psi\rangle$ is an eigenstate of time reversal symmetry $\mathcal{T}$. We therefore conclude that, with quantum disorders, *time-reversal symmetry always behaves as an average symmetry.*

After introducing the mixed state generalization of SRE states and the definition of symmetric quantum channels, we are now ready to define the concept of average SPT in terms of the density operator ρ.

2.6.2 Average symmetry-protected topological phases

We now propose the following channel definition of Average Symmetry-Protected Topological phases (ASPT) in the precense of invertible quantum disorders.

Definition 7. *Consider two SRE ensembles ρ_1 and ρ_2, with exact symmetry K and average symmetry G.*

- *ρ_1 and ρ_2 are in the same ASPT phase if there exist two symmetric finite-depth local quantum channels $\mathcal{E}$ and $\mathcal{E}'$, such that both $||\mathcal{E}(\rho_1) - \rho_2||_1$ and $||\mathcal{E}'(\rho_2) - \rho_1||_1$ vanish in the thermodynamic limit;*

- *In particular, a symmetric SRE ρ is a trivial ASPT if it is two-way connectable to a product state. Namely, there exist two symmetric finite-depth local quantum channels $\mathcal{E}$ and $\mathcal{E}'$, such that*

$$\begin{aligned} \lim_{L\to\infty} ||\rho - \mathcal{E}(\rho_{cl})||_1 \to 0, \\ \lim_{L\to\infty} ||\rho_{cl} - \mathcal{E}'(\rho)||_1 \to 0. \end{aligned} \tag{2.35}$$

  Here the density operator ρ_{cl} represents a pure symmetric product state in the Hilbert space $\mathcal{H}$ and L is the linear size of the system.

Several comments follow. (1) An SPT phase in a clean setting is an eigenstate of the protecting symmetry. As an analog, an ASPT is a mixed ensemble symmetric under the pertinent exact (average) symmetries. This property is preserved by symmetry finite-depth local quantum channels. (2) Quantum channels are generically not invertible, and form a semigroup under composition. Consequently, the above definition for ASPT is an equivalence relation, according to which states are divided into equivalence classes (phases). The physical idea is that two SRE mixed states are in the same ASPT phase if we can prepare each one from the other, using a symmetric finite-depth local channel (potentially with ancillas). In particular, an SRE ensemble is trivial when it can be prepared in this way starting from a trivial product state. (3) When constructing the symmetric finite-depth local channel, the maximal width of the gates is bounded by some constant. The depth of

a channel is allowed to be PolyLog(L) to simulate an adiabatic evolution more accurately [123, 40, 69]. However, crucially, we require it to be sub-linear in the system size L.

We also note that states nontrivial under our mixed state definition are also nontrivial under the definition used in Sec. 2.2, since classical disorders form a subset of invertible quantum disorders. However, states that are nontrivial in the sense of Sec. 2.2 may not be nontrivial in our current context.

One consequence of the Def. 7 is that an SPT in clean system $\rho = |\Psi\rangle\langle\Psi|$, which is nontrivial under any symmetric finite-depth circuit, may become trivial under a symmetric finite-depth channel. As defined in Def. 6, both $\mathcal{H}$ and the ancillary space $\mathcal{A}$ transform faithfully under the average symmetry. For an arbitrary SPT state $|\psi_g\rangle$ protected solely by the average symmetry G, one can find a G-SPT $|\psi_g^{-1}\rangle^{\mathcal{A}}$ defined in $\mathcal{A}$, such that the state $|\psi_g\rangle \otimes |\psi_g^{-1}\rangle^{\mathcal{A}}$ can be prepared from a trivial product state by a finite-depth local unitary with gates that commute with $S(g) = U(g) \otimes U(g)^{\mathcal{A}}$. This statement is known as the invertibility of SPT states [99, 53]. On the other hand, starting from a G-SPT $|\psi_g\rangle$, one can always construct a symmetric finite-depth local unitary, which brings $|\psi_g\rangle\langle\psi_g| \otimes |a\rangle\langle a|$ to $\rho_{cl} \otimes |\psi_g\rangle^{\mathcal{A}}\langle\psi_g|^{\mathcal{A}}$. After tracing out $\mathcal{A}$, this implies $|\psi_g\rangle$ becomes trivial in the mixed state setting, according to the definition Eq. (2.35). This logic also applies to any nontrivial invertible phase (such as the chiral E_8 state in $(2+1)d$), as we can also bring the ancillary degrees of freedom into the appropriate inverse state. In this sense, "gravitational response" becomes a trivial concept in the mixed state setting.

2.6.3 A simple example

We now discuss an example of nontrivial average SPT phases under the definitions used in this Section. The simplest example is in fact the one discussed in Sec. 2.4.1, where one of the $\mathbb{Z}_2$ symmetries in the $\mathbb{Z}_2 \times \mathbb{Z}_2$ cluster chain becomes an average symmetry due to a random field perturbation.

One way to characterize the clean cluster model is the nonlocal string order parameter

in the ground-state [130, 132]:

$$\lim_{|n-m|\to\infty} \langle Z_{2m-1} \prod_{k=m}^{n} X_{2k} Z_{2n+1} \rangle \neq 0. \tag{2.36}$$

The string order is made out of the symmetry operator G in the middle (but acting in a finite region), multiplied by two local endpoint operators[8]. One can construct a similar string order for the symmetry K, i.e. $Z_{2m} \prod_{k=m}^{n-1} X_{2k+1} Z_{2n}$, which also has long range order in the ground-state. For later convenience, we denote a string order associated with a symmetry K by $\mathcal{S}_K$, which is constructed by the symmetry operator s^K (acting in a finite region) in the middle, multiplied by some local endpoint operators: $\mathcal{S}_K = O_K^l s^K O_K^r$.

The topological nature of the cluster SPT is encoded in the symmetry charge of the endpoint operators: in order for the string order associated with symmetry K (G) to have long ranged order, its endpoint operators must be odd under symmetry G (K). In contrast, in a trivial SPT, e.g. a paramagnetic chain $H_{\text{triv}} = -\sum_n X_n$, the endpoint operators of a string order with a nonzero ground-state expectation cannot carry any non-trivial charges. These distinct quantized charges indicate the two models must be separated by a phase transition.

We now add the random field

$$H_{\text{dis}} = -\sum_n h_{2n} Z_{2n}, \tag{2.37}$$

where h_{2n}'s are onsite potentials distributed uniformly in $[-\delta, \delta]$. The ensemble of ground states now have exact symmetry K generated by Ising spins on the odd-sites, while the Ising symmetry on the even-sites G is only an average symmetry.

One can study the behaviours of the string orders in the presence of this disorder. Since the symmetry G is broken locally by randomness in each realization of disorder, one expects the ensemble average of the string order associated with G to decay exponentially

[8]The easiest way of seeing Eq. (2.36) is by noting that it is equal to $\prod_{k=m}^{n} Z_{2k-1} X_{2k} Z_{2k+1}$, with $Z_{2k-1} X_{2k} Z_{2k+1} = 1$ in the ground-state. Away from the exactly solvable point, the long range order is no longer perfect, but the expectation value of the string order remains nonzero – it is a general feature of 1D SPT phases [131].

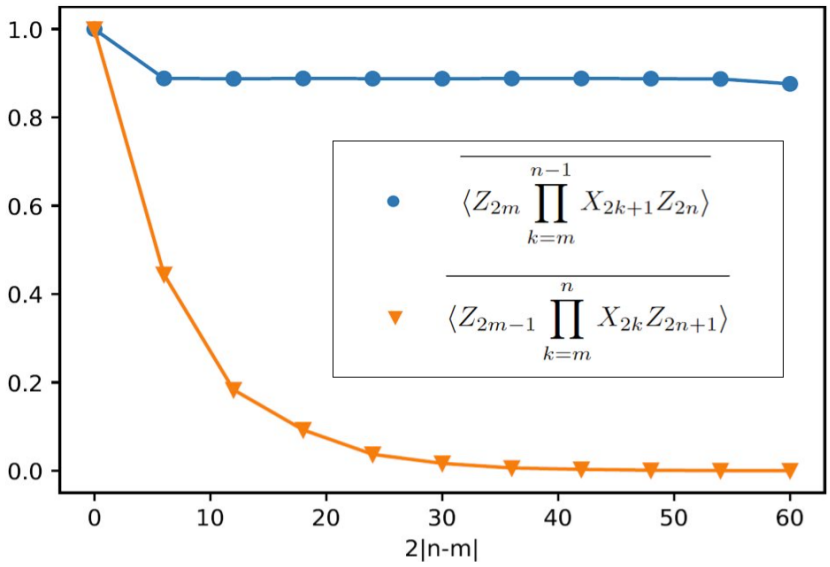

Figure 2.3: The string order parameters associated with K and G respectively, in the presence of disorder with $\delta = 0.4$. The overline denotes the ensemble average over 50 samples. The underlying clean model is in the cluster phase, perturbed away from the exactly solvable point. The numerical study is performed using the density matrix renormalization group (DMRG) technique[174, 143].

as a function of the length of the string. On the other hand, if the disorder does not close the bulk energy gap (which can be checked given the specific Hamiltonians in Eq. (2.16) and Eq. (2.18), as long as the disorder strength δ is small compared with the bulk gap), by continuity, we expect that the string order of the unbroken K with non-trivial endpoint operators remains long range ordered. These expectations are confirmed numerically, see Fig. 2.3. One can also add the disorder in Eq. (2.18) to a trivial SPT, e.g. a trivial paramagnet. In contrast, we find numerically that both string orders of K and G, with endpoint operators odd under the other symmetry, have no nonzero ensemble average.

Analogous to the clean case, one may wonder if such a nonzero string order parameter can serve as a characteristic fingerprint of a "non-trivial phase". The answer is yes, as we will show below. Specifically, we will show that if the ensemble average of the non-trivial string order parameter $\mathcal{S}_k$ (associated with an element $k \in K$) remains long-range ordered,

the mixed state ρ cannot be a trivial ASPT.

Theorem 3. *Let ρ be a symmetric SRE ensemble in which the non-trivial string order $\mathcal{S}_k$ has long-range order. The trace norm in Eq. (2.35) remains non-zero for any choice of symmetric finite-depth local channel.*

Proof: Consider a symmetric local channel $\mathcal{E}$, constructed as that in Eq. (2.33). The depth of the circuit W multiplied by the maximum range of each unitary in the circuit is bounded by some range R, which is sub-linear in L. Suppose we have a string order parameter of the exact symmetry $\mathcal{S}_k$, with two endpoint operators $O_k^l(x)$ and $O_k^r(y)$ acting in the Hilbert space $\mathcal{H}$ with non-trivial charge under $U(g)$. The length of the string $|x-y|$ is taken to be much larger than R. Under the action of the unitary circuit, $\mathcal{S}_k$ is mapped to another string operator $W^\dagger \mathcal{S}_k W$. In the region well separated from the endpoints (with a distance larger than R), the string $\mathcal{S}_k$ remains unchanged, as the circuit W commutes with the exact symmetry $S(k) = U(k) \otimes \mathbf{1}^{\mathcal{A}}$. The endpoint $O_k^l(x)$ is mapped by the circuit to a "local" operator $\tilde{O}_k^l(x) = W^\dagger O_k^l(x) W$, supported on a region within distance R of x. (The discussion for the right endpoint O_k^r is the same, hence omitted hereafter.) Therefore, $W^\dagger \mathcal{S}_k W$ is again a string order parameter associated with the group element k.

An important observation is that the new endpoint operator $\tilde{O}_k^l$ has the same charge under the average symmetry G as O_k^l, since the circuit W is symmetric:

$$\begin{aligned} & S(g)^\dagger \tilde{O}_k^l S(g) \\ =& W^\dagger (U(g) \otimes U(g)^{\mathcal{A}})^\dagger O_k^l (U(g) \otimes U(g)^{\mathcal{A}}) W \\ =& W^\dagger U(g)^\dagger O_k^l U(g) W. \end{aligned} \tag{2.38}$$

Remember that O_k^l acts only on $\mathcal{H}$, thus commutes with $U(g)^{\mathcal{A}}$. Therefore, when we compute the expectation value of $\mathcal{S}_k$ in a trivial ensemble, we have

$$\mathrm{tr}_{\mathcal{H}}[\mathcal{S}_k \mathrm{tr}_{\mathcal{A}}(W \tilde{\rho}_{cl} W^\dagger)] \sim \langle \tilde{O}_k^l(x) \rangle \langle \tilde{O}_k^r(y) \rangle = 0, \tag{2.39}$$

where $\tilde{\rho}_{cl}$ is a symmetric product state in the enlarge Hilbert space $\mathcal{H}''$, i.e. $\tilde{\rho}_{cl} = \rho_{cl} \otimes |a\rangle\langle a|$, and where $\langle ... \rangle$ denotes the expectation value with respect to this state. To get Eq. (2.39), notice that $\mathcal{S}_k = O_k^l s^k O_k^r$ and the string s^k between the endpoints acts trivially on $\tilde{\rho}_{cl}$.

We also used the cluster decomposition theorem for two well-separated endpoints. The non-trivial $S(g)$ charge of $\tilde{O}_k^{l/r}$ then forces the above expectation value to be zero. As a result, if the non-trivial string $\mathcal{S}_k$ is long range ordered in ρ, we have

$$\begin{aligned} &||\rho - \mathcal{E}(\rho_{cl})||_1 \\ &\geq |\mathrm{tr}_{\mathcal{H}}\mathcal{S}_k[\rho - \mathrm{tr}_{\mathcal{A}}(W\tilde{\rho}_{cl}W^\dagger)]|/||\mathcal{S}_k|| \sim O(1). \end{aligned} \tag{2.40}$$

This completes the proof of Theorem 3.

Theorem 3 indicates that an SPT whose protection involves the exact symmetry can not be prepared from a trivial product state. This observation will be made precise below.

2.6.4 Domain walls in an ASPT

We now show that for quantum disorders, the decorated domain wall picture again emerges naturally within the density matrix description. For simplicity, we use the cluster chain studied above as an example. In this subsection hereafter, we take $g = k = \mathbb{Z}_2$.

For symmetric SRE states, applying the symmetry in a finite but large region (much larger than the correlation length) is equivalent to applying a unitary operator just near the boundary of that region. In $(1+1)d$, the open string s^k effectively only acts near the ends,

$$s^k\rho(s^k)^\dagger = \mathrm{tr}_{\mathcal{D}}U_k^lU_k^r|\psi\rangle\langle\psi|(U_k^l)^\dagger(U_k^r)^\dagger, \tag{2.41}$$

where s^k is fractionalized on the symmetric SRE state $|\psi\rangle$, and U_k^l (U_k^r) acts non-trivially only near the left (right) edge. Notice that though the string s^k acts as an identity on the ancillary space $\mathcal{D}$, the operator $U_k^{l/r}$ might acts non-trivially on $\mathcal{D}$. The long range order of $\mathcal{S}_k = O_k^l s^k O_k^r$ implies the expectation value

$$\langle\psi|O_k^lU_k^lO_k^lU_k^r|\psi\rangle \neq 0, \tag{2.42}$$

for large separations of the two ends. By cluster decomposition theorem, one has

$$\langle\psi|O_k^lU_k^l|\psi\rangle \neq 0, \tag{2.43}$$

and similarly for the right endpoint. As $|\psi\rangle$ is symmetric, when O_k^l is charged under $\tilde{S}(g)$ (like in the case of the cluster chain), the non-vanishing expectation value requires the operator U_k^l also carries a non-trivial $\tilde{S}(g)$ charge.

Next, instead of the string of the exact symmetry (s^k), let us conjugate the density operator ρ by s^g (acts on the Hilbert space $\mathcal{H}$ only), a finite but long string of an average symmetry. Again due to the SRE nature of the purifying state, we have

$$\begin{aligned} s^g\rho(s^g)^\dagger &= \mathrm{tr}_{\mathcal{D}} s^g|\psi\rangle\langle\psi|(s^g)^\dagger \\ &= \mathrm{tr}_{\mathcal{D}} s^g \otimes s^{g\mathcal{D}}|\psi\rangle\langle\psi|(s^g)^\dagger \otimes (s^{g\mathcal{D}})^\dagger \\ &= \mathrm{tr}_{\mathcal{D}} U_g^l U_g^r|\psi\rangle\langle\psi|(U_g^l)^\dagger(U_g^r)^\dagger, \end{aligned} \tag{2.44}$$

in which we have to include a corresponding string $(s^g)^D$ acting on $\mathcal{D}$, due to the non-trivial G transformation of the ancillary space (see Eq. (2.31)). A nontrivial result of the cohomology group $H^2(\mathbb{Z}_2 \times \mathbb{Z}_2, U(1))$ [147] states that the k charge of the operator $U_g^{l/r}$ should be identical to the g charge of $U_k^{l/r}$, and is therefore nontrivial. Since the string s^g creates a g domain wall at each endpoint, we thus see that a domain wall of the average symmetry is decorated by a non-trivial charge (i.e. a 0D SPT) of the exact symmetry. This conclusion is a property of the symmetric SRE mixed ensemble ρ, which is independent of the specific choice of the purification $|\psi\rangle$.

The above discussion can be generalized to higher dimensions. For example, in $(2+1)d$, instead of string operators, we can consider membrane operators. The details, however, will be more involved and we do not attempt to provide a full exploration. Instead, we shall make the plausible conjecture that, similar to the $(1+1)d$ examples, the group-cohomology result Eq. (2.15) for decorated average domain walls captures the classification of bosonic mixed-state SPT phases (with invertible quantum disorders).

We close this section by pointing out a connection between our discussion and Ref. [42], which studied mixed state SPT in the context of open quantum systems. The definition of exact and average symmetries in this thesis mimics the definition of the strong and weak symmetry conditions for quantum channels in Ref. [42]. The two types of channels (or Lindbladians) there can thus be understood as adiabatically turning on disorder that exactly or averagely preserves the protecting symmetry of an SPT. It was observed in

Ref. [42] that a weakly symmetric channel is insufficient to preserve SPT phases. This, in our language, is the statement that an SPT protected by average symmetry alone is trivialized by disorder, presented in Sec. 2.6.2.

2.7 Discussions

Let me end this Chapter with some open directions, several of which were also mentioned in previous Sections.

1. I have focused on disordered ensembles in which any two states (with different disorder realizations) are adiabatically connected to each other (Def 1). This assumption allows us to make controlled arguments, even without assuming weak disorder strength. However, it does leave open the possibility of interesting topological phenomena in disordered ensembles not satisfying this adiabatic assumption. For example, in Sec. 2.3.1 we discussed the possibility of sample-to-sample fluctuations that are topological in nature – such phenomena will certainly require us to go beyond the adiabatic assumption. If such "topological sample fluctuation" can indeed happen, it would represent a novel topological phenomenon that intrinsically requires strong disorder.

2. It may also be possible to have "intrinsically disordered average SPT" even if the adiabatic assumption in Def. 1 is kept. For example, as we discussed in Sec. 2.3.4, among the set of consistency rules required in the standard decorated domain wall approach, there is one that is not required in the context of average SPT: the domain walls do not need to have consistent Berry phase when moved around, simply because the domain walls are anyway pinned by local disorders and do not move. This leaves open the possibility of average SPT phases not allowed in the clean limit. I will develop the theory of such phases in more detail in the next Chapter.

3. In Sec. 2.4 we showed that if the decoration dimension is greater than $(0+1)d$, then the boundary of average SPT state should almost certainly be long-range entangled, with probability approaching 1 in the thermodynamic limit. It will be desirable,

however, to obtain a more direct statement on (averaged) measurable quantities such as correlation functions or inverse energy gap. This is a natural direction for next step.

4. t'Hooft anomaly has been an extremely powerful non-perturbative tool in the study of strongly coupled gapless states of matter, including various conformal field theories that arise in exotic quantum criticality and even compressible states (some recent examples include Refs. [179, 47]). It is natural to ask whether the disordered version of these states can also be fruitfully studied using the average anomalies.

5. Since we have established the notion of average symmetry-protected topological phase, an immediate question is whether the notion of *average symmetry-enriched topological* (SET) phases can be similarly defined. In particular, are various concepts[12] in SET well defined for average symmetry? If so, what are their consequences? A theory on this topic will be presented in the next Chapter.

6. There are some other scenarios in which mixed states necessarily appear. One is in open quantum systems, where finite depth quantum channels are naturally realized by fast local Lindbladian evolutions [40, 42]. We therefore expect the results in this thesis shed light on classification and characterization of SPT phases in open systems. There are several questions remain unclear. For instance, can mixed SPT states arise as steady states of Lindbladian evolutions? Can we formulate a similar field theory, when the Hamiltonian (Lindbladian) is time-dependent? These open questions are left to future study.

Chapter 3

Topological phases with average symmetries

In this Chapter, I generalize the discussion in last Chapter to a general framework of topological phases with average symmetries. This Chapter is based on an upcoming work [116].

3.1 Average SPT: Generalities

In this section, we first give an overview of the basic notions of ASPT in two different physical scenarios, with decoherence (Sec. 3.1.1) and disorders (Sec. 3.1.2), in the simplest cases where the total symmetry $\tilde{G}$ is the direct product of the average symmetry G and the exact symmetries A. In Sec. 3.1.3 we show that for more general symmetry structures, the classification of ASPT can be described using the Atiyah-Hirzebruch spectral sequence, for both the decohered and disordered scenarios (with different input data and consistency conditions). The goal of this Section is to not only review, but significantly systematize and clarify earlier discussions in Chapter. 2.

3.1.1 Decohered ASPT

We now review the notion of a decohered ASPT state, which is relevant for open quantum systems.

Consider a mixed state ρ on a lattice system. We define ρ to be short-range entangled (SRE) [77, 115] if it can be prepared from a pure product state $|0\rangle$ via a finite-depth local quantum channel $\mathcal{E}$:

$$\rho = \mathcal{E}(|0\rangle\langle 0|). \tag{3.1}$$

Since the finite-depth channel can be viewed as a finite-depth local unitary U acting on the system together with a bath (ancilla), the short-range entangled mixed state ρ can be equivalently defined as one that can be purified to a short-range entangled state $|\Psi_0\rangle = U|0\rangle$. Another defining feature of an SRE mixed state is that all physical operators (local or extended) have only short-ranged correlation functions.

We can now enrich the structure of SRE mixed states by considering global symmetries. Let us first consider on-site unitary symmetries. A symmetry A is called *exact* if for any $a \in A$, $a\rho = e^{i\theta}\rho$. In other words, each individual state in the mixed ensemble is an eigenstate of A with the same eigenvalue. In contrast, a symmetry G is called *average* if for any $g \in G$, $g\rho g^\dagger = \rho$. This means that the density matrix ρ can be diagonalized in a G-symmetric basis, but possibly with different eigenvalues. Below we will consider the simplest situation in which the total symmetry $\tilde{G} = G \times A$, and defer the more general discussion to Sec. 3.1.3.

Recall that SPT phases of pure states are classified as equivalence classes under symmetric adiabatic evolutions or symmetric finite-depth local unitaries. For mixed states, the natural analogues of finite-depth unitaries are finite-depth quantum channels. We can always view the finite-depth local channel as a finite-depth local unitary acting on an enlarged Hilbert space (system $\mathcal{H} \oplus$ bath $\mathcal{H}_B$):

$$\mathcal{E}(\rho) = \mathrm{tr}_B \left[U(\rho \otimes |0_B\rangle\langle 0_B|)U^\dagger \right], \tag{3.2}$$

where $|0_B\rangle$ is a trivial symmetric product state in the ancillary (bath) Hilbert space. The exact and average symmetries manifest in different manners in the quantum channels

[43, 115]: for average symmetries, we demand U to be composed of symmetric local gates; for exact symmetries, we further demand that states in the bath Hilbert space $\mathcal{H}_B$ to transform trivially under the symmetries – in other words, the system and the bath do not exchange exact symmetry charges. In earlier literature on mixed states, the average and exact symmetries are also called "weak" and "strong" symmetries, respectively [4, 21, 5, 112, 43].

We then define different *decohered* ASPT phases as equivalence classes of mixed states under symmetric finite-depth local channels. Notice that the ancillary Hilbert space $\mathcal{H}_B$ will always transform nontrivially under time-reversal (because of the complex conjugation) and space symmetries. Therefore for the purpose of SPT classification, anti-unitary symmetries, and lattice symmetries should always be considered as average symmetries.

For bosonic systems, the decohered ASPT phases in D space dimensions with symmetry $\tilde{G} = A \times G$ (A being exact and G being average) are classified [115] by[1]

$$\bigoplus_{p=0}^{D} H^p(G, H^{D+1-p}(A, \mathrm{U}(1))). \tag{3.3}$$

The above formula has a decorated domain wall interpretation [34] as follows. The G-symmetric state can be obtained from a trivial spontaneous G-breaking state by proliferating domain walls (or more general defects) associated with G. On each proliferated codimension-p defect we can decorate an SPT of the exact symmetry A in $D-p$ space dimensions, labeled by an element in the group cohomology [30] $H^{D+1-p}(A, \mathrm{U}(1))$. The decoration pattern is labeled by an element in $H^p(G, H^{D+1-p}(A, \mathrm{U}(1)))$.

Recall that for pure states, with both A and G being exact symmetries, the group-cohomology classification of SPT is given by the Künneth formula

$$H^{D+1}(A \times G, \mathrm{U}(1)) = \bigoplus_{p=0}^{D+1} H^p(G, H^{D+1-p}(A, \mathrm{U}(1))). \tag{3.4}$$

The last term in the sum $H^{D+1}(G, \mathrm{U}(1))$ is absent in the mixed state classification in Eq. (3.3). This is because the term $H^{D+1}(G, \mathrm{U}(1))$, classifying SPT protected purely by the

[1] There are phases beyond group-cohomology if $D \geq 4$, but we will not discuss those.

average symmetry G, describes the nontrivial phase factors in the quantum superposition of different domain-wall configurations. In the mixed state context, the domain walls proliferate in terms of classical probability, and superposition phase factors are not well defined (equivalently, the phase factors from the bra and ket in ρ cancel out). To be more concrete, a representative wavefunction of a clean SPT phase has the following form

$$|\Psi\rangle = \sum_{\mathcal{D}} \sqrt{p_{\mathcal{D}}} e^{i\theta_{\mathcal{D}}} |\Psi_{\mathcal{D}}\rangle |a_{\mathcal{D}}\rangle \tag{3.5}$$

where $|a_{\mathcal{D}}\rangle$ in the "ancilla" space describing the quantum state of defect network of G, $|\Psi_{\mathcal{D}}\rangle$ is the decorated A-symmetric invertible phase, and $e^{i\theta_{\mathcal{D}}}$ is the phase factor that encodes the information in the $H^{D+1}(G, U(1))$ term. The clean SPT wavefunction is basically composed of the quantum superposition of different defect networks with decorated A-symmetric invertible phases. Once the G degrees of freedom are decohered, the relative phases of different quantum states with different configurations of defect networks are no longer relevant, and a mixed ensemble describes the decohered ASPT phase with the following density matrix

$$\rho = \sum_{\mathcal{D}} p_{\mathcal{D}} |\Psi_{\mathcal{D}}\rangle\langle\Psi_{\mathcal{D}}|. \tag{3.6}$$

Example: cluster chain and edge state

As an illustrative example, let us consider [115] a one-dimensional qubit chain with $\mathbb{Z}_2 \times \mathbb{Z}_2^{ave}$ symmetry, where the exact $\mathbb{Z}_2$ acts on even-sites as $\prod_{i=2n} X_i$ (i labeling the lattice sites), and the average $\mathbb{Z}_2^{ave}$ acts on odd-sites as $\prod_{i=2n+1} X_i$. ASPT phases with this symmetry are classified by $H^1(\mathbb{Z}_2, H^1(\mathbb{Z}_2, U(1))) = \mathbb{Z}_2$, with one nontrvial phase. A representative density matrix of the nontrivial phase, on a closed chain with $2N$ sites, is

$$\begin{aligned} \rho_{\text{cluster}} &= \frac{1}{2^N} \sum_{z_{2n+1}=\pm 1} |\Psi_{\{z_{2n+1}\}}\rangle\langle\Psi_{\{z_{2n+1}\}}|, \\ |\Psi_{\{z_{2n+1}\}}\rangle &= \bigotimes_{i=2n+1} |Z_i = z_i\rangle \bigotimes_{j=2n} |X_j = z_{j-1} z_{j+1}\rangle. \end{aligned} \tag{3.7}$$

Essentially, we have a classical mixture of $\mathbb{Z}_2^{ave}$ domain-wall configurations, and at each domain wall, a nontrivial exact $\mathbb{Z}_2$ charge is decorated. Alternatively, we can characterize

the nontrivial cluster chain using a string order parameter

$$\langle Z_{2n-1}X_{2n}X_{2n+2}...X_{2m}Z_{2m+1}\rangle \xrightarrow{|m-n|\gg 1} O(1). \tag{3.8}$$

It was shown in Ref. [115] that this string order parameter is robust against symmetric finite-depth channels. A similarly robust order parameter is the strange correlator defined in Refs. [182, 107].

We now show that the string order parameter Eq. (3.8) implies nontrivial edge correlations, similar to the clean SPT. Consider an open chain, say from $i = 1$ to $i = L$. Far away from the two boundaries the system should be indistinguishable from the closed cluster chain. This means that the string order parameter Eq. (3.8) should be $\sim O(1)$ as long as the two ends are not too close to the boundary. But if the system has the exact (strong) $\mathbb{Z}_2$ symmetry, $\prod_{i=2k} X_i\rho = \pm\rho$. So the string order parameter can be equivalently expressed as

$$\langle X_2...X_{2n-2}Z_{2n-1}\cdot Z_{2m+1}X_{2m+2}...X_{2\lfloor\frac{L}{2}\rfloor}\rangle \xrightarrow{|m-n|\gg 1} O(1). \tag{3.9}$$

Furthermore, average symmetry requires that

$$\langle X_2...X_{2n-2}Z_{2n-1}\rangle = \langle Z_{2m+1}X_{2m+2}...X_{2\lfloor\frac{L}{2}\rfloor}\rangle = 0. \tag{3.10}$$

Therefore a nontrivial edge correlation is enforced by the $\mathbb{Z}_2 \times \mathbb{Z}_2^{ave}$ and the bulk topology.[2]

3.1.2 Disordered ASPT

We now review the notion of disordered ASPT, which is relevant for zero-temperature systems with disordered Hamiltonians.

We consider an ensemble of disordered Hamiltonians. For concreteness, the Hamiltonian takes the form

$$H_I = H_0 + \sum_i (v_i^I \mathcal{O}_i + h.c.), \tag{3.11}$$

[2]In Ref. [115] the same state was analyzed, and it was concluded that there was no nontrivial edge correlation, and the only feature from open boundary was that the exact $\mathbb{Z}_2$ charge would fluctuate within the ensemble. What was not appreciated in Ref. [115] was that the fluctuating $\mathbb{Z}_2$ charge breaks the $\mathbb{Z}_2$ from exact to average symmetry, and since $\mathbb{Z}_2^{ave} \times \mathbb{Z}_2^{ave}$ does not have a nontrivial topological phase, the edge correlation disappears once the symmetry is lowered.

where v_i^I is a quenched disorder potential drawn from a classical probability distribution $P[v^I]$ (I labeling a particular realization and i labeling a lattice site), $\mathcal{O}$ is a local operator, and H_0 is the non-random part of the Hamiltonian. We require the disorder to be at most short-range correlated, namely $\overline{v_i^* v_j}$ (averaged over the classical probability $P[v^I]$) should decay exponentially with $|i-j|$.

We now consider the ensemble of ground states $\{|\Omega_I\rangle\}$ of the Hamiltonians $\{H_I\}$. We call the ensemble short-range entangled (SRE) if each $|\Omega_I\rangle$ is short-range entangled with a finite correlation length ξ_I that is upper-bounded in the entire ensemble[3]. Superficially, the ensemble gives a density matrix $\rho = \sum_I P_I |\Psi_I\rangle\langle\Psi_I|$ and the situation appears similar to the decohered open system. However, a crucial different for the disordered Hamiltonian system is that the states $\{|\Psi_I\rangle\}$ form a preferred basis for the ensemble. For example, two states $|\Psi_I\rangle$ and $|\Psi_{I'}\rangle$ may have equal probability of realization, which means $|\Psi_I\rangle + |\Psi_{I'}\rangle$ is an equally good eigenstate of the density matrix ρ. But in the disordered setting the latter state has no physical meaning. This makes the disordered systems physically very different from the decohered systems. However, as we will see later in Sec. 3.1.3, there is a unified mathematical framework for the classification of SPT phases for the two different settings.

Following the decohered case, we can now define exact and average symmetries. A symmetry A is exact if it commutes with H_I for any disorder realization I. An important difference with the decohered systems is that in disordered systems, time-reversal symmetry can be exact. A symmetry G is average if any element $g \in G$ takes a realization H_I to a different realization $H_{I'} = g H_I g^{-1}$ with $P[v^{I'}] = P[v^I]$. In other words, the disorder potential v may transform nontrivially under G, but the probability $P[v]$ is symmetric under G transforms. We call the ensemble of states $\{|\Psi_I\rangle\}$ symmetric if both the exact and average symmetries are not spontaneously broken. To align with the discussion for decohered systems, we also demand that the entire ensemble of states $\{|\Psi_I\rangle\}$ to transform identically under the exact symmetry A. This can be viewed as a "canonical ensemble" for a disordered system – the condition is imposed for convenience and is not strictly required

[3]It may be possible to impose only a soft bound on ξ_I to allow rare-region effects. For simplicity, we will not study such rare-region effects in this thesis.

[4].

We define two SRE ensembles (call them $\{H_I, |\Omega_I\rangle\}$ and $\{H'_I, |\Omega'\rangle\}$) to be in the same ASPT phase if $\{H_I\}$ can be continuously deformed to $\{H'_I\}$ while keeping all the conditions listed above throughout the deformation: (a) the disorder potentials remain short-range correlated; (b) the symmetries (both exact and average) are not broken explicitly or spontaneously; and (c) the ground states remain short-range entangled. We note that the conditions imposed here are slightly simpler than those originally discussed in Ref. [115] and Chapter. 2, and in Appendix B.1 we show that they are ultimately equivalent.

The disordered bosonic ASPT, as defined above, with symmetry $\tilde{G} = A \times G$ (A being exact and G being average) are classified (see Ref. [115] and Appendix B.2) by

$$\bigoplus_{p=0}^{D-1} H^p(G, h_I^{D+1-p}(A)), \tag{3.12}$$

where $h_I^q(A)$ is the classification of invertible phases in q spacetime dimension with symmetry A (for bosonic systems at $D < 3$ it is simply the group-cohomology $H^q(A, \mathrm{U}(1))$).

Similar to Eq. (3.3), the classification from Eq. (3.12) also has a decorated domain wall interpretation: on each G-domain wall we can decorate an invertible state with symmetry A. Compared to the clean case (with exact $\tilde{G}$), the $p = D$ and $p = D+1$ terms are missing. Similar to the decohered case, the $p = D + 1$ term is absent because the G-domain walls proliferate classically (probabilistically) without a superposition phase factor.

The absence of the $p = D$ term in Eq. (3.12), which describes decorating a zero-dimensional defect with an A charge, is more interesting. In the definition of SRE ensembles, we only demanded each ground state wavefunction $|\Omega_I\rangle$ to be short-range entangled, and made no requirement on the energy spectrum – we do not demand H_I to be gapped. This is appropriate for disordered systems – for example, even a fully localized Anderson insulator, with un-entangled product-state wavefunction, can be gapless. Once we

[4] This condition of fixed total charge under A is necessary for decohered mixed states, otherwise there is no difference between exact and average symmetries, since one can always simultaneously diagonalize the density matrix and the average symmetry operator. For disordered systems, however, the fixed-charge condition is optional, since there is the preferred basis given by the Hamiltonians and we are not allowed to freely re-diagonalize the density matrix.

forgo the requirement on the energy gap, zero-dimensional states with different symmetry charges can now be deformed to each other by continuously tuning the Hamiltonian (a zero-dimensional state is always SRE by definition). This means that decorating zero-dimensional defects will not produce nontrivial phases. Nevertheless, certain patterns of zero-dimensional decoration will come with nontrivial consequences, with an intriguing connection to the physics of localization – we discuss this aspect in detail in Sec. 3.1.2.

The notion of t'Hooft anomaly can also be generalized naturally to the boundary of disordered ASPT states [115]. Specifically, if the t'Hooft anomaly (labeled by the bulk ASPT phase) is nontrivial, then a symmetric boundary must be long-range entangled with probability 1 in the thermodynamic limit. More precisely, for any finite $\xi_0 > 0$, the probability of a boundary state with correlation length $\xi \leq \xi_0$ vanishes as the system size $L \to \infty$.

Interplay with localization physics

We now return to zero-dimensional decorations in the context of disordered ASPT. As discussed in Sec. 3.1.2, decorating with $(0{+}1)d$ SPT (namely charges of the exact symmetry) does not lead to nontrivial phases. This is because a $(0{+}1)d$ SPT is nontrivial only if we demand an energy gap, but in disordered systems, we do not require each individual disorder realization to be gapped – we only demand the ground state to be short-range entangled (SRE). In disordered systems, Anderson localization provides a natural mechanism to have a gapless but SRE ground state.

Let us illustrate with a familiar example. Consider a lattice-free fermion system with U(1) charge conservation and lattice translation $\mathbb{Z}^d$ symmetries, with the simplest tight-binding Hamiltonian

$$H = -t \sum_{\langle i,j \rangle} (c_j^\dagger c_i + \text{h.c.}) + \mu \sum_i c_i^\dagger c_i. \tag{3.13}$$

For $\mu > 2|t|$ or $\mu < -2|t|$, the system is an atomic insulator with U(1) charge per site $q = 0$ or $q = 1$, respectively. The system is metallic for intermediate μ, with a long-range entangled ground state. In fact, any symmetric state interpolating between

the two different atomic insulators must be long-range entangled, as guaranteed by the Lieb-Schultz-Mattis theorem.

Now we add disorders that break the exact translation symmetry to an average symmetry:

$$H_{\text{disorder}} = -\sum_j \epsilon_j c_j^\dagger c_j. \tag{3.14}$$

As is well known, for sufficiently strong disorder the metallic states (with an intermediate chemical potential μ) become Anderson localized insulators. The ground states of the Anderson insulators are SRE – they are essentially product states of fermions sitting at random locations. The probability P_i for a site i to be occupied can smoothly change from 0 to 1. This gives a smooth interpolation between the two atomic insulators with charge filling $q = 0$ and $q = 1$.

Another feature of the above localized intermediate state is that it is generally gapless, with localized excitations at arbitrarily small excitation energy in the thermodynamic limit. In order to be more precise, let us fix the total U(1) charge of the system for the entire disordered ensemble – for example at density ν we can fix $Q = \lfloor \nu L \rfloor$ where L is the system size and $\lfloor ... \rfloor$ is the integer part. Then the system must be gapless as long as the Hamiltonians are bounded, i.e. the distribution of ϵ_j is bounded (possibly with some rare tails). This is because for a large enough system, we can always find an excitation, e.g. moving a particle from an occupied site to an unoccupied site, that costs arbitrarily small energy. This forced gaplessness can be viewed as the remnant of the Lieb-Schultz-Mattis constraint for fractional charge filling.

In the above example, the lattice sites should be viewed as defects of the translation symmetries. To generalize the above observations to general ASPT with $(0+1)d$ decorations, all we have to do is to replace the lattice sites with the average G-defects, and to replace U(1) charge with general Abelian representations of the exact symmetries. The only subtlety is that we need Anderson localization for generic interacting systems – in other words, we need many-body localization (MBL). Crucially, we only need MBL for low-energy states, with vanishing energy density. Although not rigorously proven for the most general setting, it seems reasonable to assume that such low-energy MBL can be achieved in any dimension without fine-tuning [45]. With the localization assumption in

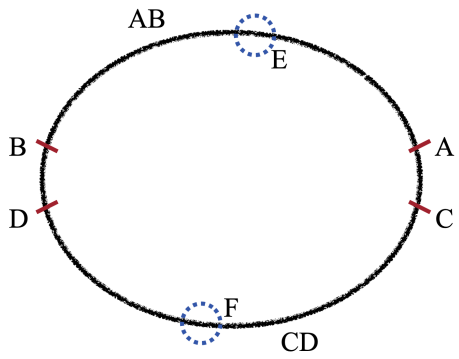

Figure 3.1: An Anderson-like insulator, when viewed as a density matrix with fixed total charge, features nontrivial long-range correlations between different subregions. This correlation forbids the density matrix to be purified to a short-range entangled state.

mind, we conclude that

> Two disordered ASPT states, with different exact symmetry charge decorations on $(0{+}1)d$ average symmetry defects, can be smoothly deformed to each other. If the disorder strength is bounded, the intermediate states must have localized excitations with excitation energy vanishing in the thermodynamic limit.

We emphasize that the story of localized states is only relevant for disordered systems, and does not affect the discussion on decohered topological phases. The reason is that even though each individual state in the ensemble of an Anderson insulator is a trivial product state, qualifying the Anderson insulator as a short-range entangled *disordered* ensemble, when viewed as a density matrix $\rho = \sum_I P_I |\Psi_I\rangle\langle\Psi_I|$ it is in fact not short-range entangled, in the sense that ρ does not have a short-range entangled purification. This can be seen as follows. Suppose ρ can be purified to an SRE state with correlation length ξ, then we consider partitioning the system as Fig. 3.1 with $|AC|, |BD| \gg \xi$. If we then project the segments AC, BD to a fixed localized product state, then the remaining two segments, AB and CD, should have no correlation. However, the exact nature of A means that the system has a fixed total A-charge Q. Since the A-charges are localized, the charge

in each segment is well defined for each eigenstate and denoted as $Q_{AB}, Q_{AC}, Q_{BD}, Q_{CD}$, respectively. Each individual charge may fluctuate within the mixed ensemble, but their sum is fixed $Q_{AB}+Q_{AC}+Q_{BD}+Q_{CD} = Q$. When we fix the charges in AC, BD, the charges in AB and CD are correlated by having a fixed sum. To make this correlation trivial, as required by the SRE assumption, Q_{AB} and Q_{CD} should not fluctuate at all if the states on AC, BD are fixed. However this is manifestly not true for an Anderson insulator – for example, starting from one localized product state, we can obtain another state by removing a charge deep inside CD (region F) and adding the charge back deep inside AB (region E), without changing anything on AC, BD. Therefore the SRE assumption must be false and Anderson insulators, when viewed as a density matrix with a fixed exact symmetry charge, should be viewed as long-range entangled. Notice that the average cluster chain in Sec. 3.1.1 avoids this contradiction, even though the exact $\mathbb{Z}_2$ charge fluctuates randomly in each segment. This is because the charge in each segment is completely determined by the product of Z operators on the segment boundary, thanks to the string order parameter Eq. (3.8). So if we fix the segment boundaries (AC and BD), the exact $\mathbb{Z}_2$ charges in AB and CD will no longer fluctuate, which makes the state compatible with the SRE condition.

There is an equivalent description: Suppose $|\psi\rangle$ is the gapped ground state with a well-defined overall charge, i.e. $|\psi\rangle$ is an eigenstate of Q. Consider an interval AB and let Q_{AB} denote the total charge in AB. One can show that

$$Q_{AB}\,|\psi\rangle \approx (K_B - K_A)\,|\psi\rangle\,, \tag{3.15}$$

where $K_{A/B}$ is an observable localized near A/B. All $\approx$ mean up to corrections exponentially small in L. By locality, K_A and K_B (almost) commute. Therefore, by measuring the two local observables K_A and K_B, we can completely fix the charge Q_{AB}. This is manifestly not true for an Anderson insulator.

Heuristically, what this means is that charge fluctuations of a subregion in an SRE (or gapped) state with a well-defined overall charge must come from entanglement between the subregion and the rest (i.e. they are very "local"), thus measured by the boundary operators. However, in an Anderson insulator, the charge of a subregion (e.g. AB) can fluctuate completely independent of the states of the other regions, so it can not be purified

into an SRE (or any gapped ground state) with a well-defined overall charge.

3.1.3 Mathematical framework: Spectral sequence

In general, for given average symmetry G and exact symmetry A, the total symmetry $\tilde{G}$ does not have to be the direct product $A \times G$. Instead, we only require A to be a normal subgroup of the full symmetry group. In the fermionic case, A contains the fermion parity $\mathbb{Z}_2^f$ as a subgroup. G and A fit into the following short exact sequence:

$$1 \to A \to \tilde{G} \to G \to 1. \tag{3.16}$$

For a $D+1$ dimensional SPT, the classification via generalized cohomology theory can be understood by decorations on G domain walls/defects. Mathematically the consistency conditions for domain wall decorations are organized into an (Atiyah-Hirzebruch) spectral sequence [172] (see Appendix B.2 for a brief review), whose E_2 page is given by

$$\bigoplus_{p+q=D+1} E_2^{p,q} = \bigoplus_{p+q=D+1} H^p(G, h^q(A)). \tag{3.17}$$

Here $h^q(A)$ is the classification of invertible phases in q spacetime dimension with symmetry A that can be decorated on G-defects. The exact form of $h^q(A)$ will depend on the physical context. In particular:

- For the standard (pure state, clean) SPT, $h^q(A)$ is the classification of all invertible phases in q spacetime dimension with symmetry A.
- For decohered ASPT, $h^q(A)$ is almost the classification of invertible phases in q spacetime dimension with symmetry A, except (1) $h^0(A) = 0$ for reasons explained in Sec. 3.1.1, and (2) $h^q(A)$ does not contain invertible phases that do not require the A symmetry at all (for example the chiral E_8 state in (2+1)d) – this is because such invertible states can be easily trivialized or prepared by a finite-depth quantum channel [115]. Hence the classification of decohered ASPT phases in bosonic systems will be reduced to the Lyndon-Hochschild-Serre (LHS) spectral sequence that replaces $h^q(A)$ by $H^q[A, U(1)]$ for $q \geq 1$.

- For disordered ASPT, $h^q(A)$ is almost the classification of invertible phases in q spacetime dimension with symmetry A, except $h^0(A) = 0$ and $h^1(A) = 0$ for reasons explained in Sec. 3.1.2.

For each decoration, we need to check the obstructions, given by the differentials:

$$d_r : E_2^{p,q} \to E_2^{p+r,q-r+1}. \tag{3.18}$$

d_r maps to a decorated domain wall configuration in $(D + 2)$ dimension. For bosonic systems with $\tilde{G} = A \times G$ these differentials automatically vanish, so we obtain Eq. (3.3) and (3.12) as the classifications. For fermion systems or boson systems with nontrivial group extension, the differentials may not vanish and represent obstructions for certain decoration patterns. The physical meanings of these differentials correspond to the three consistency conditions of constructing an SPT, as

1. $r \leq D - p$: The decorated G-defects can be gapped without breaking A-symmetry.

2. $r = D-p+1$: A-charge is preserved during a continuous deformation of the G-defect network. Since $h^1(A) = 0$ for disordered ASPT phases, this obstruction automatically vanishes for disordered ASPT.

   Physically, for clean SPTs, a nontrivial d_{D-p+1} obstruction implies that A charge will change (i.e. not be conserved) when we change the G-defect configurations through some local operation. In the disordered setting, however, we change the G-defect configurations by drawing a different disorder realization from the ensemble. Then the change of A-charge no longer require actual charge nonconservation – all we need is a localized mode, or more precisely a local conserved charge operator Q_A^{local} that changes its ground state eigenvalue as the disorder realization (which determines the G-defect configurations) changes locally. The sample-to-sample fluctuation of the local charge makes the situation similar to the localized states that interpolate between different $(0+1)d$ decorations discussed earlier in Sec. 3.1.2. Following the logic in Sec. 3.1.2, we also conclude that the localization-enabled ASPT with $(0+1)d$ decorations has to be gapless in the thermodynamic limit, as long as the disorder strength is bounded.

3. $r = D-p+2$: There is no Berry phase accumulated after a closed path of continuous F-move deformations due to the single-valued property of the SPT wavefunction. Since $h^0(A) = 0$ for both decohered and disordered ASPT, this obstruction automatically vanishes in these two contexts. Physically, the G-defects only proliferate probabilistically to form ASPT phases, so there is no need to assign consistent Berry phases.

At the level of E_2 page, ASPT contains less nontrivial phases than standard clean SPT (absence of $E_2^{p,1}$ for disordered ASPT and absence of $E_2^{p,0}$ for both disordered and decohered ASPT). However, this also means that there are fewer potential obstructions for ASPT phases since each obstruction corresponds to some nontrivial topological phase in one dimension higher. This opens the possibility of ASPT phases that are *intrinsically* disordered or decohered, in the sense that they cannot be viewed as a clean SPT perturbed by disorder or decoherence. Such "intrinsic ASPT" will be one of the main focuses of this Chapter. We dub the disordered ASPT phases enabled by vanishing d_{D-p+1} obstructions *localization-enabled* ASPT, and ASPT phases (both disordered and decohered) enabled by vanishing d_{D-p+2} obstructions *Berry-free* ASPT.

The differential (3.18) is also called the *trivialization* map for SPT phases labeled by elements in $E_2^{p+r,q-r+1}$ with decorated domain wall configurations in one higher dimension. The images of the d_r map give trivial SPT phases. The physical meaning of the trivialization map is that the images of d_r are the states with anomalous SPT states [**?**] on the boundary which is SRE, and the corresponding bulk states should be topologically trivial. We emphasize that the decoherence/disorder does not affect the trivialization of the ASPT phases: the anomalous SPT states on the boundary in the clean systems might be trivial product states with the presence of decoherence or disorder, which are also SRE and manifest the topologically trivial bulk states.

3.2 Intrinsic ASPT: examples

In this Section, we discuss the "Berry-free" and "compressible" intrinsic ASPT phases in more detail. The Berry-free intrinsic ASPT phases are enabled by the vanishing of the

Berry phase obstruction d_{D-p+2} and the compressible intrinsic ASPT phases are enabled by the vanishing of the charge-decoration obstruction d_{D-p+1}, as we discussed in Sec. 3.1.3. The Berry-free ASPT can appear in both decohered and disordered settings – the only difference is that if a phase comes from a $(0{+}1)d$ decoration it will be trivial in the disordered setting. For Berry-free ASPT states we will mostly not distinguish the two settings in this Section. The compressible ASPT can only appear in disordered settings.

3.2.1 Fixed-point model for bosonic ASPT

We will describe a class of "fixed-point" lattice models for Berry-free ASPT phases. The model is a generalization of the group-cohomology model for bosonic SPT phases [33].

Again we denote by G the average symmetry, A the exact symmetry, and the group extension $\tilde{G}$ as defined in Eq. (3.16). We denote elements of $\tilde{G}$ by $x = (g, a)$, where $g \in G$ and $a \in A$. In $(D{+}1)$-dimension, the input to the model is a (homogeneous) $(D{+}1)$-cochain $\nu(x_0, \ldots, x_{D+1})$, that satisfies the obstructed cocycle condition:

$$(d\nu)(x_0, \cdots, x_{D+2}) = O_{D+2}(g_0, \cdots, g_{D+2}). \tag{3.19}$$

Here d is the coboundary operator, g_i is the G-grading of x_i. O_{D+2} is a $(D+2)$-cocycle in $\mathcal{H}^{D+2}[G, \mathrm{U}(1)]$. To construct a clean SPT state, we will need $O_{D+2} = 1$. For the ASPT construction, this is not necessary.

We will illustrate the construction in $(2{+}1)d$ in the following, but the same construction works in any dimension. We will work with a triangular lattice. The system consists of a $\tilde{G}$ spin on each site, with an orthonormal basis labeled by group elements, i.e. $\{|x\rangle\}_{x\in\tilde{G}}$. A natural $\tilde{G}$ symmetry action is given by the left multiplication:

$$U_y |x\rangle = |yx\rangle \,, y \in \tilde{G}. \tag{3.20}$$

In addition, the lattice has to be equipped with a branching structure, which is essentially an ordering of all sites. For each triangle face Δ of the lattice, denote by i, j, k the three vertices whose ordering satisfies $i < j < k$. We also denote by $s(\Delta) = \pm 1$ the orientation, i.e. whether i, j, k is clockwise or counter-clockwise.

Firstly, we review the standard group cohomology construction when $O_4 = 1$. Define the $\tilde{G}$-invariant state on the site j:

$$|0_j^{\tilde{G}}\rangle = \frac{1}{\sqrt{|\tilde{G}|}} \sum_{x \in \tilde{G}} |x_j\rangle \,, \tag{3.21}$$

and then the trivial paramagnetic state for the whole system:

$$|\Psi_0^{\tilde{G}}\rangle = \bigotimes_j |0_j^{\tilde{G}}\rangle \,. \tag{3.22}$$

$|\Psi_0^{\tilde{G}}\rangle$ is the ground state of the following local Hamiltonian:

$$H_{\text{trivial}} = -\sum_j |0_j^{\tilde{G}}\rangle \langle 0_j^{\tilde{G}}| \,. \tag{3.23}$$

Let us now define the following finite-depth local unitary circuit

$$V = \sum_{\{x\}} \prod_{\Delta_{ijk}} \nu^{s(\Delta_{ijk})}(1, x_i, x_j, x_k) \, |\{x\}\rangle \langle\{x\}| \,. \tag{3.24}$$

V can be viewed as a composition of unitary gates each acting on a triangle. Since all the gates are diagonal in the $|\{x\}\rangle$ basis, they commute with each other and as a circuit V has depth 1. When $O_4 = 1$, one can show that the local gates do not preserve $\tilde{G}$ individually, but the unitary V as a whole does.

The SPT state is given by

$$|\Psi_{\text{SPT}}\rangle = V \, |\Psi_0^{\tilde{G}}\rangle \,. \tag{3.25}$$

The commuting-projector parent Hamiltonian for this state is

$$\begin{aligned} H = V H_{\text{trivial}} V^\dagger = -\sum_j B_j, \\ B_j = V \, |0_j^{\tilde{G}}\rangle \langle 0_j^{\tilde{G}}| \, V^\dagger. \end{aligned} \tag{3.26}$$

Here B_j is an operator that acts on the hexagon centered at j.

Now we consider what goes wrong if the cocycle ν is obstructed by a nontrivial $[O_4]$. We find that the state $|\Psi_{\text{SPT}}\rangle$ is no longer symmetric under $\tilde{G}$. More precisely, it is no longer

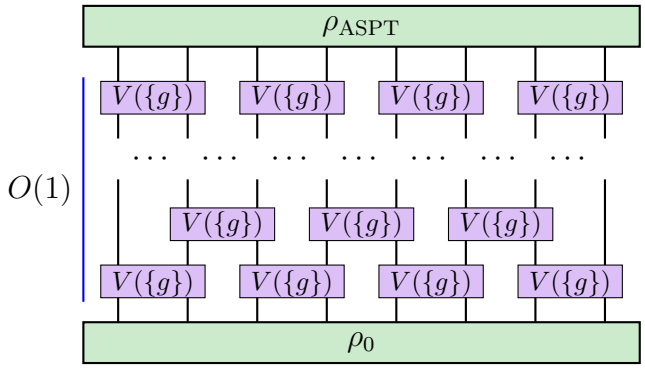

Figure 3.2: Quantum circuit as the entangler of the ASPT density matrix ρ_{ASPT}, from a trivial density matrix ρ_0. $O(1)$ depicts the finite-depth nature of $V(\{g\})$.

invariant under the symmetry transformations U_x when $x \in \tilde{G}$ has a nontrivial G-grading: $U_x |\Psi_{\text{SPT}}\rangle \neq e^{i\varphi} |\Psi_{\text{SPT}}\rangle$. However, for $a \in A$, the state is still invariant: $U_a |\Psi_{\text{SPT}}\rangle = |\Psi_{\text{SPT}}\rangle$.

Based on this observation, we now show how to construct the intrinsic ASPT phase. It is now more convenient to think of the $\tilde{G}$ spin as a G spin and an A spin, and treat the G spins as quenched disorder configurations. The configuration of G spins will be collectively denoted as $\{g\}$. In addition, for $h \in G$ under U_h the classical G spin configuration $\{g\}$ transformsd d to $\{hg\}$.

Instead of $|0^{\tilde{G}}\rangle$, we define a trivial paramagnet for the A spins:

$$|0^A\rangle = \bigotimes_j \Big(\frac{1}{\sqrt{|A|}} \sum_{a \in A} |a_j\rangle \Big), \tag{3.27}$$

and then a trivial G spin ensemble:

$$\rho_0 = \frac{1}{|G|^{N_v}} \sum_{\{g\}} |0^A\rangle\langle\otimes||\{g\}\rangle\langle,| \tag{3.28}$$

where N_v is the number of vertices of the lattice. This state can be prepared by measuring G spins in the $|0^{\tilde{G}}\rangle$ state (but no post selection). It is easy to verify that the density matrix ρ_0 does not have an exact G symmetry, but still invariant under the average G symmetry.

The follow-up finite-depth unitary circuit $V(\{g\})$ can still be defined in the same way, but now it is viewed as an operator that acts on the A spins conditioned on the G spins.

More explicitly:

$$V(\{g\}) = \sum_{\{a\}} \prod_{\Delta_{ijk}} \nu^{s(\Delta_{ijk})}(1, x_i, x_j, x_k) \left|\{a\}\right\rangle \left\langle\{a\}\right| . \tag{3.29}$$

We denote it as $V(\{g\})$ to emphasize the G spin dependence. Importantly, even though ν is not a 3-cocycle of the group $\tilde{G}$, by definition it is a 3-cocycle of A and therefore $V(\{g\})$ is a (globally) A-symmetric finite-depth circuit. On the other hand, under $h \in G$ the unitary transforms as

$$U_h V(\{g\}) U_h^\dagger = e^{i\phi(h;\{g\})} V(\{hg\}). \tag{3.30}$$

Fixing $\{g\}$, now we can define an A-SPT state:

$$\left|\Psi_{\text{ASPT}}(\{g\})\right\rangle = V(\{g\}) \left|0^A\right\rangle . \tag{3.31}$$

It then follows that

$$U_h \left|\Psi_{\text{ASPT}}(\{g\})\right\rangle = e^{i\phi(h;\{g\})} \left|\Psi_{\text{ASPT}}(\{hg\})\right\rangle . \tag{3.32}$$

Here $e^{i\phi(h;\{g\})}$ is a phase factor that can be expressed as a product over O_4, but the exact expression is not important to us – the factors from the bra and ket will cancel out in the density matrix. The parent Hamiltonian of a state $\left|\Psi(\{g\})\right\rangle$ in the ensemble is given by

$$H(\{g\}) = -V(\{g\}) \Big(\sum_j \left|0_j^A\right\rangle \left\langle 0_j^A\right| \Big) V^\dagger(\{g\}). \tag{3.33}$$

The collection of states $\left|\Psi(\{g\})\right\rangle$ for all the G spins forms a statistical ensemble. More formally, we can write it as the following density matrix:

$$\rho_{\text{ASPT}} = \sum_{\{g\}} p(\{g\}) \left|\Psi_{\text{ASPT}}(\{g\})\right\rangle \left\langle\Psi_{\text{ASPT}}(\{g\})\right| . \tag{3.34}$$

Here $p(\{g\})$ is a probability distribution of G spins. In the simplest case, we can simply set p to be a constant independent of $\{g\}$. The density matrix evidently has G average symmetry, but the A symmetry remains exact. The finite-depth quantum circuit as the entangler of an ASPT density matrix is illustrated in Fig. 3.2.

Lastly, we discuss two concrete examples. The first example is in (1+1)d, with $G = \mathbb{Z}_2, A = \mathbb{Z}_2$ and $\tilde{G} = \mathbb{Z}_4$. We will go through the construction of this example in Sec. 3.2.2.

The next example is in (2+1)d, with $G = \mathrm{SO}(5), A = \mathbb{Z}_2$ and $\tilde{G} = \mathrm{Spin}(5)$. Each state in the ensemble is a Levin-Gu SPT state [109] protected by the exact $\mathbb{Z}_2$ symmetry. To see why G must be an average symmetry, note that otherwise, we can gauge A to find a double semion topological order with four anyons $\{1, s, s', b\}$. It is enriched by the SO(5) symmetry, where b transforms as the spinor representation of SO(5) (required by the group extension). Because $b = s \times s'$, one of s or s' must also transform as a spinor representation, and we will assume it is s. Then s' transforms linearly under SO(5). In other words, we have effectively a semion topological order $\{1, s\}$ with s being a SO(5) spinor. This SET is known to have a nontrivial SO(5) 't Hooft anomaly [164]. Therefore, the original SPT state can not exist with G being an exact symmetry. However, since the only obstruction is the 't Hooft anomaly of G, once G becomes an average symmetry the obstruction no longer matters.

3.2.2 Berry-free ASPT and gapless SPT

We now discuss the relationship between the "Berry-free" intrinsic ASPT phases and the recently discussed intrinsically gapless SPT (igSPT) phases [**?**, **?**, **?**]. Firstly, let us review the physics of igSPTs in $(1+1)d$ [**?**]. They can be constructed using a "slab", where the top boundary is an "anomalous" gapped $\tilde{G}$ SPT state, obstructed only by a differential mapped into $[\omega] \in \mathcal{H}^3(G, \mathrm{U}(1))$. The bottom boundary instead has a gapless theory , e.g. a conformal field theory (CFT), where the G symmetry acts faithfully in the low-energy theory with a 't Hooft anomaly given by $[\omega^{-1}]$, and the A symmetry does not act. Together the whole slab is free of any anomaly and can be realized with a non-anomalous $\tilde{G}$ symmetry.

Starting from an igSPT state, we consider turning on a random G symmetry-breaking perturbation. Without loss of generality, we assume that the random perturbation is relevant, so it drives the gapless theory into a disordered SRE ensemble. The result is expected to be an intrinsically ASPT state. In the other direction, any symmetry-preserving clean limit of a Berry-free intrinsic ASPT state must be an igSPT state.

Let us consider an example, with $A = \mathbb{Z}_2, G = \mathbb{Z}_2$ and the extension is $\tilde{G} = \mathbb{Z}_4$. For the clean system, there is no nontrivial gapped SPT phase because $\mathcal{H}^2(\mathbb{Z}_4, \mathrm{U}(1)) = \mathbb{Z}_1$.

If we look closer, there is a nontrivial $E_2^{1,1}$ term in the LHS spectral sequence, which is however obstructed by a nontrivial d_2 differential into $\mathcal{H}^3(\mathbb{Z}_2, \mathrm{U}(1))$. The same anomaly is realized by a (1+1)d free boson CFT, and together we can construct an igSPT state. We now describe a solvable lattice model for this state. A similar model was studied in [**?**].

The Hilbert space of the model consists of Ising spins σ on the sites and τ on links. The symmetries are defined as

$$U_g = \prod_j \sigma_j^x e^{i\frac{\pi}{4}\sum_j (1-\tau^x_{j+1/2})},\ U_a = \prod_j \tau^x_{j+1/2}. \tag{3.35}$$

Here g/a is the generator of G/A. The unitaries are on-site, and satisfy $U_a^2 = 1,\ U_g^2 = U_a$. So this is a non-anomalous $\mathbb{Z}_4$ symmetry.

We define a projector:

$$P = \prod_j P_j,\ P_j = \frac{1 + \sigma_j^z \tau^x_{j+1/2} \sigma^z_{j+1}}{2}. \tag{3.36}$$

Physically, in the subspace $P = 1$ an Ising domain wall $\sigma_j^z \sigma^z_{j+1} = -1$ is decorated by a charge $\tau^x_{j+1/2} = -1$. So $P = 1$ enforces domain wall decoration corresponding to the nontrivial element in $\mathcal{H}^1(G, \mathcal{H}^1(A, \mathrm{U}(1)))$. In this subspace, U_g takes the following form:

$$U_g = \prod_j \sigma_j^x e^{i\frac{\pi}{4}\sum_j (1-\sigma_j^z\sigma^z_{j+1})}, \tag{3.37}$$

which takes the form of the anomalous $\mathbb{Z}_2$ symmetry of the Levin-Gu edge model [**?**, **?**]. It is also easy to see that U_a becomes the identity in this low-energy subspace, at least in the bulk of the spin chain. Define

$$\tilde{\sigma}_j^x = \tau^z_{j-1/2}\sigma_j^x \tau^z_{j+1/2},\ \tilde{\sigma}_j^z = \sigma_j^z. \tag{3.38}$$

$\tilde{\sigma}_j^x$ and $\tilde{\sigma}_j^z$ generate the entire algebra of operators that commute with P. They satisfy the usual commutation relations of Pauli operators.

Now we consider the following Hamiltonian:

$$H_{\mathrm{LG}} = -\sum_j \tilde{\sigma}_j^x (1 - \tilde{\sigma}^z_{j-1}\tilde{\sigma}^z_{j+1}) P. \tag{3.39}$$

Notice that since the Hamiltonian is written in terms of the $\tilde{\sigma}^{x,z}$ operator it commutes with P. In the low-energy space, Eq. (3.39) is identical to the edge Hamiltonian of the Levin-Gu model [**?**]. In addition, the Hamiltonian conserves the number of Ising domain walls, and thus also conserves the $\mathbb{Z}_4$ charge. The low-energy effective theory of this model is a $c = 1$ free boson, or a Luttinger liquid, with an anomalous U_g symmetry transformation. Thus the model realizes an igSPT phase.

To obtain an ASPT phase, we can proceed in two ways. First, we add some random Ising disorder $-\sum_j h_j \sigma_j^z$ with $h_j = \pm 1$ to break $G = \mathbb{Z}_2$ symmetry. It can be shown that this disorder is a relevant perturbation to the Luttinger liquid. In the strong disorder limit, we can ignore H_{LG} because it does not commute with the random disorder we have added. The Hamiltonian $H_{\mathcal{D}}$ and ground-state wavefunction $|\Psi_{\mathcal{D}}\rangle$ for a specific disorder realization $\{h_j\}$ is

$$\begin{aligned} H_{\mathcal{D}} &= \sum_j P_j + h_j \sigma_j^z \\ |\Psi_{\mathcal{D}}\rangle &= \bigotimes_j |\sigma_j^z = h_j\rangle \otimes |\tau_{j+1/2}^x = h_j h_{j+1}\rangle \end{aligned}. \tag{3.40}$$

Thus we obtain a disorder ensemble $\{|\Psi_{\mathcal{D}}\rangle\}$.

Alternatively, we construct the following mixed state:

$$\rho = \sum_{\mathcal{D}} p_{\mathcal{D}} |\Psi_{\mathcal{D}}\rangle\langle\Psi_{\mathcal{D}}|, \tag{3.41}$$

where $p_{\mathcal{D}}$ is the classical probability distribution of the disorder realizations. We now show explicitly that starting from the igSPT (pure) state, one can apply a finite-depth quantum channel to obtain ρ. Denote the density matrix of the igSPT state by ρ_{igSPT}. First we apply the following quantum channel $\mathcal{E}^z$:

$$\mathcal{E}^z = \mathcal{E}_1^z \circ \mathcal{E}_2^z \circ \cdots, \ \mathcal{E}_j^z[\rho] = \frac{\rho + \sigma_j^z \rho \sigma_j^z}{2}. \tag{3.42}$$

Notice that this quantum channel only preserves U_g on average, but preserves U_a exactly. After this step $\mathcal{E}^z[\rho_{\text{igSPT}}]$ already takes the form given in Eq. (3.41), but the probability distribution $p_{\mathcal{D}}$ is long-ranged. In fact, the correlation function of σ^z is the same as that in the pure state.

Then we apply another quantum channel $\mathcal{E}^x$:

$$\mathcal{E}^x = \mathcal{E}_1^x \circ \mathcal{E}_2^x \circ \cdots, \mathcal{E}_j^x[\rho] = \frac{\rho + \tilde{\sigma}_j^x \rho \tilde{\sigma}_j^x}{2}. \tag{3.43}$$

This channel preserves both U_g and U_a exactly. It is straightforward to check that $(\mathcal{E}^z \circ \mathcal{E}^x)[\rho_{\text{igSPT}}]$ gives a decohered SPT state with $p_{\mathcal{D}} \propto 1$. Notice that this does not imply that the igSPT and the decohered ASPT are in the same phase, as there is no finite-depth local quantum channel that takes ρ (which has only short-ranged correlation functions) to the igSPT (which has power-law correlation functions).

3.2.3 Fermionic intrinsic ASPT

We now turn to the fermionic case. For simplicity, we will assume that the "bosonic" symmetry group G becomes average, while the fermion parity conservation $\mathbb{Z}_2^f$ remains an exact symmetry. In the decohered case, it means that the bath is bosonic, so the coupling between the system and the environment preserves fermion parity of the system. The total symmetry group $\tilde{G}$ is a central extension of G by $\mathbb{Z}_2^f$. We further assume that G is a finite group to simplify the discussion.

The relevant groups of fermionic invertible phases that can be decorated on G-defects, up to $(3{+}1)d$, are

$$h^0 = \mathrm{U}(1), h^1 = \mathbb{Z}_2, h^2 = \mathbb{Z}_2, h^3 = \mathbb{Z}, h^4 = 0, \tag{3.44}$$

where $h^1 = \mathbb{Z}_2$ is generated by a complex fermion, $h^2 = \mathbb{Z}_2$ is generated by the Majorana chain, and $h^3 = \mathbb{Z}$ is generated by the $p + ip$ superconductor.

Following the prescription in Sec. 3.1.3, for disordered phases we set $h^0 = h^1 = 0$. Thus for disordered ASPT states, the relevant groups are

$$h^0 = 0, h^1 = 0, h^2 = \mathbb{Z}_2, h^3 = \mathbb{Z}, h^4 = 0. \tag{3.45}$$

For decohered ASPT, the groups become

$$h^0 = 0, h^1 = \mathbb{Z}_2, h^2 = \mathbb{Z}_2, h^3 = \mathbb{Z}_{16}, h^4 = 0. \tag{3.46}$$

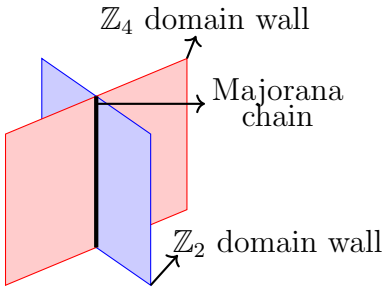

Figure 3.3: (3+1)d intrinsically decohered fermionic ASPT state from decorating a Majorana chain on the junction of $\mathbb{Z}_4$ (red) and $\mathbb{Z}_2$ (blue) domain walls.

The change of h^3 is because 16 copies of $p+ip$ superconductors are adiabatically equivalent to a E_8 state, which becomes trivialized for decohered phases (assuming the bath to be bosonic).

We now study the classifications in more details. Suppose the spatial dimension is $D \leq 3$. Let us consider the following two terms on the E_2 page: $\mathcal{H}^{D-1}(G, h^2)$ and $\mathcal{H}^D(G, h^1)$, corresponding to decorations of 1-dimensional G defect junctions by Majorana chains, and 0-dimensional G junctions by complex fermions. The potential differentials are

$$d_2 : \mathcal{H}^{D-1}(G, \mathbb{Z}_2) \to \mathcal{H}^{D+1}(G, h^1), \tag{3.47}$$

$$d_2 : \mathcal{H}^{D}(G, \mathbb{Z}_2) \to \mathcal{H}^{D+2}(G, h^0), \tag{3.48}$$

and

$$d_3 : \mathcal{H}^{D-1}(G, \mathbb{Z}_2) \to \mathcal{H}^{D+2}(G, h^0). \tag{3.49}$$

Explicit expressions for the differentials can be found in [170, 171].

First consider disordered ASPT phases, where $h^0 = h^1 = 0$ and $h^2 = \mathbb{Z}_2$. For the $\mathcal{H}^{D-1}(G, \mathbb{Z}_2)$ part, both d_2 and d_3 automatically vanish. Thus we conclude that any element of $\mathcal{H}^{D-1}(G, \mathbb{Z}_2)$ gives a disordered ASPT phase. Let us list a few examples of intrinsically disordered ASPT phases:

1. $D = 1, G = \mathbb{Z}_2, \tilde{G} = \mathbb{Z}_4^f$. This example is a Majorana chain with $\mathbb{Z}_4^f$ symmetry (i.e. a charge-4e superconductor in the clean limit), which has a d_2 obstruction in the clean

case. Below we will describe a concrete model realization of this state in a 1D Kitaev chain with random pairing.

2. $D = 2, G = \mathbb{Z}_2^{\mathsf{T}}, \tilde{G} = \mathbb{Z}_2^{\mathsf{T}} \times \mathbb{Z}_2^f$. Here $\mathbb{Z}_2^{\mathsf{T}}$ is the time-reversal symmetry. The Majorana decoration is classified by $\mathcal{H}^1(\mathbb{Z}_2^{\mathsf{T}}, \mathbb{Z}_2) = \mathbb{Z}_2$, and the nontrivial class is obstructed by d_2 in the clean case. Note that if $\tilde{G} = \mathbb{Z}_4^{\mathsf{T}f}$, then the d_2 obstruction vanishes and the result is the well-known class DIII topological superconductor in 2D (see Appendix **??** for more details).

3. $D = 3, G = \mathbb{Z}_2, \tilde{G} = \mathbb{Z}_2 \times \mathbb{Z}_2^f$. The Majorana decoration is classified by $\mathcal{H}^2(\mathbb{Z}_2, \mathbb{Z}_2) = \mathbb{Z}_2$. The nontrivial class is obstructed by d_2 in the clean case.

4. $D = 3, G = \mathbb{Z}_2 \times \mathbb{Z}_4, \tilde{G} = \mathbb{Z}_2 \times \mathbb{Z}_4 \times \mathbb{Z}_2^f$. The Majorana decoration is classified by $\mathcal{H}^2(\mathbb{Z}_2 \times \mathbb{Z}_4, \mathbb{Z}_2) = \mathbb{Z}_2^3$. Interestingly, one of them is only obstructed by d_3 in the clean case. More explicitly, denote group elements of $\mathbb{Z}_2 \times \mathbb{Z}_4$ by (a_1, a_2), where $a_1 = 0, 1$ and $a_2 = 0, 1, 2, 3$. The nontrivial cocycle in $\mathcal{H}^2(G, \mathbb{Z}_2)$ that describes Majorana chain decoration on the junction of the $\mathbb{Z}_4$ and $\mathbb{Z}_2$ domain walls (see Fig. 3.3) is given by

$$n_2(a, b) = a_1 b_2 \ (\text{mod } 2). \tag{3.50}$$

   We explicitly check that the d_2 obstruction vanishes and d_3 is nontrivial.

More examples of obstructed fermionic phases can be found in Ref. [118].

For decohered ASPTs, the differentials of the cases with Majorana-chain decoration have been analyzed in the disordered case, and the only difference is that $h^1 = \mathbb{Z}_2$ for decohered ASPTs, so the d_2 differential needs to vanish to ensure the fermion parity conservation. An example of such intrinsically decohered fermionic ASPT is given by Eq. (3.50) for $G = \mathbb{Z}_4 \times \mathbb{Z}_2$.

For the $\mathcal{H}^D$ part (complex fermion decoration), the d_2 differential always vanishes. An example of a "Berry-free" ASPT phase with complex fermion decoration is $G = \mathbb{Z}_2$, $\tilde{G} = \mathbb{Z}_2 \times \mathbb{Z}_2^f$ in $D = 3$. The fermionic SPT phase corresponding to the nontrivial element in $\mathcal{H}^3(G, \mathbb{Z}_2) = \mathbb{Z}_2$ is obstructed by d_2 in the clean case, and can now be realized an intrinsically decohered ASPT phase.

Exactly solvable lattice models of fermionic ASPT phases (without $p+ip$ decorations) can be constructed following [171]. We outline the construction in Appendix B.2 for $D = 2$. Below we describe a simple model realization of Majorana chain with an average $\mathbb{Z}_4^f$ symmetry, an example of localization-enabled compressible ASPT phase.

First let us consider a chain of spinless fermions, with the following Hamiltonian:

$$H = -\sum_j (c_j^\dagger c_{j+1} + \text{h.c.}) + \sum_j \Delta_j (c_j c_{j+1} + \text{h.c.}). \tag{3.51}$$

The $\mathbb{Z}_4^f$ symmetry is generated by $g : c_j \to ic_j$. The pairing $\Delta_j \to -\Delta_j$ under the g symmetry. When Δ_j is uniform and nonzero, this is the well-known Hamiltonian of a Kitaev chain, explicitly breaking the $\mathbb{Z}_4^f$ symmetry. When $\mathbb{Z}_4^f$ is exact, we must have $\Delta = 0$ and the ground state is a gapless metal[5]. When $\mathbb{Z}_4^f$ is an average symmetry, we can turn on a random pairing term with symmetric probability: $P[\Delta_j] = P[-\Delta_j]$. This random pairing term will localize the metallic ground state, resulting in a random Kitaev chain.

In the Hamiltonian Eq. (3.51), if the configuration Δ_j contains one sign-changing domain wall, we find it harbors a localized complex fermion zero mode. Thus when the sign of the pairing potential is disordered, we expect that there are low-energy states filling the superconducting gap, which we confirm numerically. However, this zero mode is protected by the time reversal symmetry (i.e. the complex conjugation).[6] In order to obtain a localized state, we lift the local degeneracy from the zero modes by having complex hopping or the pairing terms that break the time-reversal symmetry.

To better appreciate the nature of the the random Kitaev chain with average $\mathbb{Z}_4^f$ symmetry, it is more illuminating to consider the following "fixed point" model. On each lattice

[5]There are other terms that can gap out the metal without breaking $\mathbb{Z}_4^f$, such as a translation-breaking potential. However, to keep the system in a nontrivial Kitaev chain, we need the amplitude of such potential μ to be smaller than Δ. As we recover the exact $\mathbb{Z}_4^f$ symmetry by taking $\Delta \to 0$, we need to take $\mu \to 0$ first.

[6]In fact, $\Delta > 0$ and $\Delta < 0$ belong to distinct topological phases labeled by $\nu = \pm 1$ where $\nu \in \mathbb{Z}_8$ is the topological invariant for topological superconductors with $T^2 = 1$ time-reversal symmetry (the BDI class), so there must be a protected zero mode at the interface.

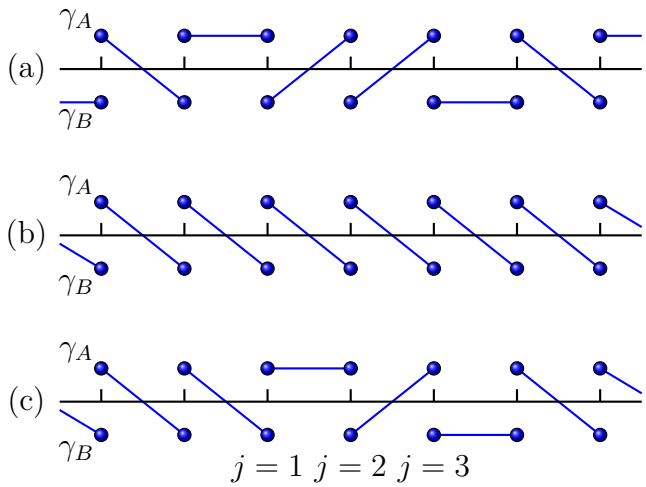

Figure 3.4: Illustration of a random Kitaev chain with average $\mathbb{Z}_4^f$ symmetry. (a) A typical Majorana bond configuration. (b) A uniform bond configuration. (c) Two nearby domain walls on top of the uniform configuration. The total fermion parity of (b) and (c) differ by (-1).

site j we have a complex fermion, which we write as two Majoranas $c_j = \frac{1}{2}(\gamma_{A,j} - i\gamma_{B,j})$. The random Hamiltonian takes the form

$$H = -\sum_j \sum_{r_j=A,B} i g_j^{r_j,r_{j+1}} \gamma_{r_j,j} \gamma_{r_{j+1},j+1}, \tag{3.52}$$

where g is a random coupling constant taking value in $\{0, \pm 1\}$ such that every lattice link $(j, j+1)$ is covered by exactly one Majorana bond, which makes each state in the ensemble a nontrivial Kitaev chain. For example, if $g_j^{AB} = 1$, then we must have $g_j^{AA} = g_j^{BB} = g_j^{BA} = 0$, and $g_{j+1}^{BA} = g_{j+1}^{BB} = g_{j-1}^{AA} = g_{j-1}^{BA} = 0$. An example of such random Majorana bond configuration is shown in Fig. 3.4 (a). Besides this nearest-neighbor constraints, the random coupling g should be uncorrelated in long distance, generated by a probability functional $P[g_j]$.

Now we examine the condition on $P[g_j]$ imposed by the average $\mathbb{Z}_4^f$ symmetry, which

is generated by $U = \exp\left(\frac{\pi}{4}\sum_j \gamma_{j,A}\gamma_{j,B}\right)$. Some simple algebra shows that

$$\begin{aligned} U(i\gamma_j^A\gamma_{j+1}^B)U^\dagger &= -i\gamma_j^B\gamma_{j+1}^A \\ U(i\gamma_j^A\gamma_{j+1}^A)U^\dagger &= i\gamma_j^B\gamma_{j+1}^B \end{aligned}. \tag{3.53}$$

The minus sign above will be important. Now for $P[g]$, we should have

$$P(g^{AB}) = P(-g^{BA}), \quad P(g^{AA}) = P(g^{BB}). \tag{3.54}$$

We can now further simplify the model by having $g^{AB}, g^{AA}, g^{BB} \in \{0, 1\}$ and $g^{BA} \in \{0, -1\}$, generated by a $\mathbb{Z}_4^f$-symmetric probability functional $P[g]$.

Now what do all these mean for the total fermion parity $i^L \prod_{j=1}^L \gamma_{j,A}\gamma_{j,B}$? If we have only AB bonds or BA bonds, the total fermion parity on a ring is fixed (-1 for periodic boundary condition). But when we have domain walls between the two bonding patterns, as required by the average $\mathbb{Z}_4^f$ symmetry, the fermion parity starts to change locally. The most illuminating case is when two domain walls are right next to each other, as shown in Fig. 3.4 (c) . In this configuration all links $(j, j+1)$ with $j < 1$ and $j > 3$ are AB bonds, while the intermediate bonds are given by $g_1^{AA} = 1$, $g_2^{BA} = -1$ and $g_3^{BB} = 1$. A simple calculation shows that, compared with the configuration with no domain wall at all ($g_j^{AB} = 1$ for all j, as in Fig. 3.4 (b)), this configuration has an additional (-1) fermion parity. This means that even though the domain wall behave like an $\mathbb{Z}_2$ object (the bonding configurations return to the original ones after passing through two domain walls), "fusing" two nearby domain walls together will change the fermion parity. As a result, in the clean limit the domain walls cannot condense to recover the exact $\mathbb{Z}_4^f$ symmetry. This is nothing but the manifestation of the d_2 obstruction. In general, the fermion parity of the state depends on the configurations of the g's and fluctuate randomly within the ensemble. In a disordered system the nontrivial domain-wall fusion does not lead to any obstruction for short-range entanglement, since the domain walls are pinned by the disorders. The above discussion eventually leads to a long-distance picture, which contains localized fermions (that carry nontrivial fermion parity) randomly located at the $\mathbb{Z}_4^f$-domain walls. If we take the absolute ground state of each Hamiltonian realization, different states in the ensemble will have different total fermion parity. If we take a "canonical ensemble" and fix the total fermion parity for the entire ensemble, then half of the ensemble will be put in excited

states (to match the fermion parity), and the excitation spectral above such states will in general be gapless (assuming a bounded distribution of g_j).

3.3 Average symmetry-enriched topological orders

3.3.1 General structures

We will focus on SET phases in (2+1)d, and comment on generalizations to higher dimensions.

In general, a (2+1)d bosonic topological order is described by a mathematical structure called unitary modular tensor category, denoted by $\mathcal{C}$. Physically, $\mathcal{C}$ consists of a set of topological charges (i.e. anyon types), as well as consistent data specifying their fusion and braiding. When the system has a global symmetry $\tilde{G}$, $\mathcal{C}$ gets enriched in three ways [12]:

1. There is a group homomorphism from $\tilde{G}$ to the group of auto-equivalence maps $\mathrm{Aut}(\mathcal{C})$ of $\mathcal{C}$,
$$\rho : \tilde{G} \to \mathrm{Aut}(\mathcal{C}), \tag{3.55}$$
Here $\mathrm{Aut}(\mathcal{C})$ consists of all the permutations of anyon types which keep the fusion and braiding properties invariant [7]. Basically, ρ tells us how $\tilde{G}$ permutes anyons.

2. The anyons may carry fractional quantum numbers under $\tilde{G}$. In particular, given ρ, there is a possible obstruction to symmetry fractionalization, which is an element in $\mathcal{H}^3_\rho(\tilde{G}, \mathcal{A})$. When the $\mathcal{H}^3$ class vanishes, distinct symmetry fractionalization classes form a torsor over $\mathcal{H}^2_\rho(\tilde{G}, \mathcal{A})$, where $\mathcal{A}$ is the group of Abelian anyons.

3. Once ρ and the symmetry fractionalization of anyons are known, we then need to specify the fusion and braiding properties of $\tilde{G}$ symmetry defects. In particular, given ρ and the symmetry fractionalization of anyons, the global symmetry may have a 't

[7] Note that more precisely, $\mathrm{Aut}(\mathcal{C})$ is the group of braided tensor auto-equivalences of $\mathcal{C}$ and there can be nontrivial elements which do not permute any anyons. However, such examples are only known to occur for very complicated $\mathcal{C}$, and for simplicity, we do not consider them.

Hooft anomaly valued in $\mathcal{H}^4(G, \mathrm{U}(1))$. When the $\mathcal{H}^4$ anomaly class vanishes, distinct equivalence classes form a torsor over $\mathcal{H}^3(\tilde{G}, \mathrm{U}(1))$, up to further identifications [1, 36].

It is again useful to think of the SET phases in terms of fluctuating symmetry defect lines. Each defect line is associated with an anyon permutation action given by ρ. The $\mathcal{H}^3$ obstruction means that defect fusion may fail to be associative: an F move of defect lines may nucleate an extra Abelian anyon, violating the locality requirement. When the $\mathcal{H}^3$ class vanishes, the extra Abelian anyon can be "absorbed" into decorations of tri-junctions of defects by Abelian anyons. In-equivalent patterns of decorations are classified by a torsor over $\mathcal{H}^2_\rho(\tilde{G}, \mathcal{A})$. Lastly, once we have well-defined defect fusions, including decorations on tri-junctions, there may be a Berry phase in the space of states with defects, which gives the $\mathcal{H}^4$ anomaly. From this interpretation, it is clear that with a non-trivial $\mathcal{H}^3_\rho(\tilde{G}, \mathcal{A})$ class the map ρ does not make sense in a pure 2+1d system. The $\mathcal{H}^4$ anomaly means that the $\tilde{G}$ symmetry has a 't Hooft anomaly. Examples include the surface of a 3+1d bosonic SPT state or 2+1d lattice models that satisfy Lieb-Schultz-Mattis-type theorems.

We now generalize the classification to disorder ensembles with topological order. First let us define what we mean by LRE ensembles, which is a natural extension of the notion of SRE ensembles. To formulate the definition it is convenient to choose a "reference state", which can be the ground state of a gapped Hamiltonian in the clean system, and identify its topological order described by the anyon theory $\mathcal{C}$. We require that all states in the ensemble are smoothly connected to the reference state, thus described by the same topological order $\mathcal{C}$. Such an ensemble is said to be LRE with topological order $\mathcal{C}$.

Let us now assume that $\tilde{G}$ fits into the group extension (3.16), with exact symmetry A and average symmetry G, and see how the classification above is modified. We again expect $\tilde{G}$ to be mapped to $\mathrm{Aut}(\mathcal{C})$ through a group homomorphism ρ, which is an invariant of the disorder ensemble. The only way to change ρ is to go through a phase transition, which violates the adiabatic connectability within a single disorder ensemble. It is then useful to think of each state in the disorder ensembles as a topological order with exact A symmetry (i.e. fluctuating A symmetry defects) and a static G defect network.

Generalizing the discussions in Sec. 3.1.2, in the presence of disorder it is possible to localize Abelian anyons (as long they do not carry any zero modes protected by the exact

symmetry, see below). As a result, there is no longer any energetic requirement to have fixed Abelian anyons decorated on G defect junctions. This is in parallel with dropping the 0D charge decoration in the classification of disordered ASPT phases. In fact, one can gauge the exact symmetry A in a disordered ASPT state to get a disordered ASET state.

We first consider a simpler problem, where the entire symmetry group $\tilde{G}$ becomes average (i.e. A is trivial). In this case, all Abelian anyons can be localized and both the $[O_3]$ obstruction class and the symmetry fractionalization class (i.e. decorations of defect junctions by Abelian anyons) lose their meaning. The same is true for the $\mathcal{H}^4(\tilde{G}, \mathrm{U}(1))$ anomaly and $\mathcal{H}^3(\tilde{G}, \mathrm{U}(1))$ torsor since the disordered SET is an ensemble of defects. We thus conclude that with a trivial A, disordered ASET phases are completely classified by the maps ρ, including those with nontrivial $\mathcal{H}^3$ obstructions. An example of such an intrinsically disordered ASET is given below in Sec. 3.3.3.

Next we consider ASETs with a nontrivial A, with a given $\rho : \tilde{G} \to \mathrm{Aut}(\mathcal{C})$. The map ρ is associated with an obstruction class $[O_3] \in \mathcal{H}^3_\rho(\tilde{G}, \mathcal{A})$. The group $\mathcal{H}^3_\rho(\tilde{G}, \mathcal{A})$ can also be decomposed using the Leray-Serre spectral sequence, whose E_2 page consists of

$$E_2^{p,3-p} = \bigoplus_{p=0}^{3} \mathcal{H}^p(G, \mathcal{H}^{3-p}(A, \mathcal{A})). \tag{3.56}$$

Here we suppress the group action subscripts for clarity. It should be understood that A acts on $\mathcal{A}$ through ρ, and G acts on the coefficient group $\mathcal{H}^{3-p}$ via both ρ and the G action on A.

Let us start with the component that only involves G, i.e. $E^{3,0} = \mathcal{H}^3_\rho(G, \mathcal{A})$. Since now we only have an ensemble of G defects, if the additional Abelian anyon from a F move of G defects can be localized then this component of the obstruction class no longer makes sense. However, given the exact A symmetry, localization requires that the Abelian anyons involved in the F move do not transform under A symmetry action, and carry no projective multi-dimensional representations of A (a projective one-dimensional representation, i.e. a fractional charge, is allowed).

The other components in the decomposition with $p < 3$ all involve A defects, and hence even when G becomes an average symmetry they still represent nontrivial obstructions.

Having dealt with the $\mathcal{H}^3$ obstruction, we move to the $\mathcal{H}^2_\rho(\tilde{G},\mathcal{A})$ torsor. Again we can decompose it using the LHS spectral sequence:

$$E_2^{p,2-p} = \mathcal{H}^2_\rho(G,\mathcal{A}) \oplus \mathcal{H}^1(G,\mathcal{H}^1(A,\mathcal{A})) \oplus \mathcal{H}^2_\rho(A,\mathcal{A}). \tag{3.57}$$

Here we also supress the group action subscripts in the middle term. Via the same reasoning, with localization of Abelian anyons, $\mathcal{H}^2_\rho(G,\mathcal{A})$ may become trivialized, provided that the Abelian anyons involved in this decoration transform trivially (at most as 1D projective reps) under A. The next two terms are still meaningful for disordered ASETs. Perhaps the most interesting part is the $\mathcal{H}^1(G,\mathcal{H}^1(A,\mathcal{A}))$ torsor. When ρ is the identity, in a clean SET this term means that G and A symmetries do not commute when acting on certain anyons. When the G symmetry becomes average, one can interpret this term as the A charge carried by the anyon changes when it passes through certain G defects.

We can similarly discuss what changes need to be made for the $\mathcal{H}^3$ torsor and $\mathcal{H}^4$ anomaly, however, this is identical to the ASPT classification and we will not repeat it.

3.3.2 Example: $\mathbb{Z}_2 \times \mathbb{Z}_2$ toric code with $\mathbb{Z}_2^{\mathrm{A}}$ symmetry

We consider a fascinating example from a (2+1)d ASPT phase with $A = \mathbb{Z}_2 \times \mathbb{Z}_2$ and $G = \mathbb{Z}_2$ while the extension is trivial. The type-III SPT can be constructed from decorating a 1d cluster state protected by A on the domain wall of G.

If we gauge the exact symmetry A to obtain a double toric code topological order, with anyons labeled as $\{e_1, m_1, e_2, m_2\}$ and their combinations, then the average symmetry G will permute the anyons according to

$$\rho: \quad \begin{cases} e_1 \leftrightarrow e_1 \\ e_2 \leftrightarrow e_2 \end{cases}, \quad \begin{cases} m_1 \leftrightarrow m_1 e_2 \\ m_2 \leftrightarrow m_2 e_1 \end{cases} \tag{3.58}$$

See Fig. 3.5. This anyon permutation can be seen by firstly considering moving an m_1 anyon across a $\mathbb{Z}_2^A$ domain wall which should be decorated with a 1d cluster state in the ungauged system. We can relabel the anyons as $\tilde{e}_1 = e_1 m_2$, $\tilde{e}_2 = e_2 m_1$, $\tilde{m}_1 = m_1$, and $\tilde{m}_2 = m_2$, and the theory is rephrased as two copies of $\mathbb{Z}_2$ gauge theories, with $\mathbb{Z}_2^A$ simply exchanges the two copies.

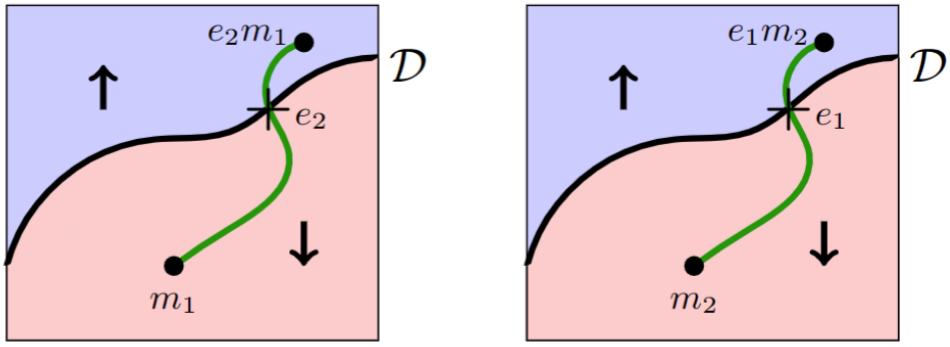

Figure 3.5: Anyon permutation of double toric code model with average symmetry $\mathbb{Z}_2^A$. $\mathcal{D}$ is the symmetry domain wall of $\mathbb{Z}_2^A$ separating the red and blue regimes (with Ising spin-$\uparrow$ and spin-$\downarrow$), and the green curve depicts the string operator of a $\mathbb{Z}_2$ gauge group connecting two anyons m_1/m_2 and e_2m_1/e_1m_2.

3.3.3 Intrinsically disordered ASET with $\mathbb{Z}_2^A$ symmetry

It is instructive to study a lattice model for an intrinsically disordered $\mathbb{Z}_2^A$ ASET phase. The model realizes a $\mathbb{D}_{16} = \mathbb{Z}_8 \rtimes \mathbb{Z}_2$ gauge theory, denoted by $\mathrm{D}(\mathbb{D}_{16})$. The group has two generators a and r that satisfy $a^8 = r^2 = 1, rar = a^{-1}$.

For a topological gauge theory with a finite gauge group H, a large class of anyonic symmetries can be understood as outer automorphisms $\mathrm{Out}(H)$ of the gauge group. Here $\mathrm{Out}(H)$ is the quotient $\mathrm{Aut}(H)/\mathrm{Inn}(H)$, where Aut is the group of automorphisms and Inn is the group of inner automorphisms (i.e. conjugation by a group element). Physically, the inner automorphisms are gauge transformations, so they do not correspond to faithful symmetry actions. Hence each element in $\mathrm{Out}(H)$ corresponds uniquely to an element in $\mathrm{Aut}(\mathrm{D}(H))$ that does not mix electric and magnetic charges of the gauge theory. Adopting the general framework, different ASETs with an average symmetry group G are classified by homomorphisms $\rho : G \to \mathrm{Out}(H)$. Mathematically, ρ is associated with a $\mathcal{H}^3(G, Z(H))$ obstruction class, where $Z(H)$ is the center of the group H. It can be shown that this is the same $\mathcal{H}^3$ obstruction.

We now specialize to the $\mathbb{D}_{16}$ gauge theory. Write $G = \mathbb{Z}_2 = \{1, g\}$. We assume that

the image of g under ρ is the following automorphism:

$$\rho_g : a \to a^5, r \to ra. \tag{3.59}$$

The permutation action on anyons is order 2 because ρ_g^2 is the conjugation by a^{-3}. It is shown in Ref. [50] that this ρ has a nontrivial $\mathcal{H}^3(\mathbb{Z}_2, \mathbb{Z}_2)$ class: $O_3(g, g, g) = [a^4]$. Here $[a^4]$ should be understood as the a^4 gauge flux in the $\mathbb{D}_{16}$ gauge theory, which is a $\mathbb{Z}_2$ Abelian boson. Intuitively, inserting a g defect loop introduces an additional $[a^4]$ anyon.

Ref. [50] introduced a generalization of Kitaev's quantum double model [94] for this anomalous SET state. Schematically, the model is defined on a quasi-2D lattice. Each link has a 16-dimensional Hilbert space, with an orthonormal basis labeled by elements of $\mathbb{D}_{16}$. They can be viewed as lattice gauge fields. The Hamiltonian takes the following form:

$$H_{\text{clean}} = -\sum_v A_v - \sum_p (\delta_{F_p,1} + \delta_{F_p,a^4}). \tag{3.60}$$

Here A_v implements the Gauss's law at each vertex, and F_p is the gauge flux through a plaquette p. Note that the second term imposes the condition that through each plaquette the gauge flux is either 1 or a^4 (note $Z(\mathbb{D}_{16}) = \{1, a^4\}$). This is distinct from the standard quantum double construction where the plaquette term enforces F_p to be 1. H_{clean} has an extensive ground state degeneracy since we can have 1 or a^4 flux through each plaquette. However, if the fluxes are fixed, the ground state is indeed a $\mathbb{D}_{16}$ gauge theory (with background fluxes).

The $\mathbb{Z}_2$ symmetry transformation can be defined so that it implements the ρ symmetry in the $\mathbb{D}_{16}$ gauge theory. However, under this $\mathbb{Z}_2$ symmetry transformation we have $F_p \to F_p a^4$, which explains the form of the plaquette term.

Now we turn this extensive number of ground states into a disorder ensemble:

$$H[\sigma_p] = H_{\text{clean}} - \sum_p \varepsilon_p (\delta_{F_p,1} - \delta_{F_p,a^4}). \tag{3.61}$$

Here ε_p are independent random variables drawn symmetrically from the $[-W, W]$ with $W < 1$. Under $\mathbb{Z}_2^A$ they transform as $\varepsilon_p \to -\varepsilon_p$.

In accordance with the general principle, the model supports gapless modes for the flux anyon $[a^4]$ localized at certain plaquettes, in order to accommodate the $\mathcal{H}^3$ obstruction. We can think of the ground state as a localized state of the $[a^4]$ flux anyons.

3.3.4 ASET with 't Hooft anomaly: an example with $\mathbb{Z}_2 \times \mathbb{Z}_2^A$

We consider the surface of a (3+1)d ASPT with $\mathbb{Z}_2 \times \mathbb{Z}_2^A$ symmetry. The generator of the $\mathbb{Z}_2$ ($\mathbb{Z}_2^A$) will be denoted by g (g_A). In the bulk ASPT state, on each (2+1)d domain wall of the average $\mathbb{Z}_2^A$ symmetry we decorate a Levin-Gu state [109] of the exact $\mathbb{Z}_2$ (see Fig. 3.6), with the following topological action on a 4-manifold X_4:

$$S = \int_{X_4} a^3 \cup b \tag{3.62}$$

where a and b are background gauge fields of $\mathbb{Z}_2$ and $\mathbb{Z}_2^A$, respectively. Notice that when both symmetries are exact, there are two other nontrivial topological terms. One of them is given by

$$S' = \int_{X_4} a \cup b^3. \tag{3.63}$$

It corresponds to decoration of exact $\mathbb{Z}_2$ charges on junctions of the $\mathbb{Z}_2^A$ symmetry. As explained in Sec. 3.1.2, this action S' is trivialized when $\mathbb{Z}_2^A$ becomes average in a disordered ensemble. The other action is $S + S'$, which is now identified with S.

On the (2+1)d surface of this state, we have a random network of $\mathbb{Z}_2^A$ domain walls, each decorated with a Levin-Gu edge theory described by a Luttinger liquid [$\varphi^T = (\varphi^1, \varphi^2)$],

$$\mathcal{L} = \frac{K_{IJ}}{4\pi} \left(\partial_x \varphi^I\right) \left(\partial_t \varphi^J\right) + \frac{V_{IJ}}{8\pi} \left(\partial_x \varphi^I\right) \left(\partial_x \varphi^J\right) \tag{3.64}$$

where the K-matrix $K = \sigma^x$. The nontrivial $\mathbb{Z}_2$ symmetry action is defined as

$$\varphi^{1,2} \mapsto \varphi^{1,2} + \pi. \tag{3.65}$$

We now want to gap out these domain wall modes in a $\mathbb{Z}_2$ symmetric way, which can be achieved by placing a semion topological order/chiral spin liquid (CSL) on the surface. Then on each domain wall, we have not only the Levin-Gu edge state but also two counter-propagating chiral Luttinger liquids as the edge modes of the semion topological orders on both sides of the domain wall. The total (1+1)d domain wall theory is

$$\mathcal{L} = \frac{K'_{IJ}}{4\pi} \left(\partial_x \varphi^I\right) \left(\partial_t \varphi^J\right) + \frac{V'_{IJ}}{8\pi} \left(\partial_x \varphi^I\right) \left(\partial_x \varphi^J\right) \tag{3.66}$$

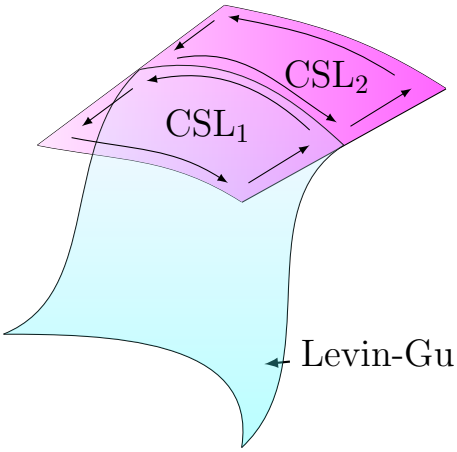

Figure 3.6: Surface topological order of (3+1)d ASPT with $\mathbb{Z}_2 \times \mathbb{Z}_2^A$ symmetry. The indigo surface depicts the $\mathbb{Z}_2^A$ domain wall decorated by a Levin-Gu state, and the violet surface depicts the surface chiral spin liquid enriched by $\mathbb{Z}_2 \times \mathbb{Z}_2^A$ symmetry.

where $\varphi^T = (\varphi^1, \varphi^2, \varphi^3, \varphi^4)$, and the K-matrix $K' = \sigma^x \oplus 2\sigma^z$. A semion is created by the operator $e^{i\varphi^3}$ on one side of the domain wall, or $e^{i\varphi^4}$ on the other side. Originally, without Levin-Gu edge modes, the domain wall can be gapped by adding a Higgs term $\cos(2\varphi^3 - 2\varphi^4)$, which induces coherent tunneling of the semions across the domain walls. Alternatively, with the Levin-Gu edge modes, we can gap out the theory in a $\mathbb{Z}_2$ symmetric way by the following Higgs terms,

$$\cos(\varphi^1 + \varphi^2 - 2\varphi^4) + \cos(\varphi^1 - \varphi^2 - 2\varphi^3). \tag{3.67}$$

In order for this term to preserve the $\mathbb{Z}_2$ symmetry, $e^{2i\varphi^4}$ and $e^{2i\varphi^3}$ should be invariant under $\mathbb{Z}_2$.

We now analyze the symmetry fractionalization between $\mathbb{Z}_2$ and $\mathbb{Z}_2^A$ in the semion surface theory. It is instructive to start with the clean case, when both symmetries are exact (we will continue denote the symmetry group as $\mathbb{Z}_2 \times \mathbb{Z}_2^A$). Denote the local h symmetry action on a semion by U_h for every $h \in \mathbb{Z}_2 \times \mathbb{Z}_2^A$. The group relations in $\mathbb{Z}_2 \times \mathbb{Z}_2^A$ lead to the following invariants:

$$\begin{aligned} \lambda_h &= U_h^2, h \in \mathbb{Z}_2 \times \mathbb{Z}_2^A \\ \eta &= U_g U_{g_A} U_g^{-1} U_{g_A}^{-1}. \end{aligned} \tag{3.68}$$

η	λ_g	λ_{g_A}	S_{anomaly}
1	± 1	± 1	0
-1	1	1	$a \cup b^3 + a^3 \cup b$
-1	1	-1	$a^3 \cup b$
-1	-1	1	$a \cup b^3$
-1	-1	-1	0

Table 3.1: 't Hooft anomalies for the projective $\mathbb{Z}_2 \times \mathbb{Z}_2^A$ symmetry actions in clean semion topological order.

All of them take ± 1 value. They are related by the algebraic identity: $\lambda_g \lambda_{g_A} \lambda_{gg_A} = \eta$. So there are three independent $\mathbb{Z}_2$ invariants for the projective symmetry action, consistent with the $\mathcal{H}^2(\mathbb{Z}_2 \times \mathbb{Z}_2, \mathbb{Z}_2) = \mathbb{Z}_2^3$ classification. The four $\eta = 1$ classes can all be realized by one-dimensional representations, while the $\eta = -1$ classes must be realized by at least two-dimensional representations. In particular, the one with $\lambda_g = \lambda_{g_A} = \lambda_{gg_A} = -1$ is realized in the semion chiral spin liquid, where $\mathbb{Z}_2 \times \mathbb{Z}_2^A$ is a subgroup of the SO(3) symmetry. The other three classes with $\eta = -1$ are all anomalous with respect to the (exact) $\mathbb{Z}_2 \times \mathbb{Z}_2^A$ symmetry. Their 't Hooft anomalies were computed in [29] and we recall the results in Table 3.1.

When $\mathbb{Z}_2^A$ becomes average, as discussed in Sec. 3.3.1, the invariants λ_{g_A} and λ_{gg_A} are ambiguous due to the localization of semions. However, λ_g and η should remain well-defined. The former should be fairly clear since $\mathbb{Z}_2$ is an exact symmetry, so we now explain how to define η. Since $U_g U_{g_A} = \eta U_{g_A} U_g$, under the g_A action the $\mathbb{Z}_2$ charge, measured by the eigenvalue of U_g, changes by η. Therefore, η can be measured as the change of the $\mathbb{Z}_2$ charge when when adiabatically moving a semion across a g_A defect (which implements the g_A symmetry on the semion).

First we determine λ_g. In the Luttinger liquid formulation (3.64), $\lambda_g = -1$ means that under the $\mathbb{Z}_2$ symmetry, φ^3 and φ^4 must shift by an odd multiples of $\pi/2$, and therefore $e^{2i\varphi^{3/4}}$ should be odd under $\mathbb{Z}_2$. However, we have seen that for the Higgs term to preserve symmetry $e^{2i\varphi^{3/4}}$ have to be $\mathbb{Z}_2$ even. Thus we must have $\lambda_g = 1$.

η	λ_g	S_{anomaly}
1	± 1	0
-1	1	$a \cup b^3$
-1	-1	0

Table 3.2: Average 't Hooft anomalies in disordered semion topological order.

From Eq. (3.65) and (3.67), we find that at the domain wall φ^4 is identified with $\varphi^3 + \varphi^2$, therefore under the $\mathbb{Z}_2$ symmetry, $e^{i\varphi^4}$ has opposite $\mathbb{Z}_2$ charge to that of $e^{i\varphi^3}$. In other words, adiabatically moving a semion across a domain wall changes its global $\mathbb{Z}_2$ charge by -1. This is the manifestation of the non-commutativity between $\mathbb{Z}_2$ and $\mathbb{Z}_2^A$ acting on the semion in the ensemble.

Let us now discuss how the anomaly inflow works in the average SET. We have shown that λ_g and η remain good invariants, and λ_{g_A} and λ_{gg_A} are not well-defined individually, but their ratio is fixed by $\lambda_g\eta$. Interestingly, with $\eta = -1$ fixed, the anomalies in Table 3.1 separate into two groups corresponding to $\lambda_g = \pm 1$. The two classes inside each group differs just by the $a \cup b^3$ term, which describes decorations of $\mathbb{Z}_2$ charges on $\mathbb{Z}_2^A$ defect junctions, and becomes trivial due to the localization. This ties nicely with the observation that λ_{g_A} is now ambiguous. The new bulk-boundary correspondence for the semion theory with average $\mathbb{Z}_2 \times \mathbb{Z}_2^A$ symmetry is now summarized in Table 3.2.

This example illustrates that for a mixed group of exact and average symmetry, "symmetry fractionalization" can be well-defined on anyons. We have also derived the complete average 't Hooft anomaly matching for $\mathbb{Z}_2 \times \mathbb{Z}_2^A$ symmetry in the semion topological order.

3.3.5 An example with Lieb-Schultz-Mattis anomaly

We consider a $2d$ lattice system with average $\mathbb{Z}\times\mathbb{Z}$ translation symmetry, exact spin $SO(3)$ rotation symmetry and a spin-1/2 moment per lattice unit cell. This system has a t'Hooft anomaly from Lieb-Schultz-Mattis (LSM) constraints

$$S = \int_{X_4} x \cup y \cup w_2^{SO(3)}, \tag{3.69}$$

where x, y are background gauge fields of the x, y translation symmetries, and $w_2^{SO(3)}$ is the second Stiefel-Whitney class of the background $SO(3)$ gauge field. This anomaly remains nontrivial as the $\mathbb{Z} \times \mathbb{Z}$ translation symmetry becomes average.

In the clean limit, one of the most well-known topological orders that match with the LSM anomaly is a $\mathbb{Z}_2$ topological order. In this $\mathbb{Z}_2$ topological order, the e particle carries a nontrivial $H^2(SO(3), \mathbb{Z}_2)$ symmetry fractionalization (in common term, it carries spin-1/2); the m particle carries a nontrivial $H^2(\mathbb{Z} \times \mathbb{Z}, \mathbb{Z}_2)$ symmetry fractionalization, in the sense that $T_x T_y = -T_y T_x$ when acting on m, where $T_{x,y}$ are the generators of the x, y translations. These symmetry fractionalizations are required for the $\mathbb{Z}_2$ topological order to match the anomaly. While the spin-1/2 moment on the e particle is not affected by disorder, we do need to explain the meaning of "$T_x T_y = -T_y T_x$" on the m particle. As discussed in Sec. 3.3.1, the expression $T_x T_y = -T_y T_x$ on m can be interpreted as having an e particle localized at each unit cell (the intersection of a T_x domain wall and a T_y domain wall). If e particle does not carry any degeneracy, then we can deform the state by randomly distributing localized e particles among all unit cells, and states with different e particle distributions will be smoothly connected. However, since e particle carries spin-1/2 moment, the additional localized e particles must find their way to form an $SO(3)$ invariant (singlet) state. We do not expect the singlet state to be achievable without developing further long-range entanglement. Therefore the notion of "one e particle per unit cell" is robust. Equivalently, $T_x T_y = -T_y T_x$ on m particle and the $\mathbb{Z}_2$ topological order indeed matches the LSM anomaly.

3.4 Dicussions

In this Chapter I systematically classified and characterized topological phases, both SPT and SET, with average and exact symmetries. This allowed us to clarify many subtle issues from previous literature, and discover new physics that are intrinsically associated with mixed states.

First, I discussed the general framework to classify ASPT, in both decohered and disordered systems. Even though the physical states in both scenarios can be described by

density matrices of the form $\rho = \sum_I P_I |\Psi_I\rangle\langle\Psi_I|$, in a disordered system the state is also further endowed with an ensemble of Hamiltonians $\{H_I\}$ with probability $\{P_I\}$. This makes the physics of the two scenarios quite different. In particular the classification of ASPT phases will be different in the two scenarios. Pleasantly, despite of the physical difference between decohered and disordered systems, the ASPT phases in both scenarios can be characterized and classified under the unified mathematical framework of spectral sequence. The physics behind the spectral sequence framework is the decoration of symmetry defects [34, 60, 172], which is familiar from the classification of pure state SPT phases.

As an appealing consequence of our classification, we discovered a family of ASPT phases that are *intrinsically mixed*. These are SPT phases that can only exist with average symmetries, in decohered or disordered system, and by definition cannot exist as pure state SPT. In fact if we try to deform an intrinsically mixed ASPT to a pure state, for example by reducing the disorder strength, the state reduces to the so-called "intrinsically gapless SPT" [157].

I then moved on to nontrivial intrinsic topological orders in (2+1)d in the presence of quenched disorders, and discuss how average (and exact) symmetries enrich the structure of topological orders. I showed that average symmetries can permute anyons, as ordinary exact symmetries. Furthermore an average symmetry and an exact symmetry can jointly fractionalize on anyons. However, the fractionalization of average symmetry alone becomes ill-defined on the anyons – unless the fractionalization pattern involves certain 't Hooft anomalies. Another interesting feature of disordered systems is that certain obstructions of symmetry enrichment, known as $\mathcal{H}^3$ obstruction, are lifted once the symmetries involved become average. Such intrinsically disordered ASET comes with additional features. For instance, the system will have localized anyons that lead to a gapless spectrum, yet the system still hosts short-range correlated ground states.

In this Chapter I only studied bosonic ASETs in (2+1)d disordered systems. A natural open question is to extend the theory to fermionic systems. In the clean limit, classifications of fermionic SET phases have been developed recently in [17, 18]. While certain basic elements of the theory are parallel to the bosonic case, there are important new ingredients and subtleties, especially when 't Hooft anomalies are concerned. A systematic study on

fermionic ASET in disordered ensembles is left to future study.

Chapter 4

Critical Systems under Measurements and Decoherence

This Chapter is based on a recent work [114]. In this Chapter I will provide a description of the universal features of an open critical system under measurements and decoherence, via a replicated Keldysh field theory. The use of the Keldysh effective theory provides a valuable quantum field theory toolbox, which offers two key advantages: (1) It makes the microscopic and replica symmetries and fundamental consistency conditions of a density matrix manifest. (2) It enables the identification of the physically relevant degrees of freedom at low energies (IR). In general, our approach is to identify the internal symmetries of the system at microscopic scales (UV) and then construct the most general low energy effective theory that satisfies the symmetry, using IR degrees of freedom. The IR behaviors can then be deduced from this IR effective theory.

As an example, we apply this approach to critical Ising model with a $\mathbb{Z}_2$ global symmetry in both one and two spatial dimensions. Specifically, we consider measurements and decoherence in either a $\mathbb{Z}_2$ even or odd basis. Our results show that, in one spatial dimension, after averaging over the entire ensemble of measurement outcomes: (1) measurements in a $\mathbb{Z}_2$ even basis over *a finite period of time* do not alter the scaling behaviors of correlation functions and entanglement entropy compared to the initial critical state; (2) measurements in a $\mathbb{Z}_2$ odd basis cause the entanglement entropy to saturate to a constant

for large subsystems. Furthermore, we find that different decoherence noises over a finite time can be mapped to distinct boundary conditions of a critical Ashkin-Teller model, and entanglement characteristics of the resulting mixed state, such as the g-function and the subsystem entropy, can be calculated accordingly. As an illustration, the mixed state arising from decoherence in the longitudinal direction is characterized by a value of $g = 1/2$, and a subdominant logarithmic term in the second Renyi entropy, with a coefficient equal to $1/8$. On the other hand, when measured or decohered in a $\mathbb{Z}_2$ even basis, *in the stationary state* the von Neumann entanglement entropy can still exhibit a logarithmic scaling for large subsystems. Conversely, when measured or decohered in a $\mathbb{Z}_2$ odd basis, the stationary state exhibits an area law entanglement for arbitrarily small measurement/decoherence rate. These results are organized by their symmetry breaking patterns and are summarized in the boxes in Sec. 4.2. The discussion of the IR behaviours in two spatial dimensions follows a similar approach. Several physical setups that are analyzed in this study have been previously investigated in the literature [173, 113, 63, 177].

This Chapter is structured as follows. In Section 4.1, we present the general framework of the replicated Keldysh effective theory. Specifically, in Section 4.1.1, we introduce the Keldysh path integral for an open system undergoing a Markovian quantum dynamics, which describes decoherence. We also discuss two different microscopic symmetry conditions. Furthermore, in Section 4.1.2, we elaborate on the fundamental consistency conditions of the Keldysh formalism, which are due to consistency conditions of a density matrix. The effect of measurements is discussed in Section 4.1.3, where we re-write it as a Keldysh path integral using the quantum state diffusion framework [83]. In Section 4.1.4, we provide a detailed discussion of the replica symmetries of various cases, in the entire space-time and on its boundary (the time slice where the measurements/decoherence are performed), serving as a guideline for our n-replica IR theory. We then apply this formalism to the critical Ising model in one and two spatial dimensions in Section 4.2. Finally, in Section 4.3, we present a summary of the study in this Chapter and discuss several open questions for future study.

4.1 Generalities

In this section, I present an analysis of the effects of measurement and decoherence on an open quantum system through a replicated Keldysh field theory. For this purpose, it is assumed that the system is nearly critical, where the correlation length is much larger than the lattice spacing, to allow for a valid coarse-grained continuum description. Measurement and decoherence give rise to certain interactions in the effective field theory, and the universal long wave-length physics is studied in Section 4.2 using standard techniques.

To define the question more precisely, let us denote the linear size of our system by L. In this thesis I will focus on two possible physical settings, distinguished by the time scales of the system being measured or experiencing decoherence:

1. One can consider a critical quantum system initially in a pure state that undergoes measurement and decoherence for a finite time interval. It is essential to note that this interval is of the order of unity [$\sim O(1)$] and does not depend on the size of the system. In the thermodynamic limit, interactions resulting from the perturbations are confined to a single time slice in the field theory description. Physical characteristics of the modified quantum state can be determined by studying correlation functions at this time slice.

2. In the second scenario, measurement or decoherence persists over an extensive duration of time, typically of $O(L)$ in the thermodynamic limit. This setup enables an exploration of the properties of stationary states and response functions. Accordingly, interactions resulting from measurement or decoherence are included throughout the time evolution in the Keldysh field theory.

Examples for both scenarios will be provided in Sec. 4.2. The connection between the effect of measurement/decoherence and the boundary or defect properties has been pointed out in recent literature [63, 106]. As typical discussions about low energy physics, we constrain the form of the IR effective field theory based on (1) symmetry of the time evolution; (2) intrinsic consistency conditions of the Keldysh formalism, which emerge from the fundamental properties of a density matrix. To illustrate these constraints, we

examine the Lindblad quantum master equation that describes decoherence in the next two subsections. For the case of measurement, a formalism for trajectory-averaged properties has been proposed in Ref. [16, 102] for measurement-induced phase transitions of Dirac fermions, which will be reviewed in Sec. 4.1.3 and applied to more general cases in Sec. 4.1.4.

4.1.1 The Keldysh action and symmetries

The Keldysh functional integral formulates the time evolution of a density matrix. As an example, we start with a Lindblad quantum master equation that describes an open quantum system under decoherence,

$$\frac{d}{dt}\rho = \mathcal{L}\rho = -i[H,\rho] + \sum_{\alpha} \gamma_\alpha [2L_\alpha \rho L_\alpha^\dagger - \{L_\alpha^\dagger L_\alpha, \rho\}], \tag{4.1}$$

where the Liouvillian $\mathcal{L}$ acts on the density operator ρ from both the ket and the bra sides. The *quantum jump* operators L_α encode the dissipative couplings of the system with its environment. The (single replica) Keldysh partition function is defined as $Z_1 = \mathrm{tr}[\rho(t_f)]$, in which we take the trace of the density matrix at a time t_f. Upon the introduction of external source fields, the partition function plays the role of the generating functional for correlation functions. In terms of coherent state path integral, the non-trivial action of $\mathcal{L}$ on both sides of ρ leads to a doubling of degrees of freedom, characteristic of the Keldysh formalism [87, 149],

$$\begin{aligned} Z_1 &= \int \mathrm{D}\phi_+ \mathrm{D}\phi_- \exp(iS[\phi_+,\phi_-]), \\ S[\phi_+,\phi_-] &= \int_{t,x}^{t_f} \bar{\phi}_+ i\partial_t \phi_+ - \bar{\phi}_- i\partial_t \phi_- - \mathcal{L}[\phi_+,\phi_-], \\ \mathcal{L}[\phi_+,\phi_-] &= H_+ - H_- + i\sum_\alpha \gamma_\alpha [2L_{\alpha,+}L_{\alpha,-}^\dagger \\ &\quad - L_{\alpha,+}^\dagger L_{\alpha,+} - L_{\alpha,-}^\dagger L_{\alpha,-}], \end{aligned} \tag{4.2}$$

where $H_+ = H[\phi_+]$ etc., ϕ_+ and ϕ_- represent the dynamical fields on the forward and backward branches of the Keldysh contour, respectively. We shall employ the notation S_D to represent the decoherence action, which corresponds to the contribution from the quantum jump operator L in the Keldysh action in Eq. (4.2).

Upon doubling the degrees of freedom in the Keldysh functional integral approach, it becomes evident that the Keldysh action may possess a doubled symmetry. Consider a Hamiltonian that is symmetric under a group G, as well as an initial pure state that shares this symmetry. In the absence of dissipative couplings or when all L_α are G invariant, the Keldysh action would exhibit a symmetry of $G_+ \times G_-$, which act on ϕ_+ and ϕ_-, respectively. In terms of the density matrix, they separately operate on the ket and bra sides of ρ. When the system-environment interaction L_α transforms in a non-trivial representation under G, the presence of dissipative coupling reduces the symmetry of the Keldysh action to G. This corresponds to the diagonal subgroup of $G_+ \times G_-$ that operates on the two sides of ρ adjointly.

In Sec. 4.2 we explore both symmetry conditions of the Keldysh action. In Ref. [22, 43], the doubled symmetry is referred to as the *strong* symmetry and the diagonal subgroup as the *weak* symmetry. We adopt this nomenclature throughout this Chapter.

4.1.2 Consistency conditions

The definition of the partition function leads to a series of consistency conditions that the Keldysh action must satisfy, which, together with the symmetries discussed in Sec. 4.1.1 and their n-replica generalizations in Sec. 4.1.4, will serve as the guiding principles for our low energy effective theory. To facilitate our analysis, we introduce a new set of variables,:

$$\phi_c = \phi_+ + \phi_-, \quad \phi_q = \phi_+ - \phi_-. \tag{4.3}$$

The two new fields are usually called the classical and quantum component in literature [86]. Importantly, the Keldysh formalism imposes three consistency conditions.

(1) Conservation of probability: When $\phi_q = 0$, the Keldysh action vanishes identically:

$$S[\phi_c, \phi_q = 0] = 0. \tag{4.4}$$

Intuitively, in the case of $\phi_+ = \phi_-$ the action on the forward branch exactly cancels that on the backward part. More precisely, this requirement is due to the trace-preserving property of the Lindblad master equation Eq. (4.1) and ensures the normalization of the partition function, $Z_1 = \mathrm{tr}[\rho(t_f)] = 1$.

(2) Hermiticity: The density operator ρ should always be Hermitian during the time evolution. In this regard, we consider the path integral representation of matrix elements:

$$\begin{aligned}\langle\phi_1|\rho(t)|\phi_2\rangle &= \int_{\phi_-(t)=\phi_2}^{\phi_+(t)=\phi_1} \mathrm{D}\phi_\pm \exp(iS[\phi_+,\phi_-]) \\ =&\langle\phi_2|\rho(t)|\phi_1\rangle^* = \int_{\phi_-(t)=\phi_1}^{\phi_+(t)=\phi_2} \mathrm{D}\phi_\pm \exp(-iS^*[\phi_+,\phi_-]) \\ =&\int_{\phi_-(t)=\phi_2}^{\phi_+(t)=\phi_1} \mathrm{D}\phi_\pm \exp(-iS^*[\phi_-,\phi_+]),\end{aligned} \tag{4.5}$$

in which the last line is merely a change of integration variables. The two matrix elements calculated above should be equal at any time t, indicating that

$$S[\phi_c,\phi_q] = -S^*[\phi_c,-\phi_q]. \tag{4.6}$$

Given the involvement of complex conjugation, one may consider the Hermiticity condition as an effective time-reversal symmetry. Hereafter, we refer to this constraint as the $\mathbb{Z}_2^T$ symmetry. It is worth noting that in order for this constraint to be fulfilled, the presence of an anti-unitary symmetry at the microscopic level is not a requirement for the system.

(3) Non-negativity: The preservation of non-negativity of ρ during the time evolution is a crucial consideration, particularly in the case of decoherence where the density operator becomes mixed. In the framework of Lindblad dynamics which describes the decoherence process, the non-negativity condition necessitates that all dissipation rates γ_α appearing in the master equation Eq. (4.1) are non-negative [66]. This condition on the other hand also ensures the convergence of the Keldysh path integral. Additionally, this requirement is equivalent to the criterion that the decoherence must be completely positive when viewed as a quantum channel. For $\gamma_\alpha > 0$, one can see that decoherence pushes the density matrix towards its diagonal, which agrees with our physical expectations.

4.1.3 Measurements

In Ref.[16, 102], a formalism for many body systems under continuous measurements was proposed, and used to study monitored fermion dynamics. In this subsection, we will

summarize the results in a manner appropriate for our purposes. A brief derivation of the results can be found in Appendix. C.1.

To achieve a continuum description, we investigate the scenario of weak measurement, where information on a local degree of freedom is acquired at a finite rate, causing continuous changes to the state [83, 15]. On the other hand, local measurements are extensively performed on the entire system. We stress that after a measurement, a pure state still remains pure. The system's collective behavior is captured through various correlation functions that are averaged over the ensemble of post-measurement states. This approach is akin to the calculation of observables in disordered systems, where one averages over the realizations of disorder.

In the first scenario, where measurements are performed at one time slice $t = t_f$, the ensemble of final state is labeled by their outcomes at different measurement locations. The post-measurement density matrix of a specific outcome is represented as

$$\begin{aligned} \rho(t_f) &= V\rho_\Omega V^\dagger, \\ V &= \exp[-\Gamma \int_x M(x)^2 + \sqrt{\Gamma}\int_x W_{t_f}(x)M(x)], \end{aligned} \tag{4.7}$$

where $\Gamma > 0$ is a (small) effective measurement strength, and ρ_Ω denotes the state before measurements. $M(x)$ is the normal-ordered measurement operator – the observable $O(x)$ being measured, subtracted by its expectation value in the initial state ρ_Ω. $W_{t_f}(x)$ is a Gaussian random variable that reflects the stochastic nature of the post-measurement state update. It has zero mean and $\overline{W_{t_f}(x)W_{t_f}(y)} = \delta(x-y)$, where the overline denotes averaging over the ensemble of measurement outcomes.

We also consider continuous measurements that extend over a long period of time. Through time evolution, we generate an ensemble of pure state trajectories, each of which corresponds to a distinct sequence of measurement outcomes. To describe the stochastic evolution of the density operator, we adopt the quantum state diffusion framework [65, 175].

Conditioned on a particular trajectory, the state-update can be expressed as follows:

$$\begin{aligned}\rho(t+dt) =& V_{dt}\rho(t)V_{dt}^{\dagger},\\ V_{dt} =& \exp[-\int_x (iH+\gamma M_t(x)^2)dt\\ &+\sqrt{\gamma}\int_x W_t(x)M_t(x)].\end{aligned} \tag{4.8}$$

Here the local measurement operator is defined as $M_t(x) = O(x) - \mathrm{tr}[\rho(t)O(x)]$, where $O(x)$ is the Hermitian local operator being measured, subtracted by its expectation value before the measurement. The explicit dependence of $M_t(x)$ on the expectation value reflects the measurement feedback to the time evolution. The parameter $\gamma > 0$ represents the measurement strength. $W_t(x)$ is again a Gaussian random variable with zero mean and $\overline{W_t(x)W_{t'}(y)} = dt\delta(x-y)\delta(t-t')$, where the overline denotes averaging over the ensemble of trajectories. The proposed time evolution in Eq. (4.8) can be rationalized by taking the limit of $\gamma \to \infty$, corresponding to a projective measurement where the quantum state rapidly collapses onto an eigenstate of the measured operator O.

The time evolution with measurement can be expressed as a Keldysh path integral straightforwardly. For example, after the Keldysh doubling, the evolution operator V in Eq. (4.8) gives rise to an additional term in Eq. (4.2), given by:

$$S_M[\phi_\pm] = i[\int_{x,t} dt\gamma M_{t,+}^2 - \sqrt{\gamma}W_t M_{t,+} + (+\to -)]. \tag{4.9}$$

An observation is that averaging over the ensemble of state trajectories in a single replica formalism yields the Lindblad form described by Eq.(4.2) with $L_\alpha = O$. This observation can be interpreted as the averaging of the measurement outcome with the corresponding measurement probability, leading to the erasure of the outcome information and resulting in an equivalent decoherence process with a corresponding quantum jump operator.

4.1.4 Replica field theory

This subsection extends the previous discussions in the preceding sections to an n-replica theory. As previously stated in the Introduction, the Keldysh formalism of measurement

and decoherence opens a powerful toolbox of modern quantum field theory. Specifically, symmetries at high energy scales must be preserved under RG flow to long distances. Thus, in a strongly interacting theory, one can examine the long-wavelength physics by writing a generic IR effective action that preserves the symmetry, disregarding the details of the RG flow. In any local quantum field theory, it is essential to differentiate between two notions of symmetry: the symmetry of the effective action in space-time (bulk), and the symmetry of the boundary condition, which, in this case, is the time slice $t = t_f$ [1]. In our forthcoming discussion of n-replica theory, this distinction becomes crucial.

(1) Consider first the measurement scenario, where we are interested in the n-replica partition function $Z_n = \mathrm{tr}[\overline{\rho(t_f)^{\otimes n}}]$, where the trace is taken over a tensor product of n Hilbert spaces and the overline denotes ensemble average. As an example, when measurements are performed throughout the time evolution, the measurement action in Eq. (4.9) becomes

$$\begin{aligned} S_M[\phi_\pm] = i[\int_{x,t} dt\gamma \sum_\alpha (M^{(\alpha)}_{t,+})^2 \\ - \sqrt{\gamma} W_t \sum_\alpha M^{(\alpha)}_{t,+} + (+ \to -)], \end{aligned} \tag{4.10}$$

where α denotes the replica index. Crucially, the stochastic variable W_t couples to all replicas and both branches for each replica in an identical fashion, analogous to the case in disordered systems where the disorder potential couples to all replicas identically. This reflects the fact that all replicas of a single trajectory undergo the same stochastic state update, and the label of this trajectory, i.e., the sequence of measurement outcomes, carries physical significance, as previously stated in the Introduction. The correspondence between the dynamics with measurements and the effects of static disorders was also noted in a previous study [84].

In the absence of measurement, the discussion in Sec. 4.1.1 can be straightforwardly generalized to the n-replica case, revealing that the Keldysh-doubled effective action exhibits a global symmetry $(G_+^{\otimes n} \rtimes S_n) \times (G_-^{\otimes n} \rtimes S_n)$ [10]. Here, the two S_n's represent the permutation group of the $+$ and $-$ branches, respectively. Upon introducing the measure-

[1] In this Chapter, we use the terms "boundary" and "$t = t_f$" interchangeably.

ment action S_M at UV energy scales, the most important information we can extract is about the UV internal symmetry of the theory. Of particular interest are two possibilities:

- We first consider the case where the measurement action S_M preserves the strong $G_+ \times G_-$ symmetry discussed in Sec. 4.1.1. This implies that the stochastic variable W transforms trivially under G, i.e. the measurement is in a local symmetric basis. The bulk of the theory preserves the $(G_+^{\otimes n} \rtimes S_n) \times (G_-^{\otimes n} \rtimes S_n)$ symmetry. However, the boundary condition at $t = t_f$ has only a reduced symmetry of $G^{\otimes n} \rtimes S_n$. This can be understood by noting that, upon taking the trace in the partition function (gluing the boundaries), we make the identification:

$$\phi_+^{(\alpha)}(t_f) = \phi_-^{(\alpha)}(t_f) = \phi_{(\alpha)}. \tag{4.11}$$

  Thus the boundary condition preserves only the simultaneous action on the identified boundaries, along with an S_n permutation of replicas.

- In situations where measurements are conducted in a basis that transforms non-trivially under G, the stochastic variable W is associated with a non-trivial G representation. The measurements action breaks the strong $G_+ \times G_-$ symmetry described in Sec. 4.1.1 down to the weak subgroup. The bulk theory exhibits either the full $(G_+^{\otimes n} \rtimes S_n) \times (G_-^{\otimes n} \rtimes S_n)$ symmetry when the measurement is conducted over a short timescale ($O(1)$), or a reduced $G \times (S_n \times S_n)$ symmetry for an $O(L)$ time measurement. The reason behind this symmetry reduction is the fact that the stochastic variable W couples identically to all the $2n$ Keldysh branches. On the other hand, for our specific interest, the measurement action S_M is always present on time slice $t = t_f$. Upon making the identification Eq. (4.11) at time slice $t = t_f$, the boundary condition has a symmetry $G \times S_n$.

The examples discussed in Sec. 4.2 will be organized based on their patterns of symmetry breaking.

(2) We now shift our attention to the scenario of decoherence. In this case, the n-replica partition function is defined as $Z_n = \mathrm{tr}[\rho(t_f)^n]$. [2] Its path integral representation is given

[2] In the presence of both measurements and decoherence, a unified partition function can be defined as

by the Keldysh effective action in the Lindblad form in Eq. (4.2), with an additional summation over the contributions of the n replicas. The Lindblad action, which describes the system at high energy scales, features an *intra-replica* coupling between the two branches. The underlying interpretation, as explained in the Introduction, is that decoherence erases the measurement outcomes (integrates out the environment) in the first place, and the ensemble representation of a mixed state does not have a preferred basis.

Similarly, we focus on two distinct symmetry conditions:

- First, we examine cases where the strong $G_+ \times G_-$ symmetry is preserved by the decoherence. Depending on the decoherence timescale, the bulk theory may possess either the full $(G_+^{\otimes n} \rtimes S_n) \times (G_-^{\otimes n} \rtimes S_n)$ symmetry for $O(1)$ time decoherence, or a reduced $(G_+ \times G_-)^{\otimes n} \rtimes S_n$ symmetry for $O(L)$ time decoherence. Notably, the intra-replica branch coupling prohibits independent permutation of the two branches. In contrast, the decoherence action S_D is always present at the final time slice, $t = t_f$. To compute the partition function in the case of decoherence, we need to specify the boundary condition

$$\begin{aligned} \phi_+^{(\alpha)}(t_f) &= \phi_-^{(\alpha+1)}(t_f) = \phi_{(\alpha)}, \\ \phi_-^{(\alpha)}(t_f) &= \phi_+^{(\alpha-1)}(t_f) = \phi_{(\alpha-1)}. \end{aligned} \tag{4.12}$$

  The boundary condition exhibits a reduced $G^{\otimes n} \times \mathbb{Z}_n$ symmetry, where $\mathbb{Z}_n$ corresponds to the cyclic permutation of replicas.

- In cases where the decoherence preserves only the weak G symmetry, depending on the time scale of the decoherence, the bulk theory has either the full $(G_+^{\otimes n} \rtimes S_n) \times (G_-^{\otimes n} \rtimes S_n)$ symmetry, or a reduced $G^{\otimes n} \rtimes S_n$ symmetry for $O(L)$ time decoherence. At the boundary $t = t_f$, the symmetry is reduced to $G \times \mathbb{Z}_n$ by the boundary condition in Eq. (4.12).

All the symmetry conditions enumerated in this subsection are considered as internal symmetries of the system under measurement or decoherence at UV energy scales, which

$Z_n = \mathrm{tr}[\overline{\rho(t_f)^n}]$. In this thesis, we consider the effects of measurements and decoherence separately for the sake of simplicity.

must be preserved along the RG flow. Besides the symmetries discussed above, an extra time reversal symmetry $\mathbb{Z}_2^T$ arising from the Hermiticity of the density matrix is imposed for both the measurement and the decoherence scenarios.

After presenting the general formalism and fundamental constraints in this section, we are now prepared to investigate the impact of measurement and decoherence on the long wave-length behavior of specific critical systems. Our strategy is to construct the most general IR effective theory that are allowed by the UV internal symmetries. The IR counterparts of the local measurement operator M and the quantum jump operator L can also be identified, guided by symmetry considerations. Moreover, the Keldysh action must satisfy the consistency conditions outlined in Section 4.1.2.

4.2 Examples: the Ising model

Our analysis focuses on a transverse field Ising model with a $\mathbb{Z}_2$ global symmetry, in one ($1d$) or two ($2d$) spatial dimensions, and is tuned to the vicinity of the Ising critical point. The $\mathbb{Z}_2$ charged operators include the spin Z operator acting on each lattice site. The product of spin X on each site serves as the symmetry generator.

4.2.1 Finite time perturbations: one dimension

To begin, we examine the scenario where the system is subjected to a perturbation, i.e. measurements or decoherence, for a duration of $O(1)$ time. We categorize the possible perturbations based on their symmetry properties. The Ising Hamiltonian exhibits a $\mathbb{Z}_2$ spin flip symmetry, which after the Keldysh doubling, gives rise to a $\mathbb{Z}_2^+ \times \mathbb{Z}_2^-$ symmetry in the long wavelength field theory. Specifically, the $\mathbb{Z}_2^+$ ($\mathbb{Z}_2^-$) symmetry acts on the bra (ket) side of the density matrix.

We first consider the effects of measurements. Using the Keldysh formalism, we prepare the density matrix before measurement by allowing a purely Hamiltonian dynamics to evolve for an infinitely long time, resulting in the projection of the system to the pure ground state. In this setting, the action induced by the measurement described in Eq. (4.7)

is solely present at the final time slice t_f. The partition function can then be calculated by closing the time contour. In a single replica formalism, performing the trajectory-average leads to

$$S_M = i\frac{\Gamma}{2}\int_x (M_+ - M_-)^2, \tag{4.13}$$

which vanishes identically when the time contour is closed and the ket side is identified with the bra side. This observation implies that weak measurements do not affect the scaling behaviors of correlation functions of local operators that are linear in the density matrix. Specifically, the correlation function $\overline{\langle O(0)O(x)\rangle} = \mathrm{tr}[\bar{\rho}(t_f)O(0)O(x)]$ retains the same scaling form as it had in the pre-measurement state, where O denotes a local operator.

However, the situation becomes different when we consider quantities non-linear in density matrix, e.g. the famous von Neumann entropy. We primarily construct a theory with two copies of the density matrix, for the sake of simplicity. We begin by considering the following quantity (at time slice t_f, after measurements):

$$\rho_2 = \overline{\rho \otimes \rho}, \tag{4.14}$$

which is a tensor product of two identical density matrices (conditioned on the same measurement outcome trajectories), and then averaged over the trajectory ensemble. This quantity can be constructed using a two-replica Keldysh effective theory, and the measurement-induced coupling can be expressed, at UV energy scales, as follows:

$$S_M = i\Gamma\int_x \{\sum_{\sigma=\pm}\sum_{\alpha=1}^{2}[M_\sigma^{(\alpha)}]^2 - \frac{1}{2}[\sum_{\sigma,\alpha} M_\sigma^{(\alpha)}]^2\}, \tag{4.15}$$

where $\alpha = 1, 2$ is the replica index.

In order to compute the two-replica partition function $Z_2 = \mathrm{tr}[\overline{\rho(t_f)^{\otimes 2}}]$, it is necessary to glue the time slice t_f with the boundary condition in Eq. (4.11). It should be noted that the bulk far from the time slice t_f is always described by an Ising conformal field theory (CFT). Depending on the basis in which the system is being measured, we consider two scenarios, distinguished by symmetry of the measurement operator.

(1) When measuring a system in a symmetric basis, such as along the X basis, the measurement operator conserves the spin flip symmetry. In the case of two replicas, the

internal symmetry of the UV theory described by Eq. (4.15) reduces to $\mathbb{Z}_2^2 \times \mathbb{Z}_2^{(p)}$ at the boundary $t = t_f$. Here $\mathbb{Z}_2^{(p)}$ denotes the replica permutation symmetry. To capture the effects of measurement at low energies, we must enumerate all local interactions in the IR effective theory that are consistent with this symmetry. The dominant contribution to the IR effective theory can be expressed as

$$S_M^{IR} = -i\Gamma\epsilon_{(1)} \cdot \epsilon_{(2)} + ..., \tag{4.16}$$

where terms with higher scaling dimensions have been omitted. Meanwhile, the dominant contribution to the measurement operator M at low energies can be identified as $M \sim \epsilon$. Several comments follow:

1. The derivation of the IR effective action S_M^{IR} from the UV theory in Eq. (4.15) is generally not feasible due to the strongly-interacting nature of the underlying system. The only information we have is that S_M^{IR} retains the global symmetry of the UV theory.

2. An additional term proportional to $\epsilon_{(1)} + \epsilon_{(2)}$ in Eq.(4.16) could also preserve the symmetry of the boundary condition. However, the $(1+1)d$ Ising model has an emergent symmetry – the Kramers-Wannier duality which flips the sign of $M_{(1)} \sim \epsilon_{(1)}$ and $M_{(2)} \sim \epsilon_{(2)}$ simultaneously in Eq. (4.15). As a consequence, this symmetry forbids the inclusion of the aforementioned coupling. It should be noted that this is a specific feature of the $(1+1)d$ Ising model[3].

3. It is worth noting that the interaction given in Eq. (4.16) preserves the $\mathbb{Z}_2^T$ time reversal symmetry, which acts on the $t = t_f$ slice as a complex conjugation. Note that according to our convention in Eq.(4.6), a minus sign obtained by S_M^{IR} under $\mathbb{Z}_2^T$ implies time reversal invariance.

[3]Strictly speaking, here the unperturbed UV fixed point is considered as an Ising CFT with an enlarged symmetry. In terms of a lattice model perspective, this corresponds to a scenario in which the measurement operator M transforms nicely (with only a -1 factor) under the Kramers-Wannier duality even at high energy scales.

As the scaling dimension of ϵ in the $(1+1)d$ Ising CFT is $\Delta_\epsilon = 1$, S_M^{IR} is irrelevant on the 1D time slice t_f. The full symmetry of the original UV theory will remain preserved in the IR, and the scaling of correlation functions and the Renyi entropy remains unchanged.

Before proceeding, let me briefly comment on the scenario where the operator M severely breaks the Kramers-Wannier duality at UV energy scales. It is then necessary to include the perturbation $S_M^{IR} = -i\Gamma'[\epsilon_{(1)} + \epsilon_{(2)}]$ which is exactly marginal at the defect $t = t_f$. Consequently, the scaling of the Renyi entropy and correlation functions exhibits continuous variation depending on the measurement strength [44, 128, 14]. However, if one performs an analytical continuation of the number of replicas to $n \to 1^+$, the coefficient Γ' must vanish due to the reasoning around Eq. (4.13) – the single replica measurement action (for $O(1)$ time measurements) vanishes identically. Therefore, in the $n \to 1^+$ limit these scalings, such as the von Neumann entanglement entropy, would remain unaffected by this exactly marginal ϵ linear term, see Eq. (4.18). As a result,

> Measurements performed in a symmetric basis over a finite period of time, in $(1+1)d$ Ising CFT do not affect the scaling properties of trajectory-averaged correlation functions linear or non-linear in the density operator, as well as that of the von Neumann entanglement entropy.

(2) In the case of measurements performed in a $\mathbb{Z}_2$ odd basis, such as the local Z basis, for the two-replica case the symmetry at $t = t_f$ becomes $\mathbb{Z}_2 \times \mathbb{Z}_2^{(p)}$. At long distances the operator M should be identified with the most relevant local operator with the same symmetry property, namely $M \sim \sigma$, the spin field. A similar enumeration yields the measurement-induced coupling for measurements performed in a $\mathbb{Z}_2$ odd basis

$$S_M^{IR} = -i\Gamma\sigma_{(1)} \cdot \sigma_{(2)}, \tag{4.17}$$

where the most relevant contribution is retained. Unlike the symmetric measurement, here we have a relevant perturbation on the time slice given $\Delta_\sigma = \frac{1}{8}$. In effect, we have two copies of Ising CFT coupled to each other on a line defect (the time slice $t = t_f$). Each copy acts as a symmetry-breaking field for the other – therefore both copies would be

cut open at the $1d$ defect $t = t_f$, and in total we have four decoupled halves. Given the measurement rate $\Gamma > 0$ [4], this coupling favors configurations in which spins at the edge of the four halves are parallel.

How to characterize the trajectory ensemble under $\mathbb{Z}_2$ odd measurements? Cardy established [26, 27] that there are only three universality classes of boundary conditions for an Ising CFT on a semi-infinite plane: fixed-up ($\uparrow$), fixed-down ($\downarrow$), and free (f). As discussed earlier, the two copies of Ising CFT are cut open at the line defect, and the spins on the edge of the four halves have a parallel orientation. Despite the naive expectation of spontaneous breaking of the $\mathbb{Z}_2$ spin flip subgroup of the boundary symmetry, we do not anticipate any genuine symmetry breaking in the $(1+0)d$ time slice at $t = t_f$. Therefore, each of the four halves has a fixed boundary condition, and the boundary state can be written symbolically as $|\uparrow\uparrow\uparrow\uparrow\rangle + |\downarrow\downarrow\downarrow\downarrow\rangle$.

This finding has significant implications on the entanglement entropy of the system subject to measurements. Consider a subsystem A of length l, and let us compute the trajectory-averaged 2nd Renyi entropy defined as $S_A^{(2)} = -\overline{\ln(\mathrm{tr}\rho_A^2)}$, where ρ_A is the reduced density matrix of A. It has been demonstrated in Ref. [24, 23] that the Renyi entropy can be computed on a space-time manifold with a boundary condition at the time slice $t = t_f$, such that (1) Inside A, the n replicas are sewn together cyclically, leading to the identification in Eq. (4.12); (2) Outside A, each replica is sewn with itself, as that in Eq. (4.11). In the specific case of the Ising model, it can be checked that the boundary state inside and outside the subsystem A remains the same, see Fig. 4.1.[5]

[4] In principle, the functional dependence of the IR coupling constant on the microscopic measurement rate Γ can be complicated. Nonetheless, we anticipate that it will remain non-negative due to the physical expectation that measurements tend to project the density matrix onto its diagonal elements, as outlined in the Introduction. Moreover, this term has a clear UV correspondence in the measurement action at high energies if one substitutes $M \sim \sigma$ into Eq. (4.15), where the coefficient is indeed the (positive) microscopic measurement rate. As a relevant coupling, we expect it to increase monotonically along the RG flow. Hence, we use the notation Γ for both the microscopic measurement rate and the IR coupling constant.

[5] Upon examination of the boundary condition at $t = t_f$, the measurement action S_M within subsystem A is found to exhibit either a $G^{\otimes n} \times \mathbb{Z}_n$ symmetry (for measurements in a symmetric basis) or a $G \times \mathbb{Z}_n$ symmetry (for measurements in a G non-trivial basis) at high energies. For $n = 2$, the symmetries inside and outside of subsystem A coincide.

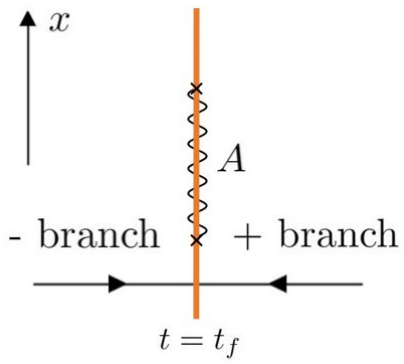

Figure 4.1: Illustration of the boundary condition at $t = t_f$. Time evolution of the density matrix is captured by two Keldysh branches running horizontally, while the vertical line denotes the spatial dimension. The orange line marks the region where S_M is non-vanishing, and the wavy line represents subsystem A (the branch cut), where the entanglement entropy is calculated.

In the case of measurements performed in a symmetric basis, the measurement induced coupling Eq. (4.16) on the defect is irrelevant (provided that the Kramers-Wannier duality is present). Thus the Renyi entropy remains the same as the case without the defect. Ref. [24] demonstrated that the Renyi entropy can then be related to scaling dimension of the twist field in Ising CFT (located at endpoints of the subsystem A), given by $S_A^{(2)} = \frac{1}{8}\ln l + O(1)$. In the limit $n \to 1^+$, the scaling of the ensemble-averaged von Neumann entanglement entropy $S_A = -\overline{\mathrm{tr}(\rho_A \ln \rho_A)}$, for any generic $\mathbb{Z}_2$ symmetric measurements (with or without the Kramers-Wannier duality) , behaves as

$$S_A = \frac{1}{6}\ln l + O(1). \tag{4.18}$$

In the scenario where measurements in a $\mathbb{Z}_2$ odd basis are carried out, the induced coupling by the measurement is relevant, thereby causing the system to be cut open at the $1d$ defect. The Renyi entropy is then calculated by the scaling dimension of certain boundary condition changing operator of the Ising boundary CFT. It is observed that, no matter inside or outside the subsystem A, the defect will always flow to the fixed boundary

condition with the aforementioned boundary state. Consequently, the boundary condition changing operator at endpoints of A is trivial. It is then deduced that the 2nd Renyi entropy saturates for large l, $S_A^{(2)} = O(1)$. In the limit of $n \to 1^+$, the validity of this area law remains for the von Neumann entanglement entropy.

> In a $(1+1)d$ Ising CFT, when measurements are performed in a $\mathbb{Z}_2$ odd basis over a finite time, the trajectory-averaged entanglement entropy of a subsystem saturates to a constant for sufficiently large subsystems.

The effect of decoherence, which is described by a Keldysh effective action in the Lindblad form, can be studied similarly. The fundamental quantity of interest is the n-replica Keldysh partition function, $Z_n = \mathrm{tr}[\rho(t_f)^n]$. It is instructive to note a basic observation before examining specific decoherence. Let us denote the decoherence action by S_D, which is non-zero only at the time slice t_f. Consider the effect of decoherence over a finite time in a single replica formalism. When taking the trace in the partition function, $\phi_+(t_f)$ and $\phi_-(t_f)$ are identified. Conservation of probability, as given by Eq. (4.4), leads to the vanishing of the decoherence action S_D. This, combined with our previous statement, yields the following results:

> Weak measurement and decoherence over a finite period of time have no impact on the scaling behaviors of local operator correlation functions that are linear in the density operator.

This is a general statement that extends to higher-dimensional systems as well. In the following discussion, we will concentrate on quantities that are non-linear in the density operator. Depending on the symmetry of the Lindbladian, we consider two possible scenarios.

(1) Let us first consider decoherence which preserves the strong $\mathbb{Z}_2^+ \times \mathbb{Z}_2^-$ symmetry, for example, a dephasing in the X basis. Based on this symmetry, the low energy incarnation of the quantum jump operator should be identified as $L \sim \epsilon$. As previously mentioned, the

boundary condition at $t = t_f$ preserves a $\mathbb{Z}_2^2 \times \mathbb{Z}_2^{(p)}$ symmetry, as well as a $\mathbb{Z}_2^T$ time reversal invariance.

Now the aim is to enumerate all possible local interactions that maintain the $\mathbb{Z}_2^2 \times \mathbb{Z}_2^{(p)}$ symmetry of the UV theory. The leading contribution is

$$S_D^{IR} = -i\gamma_D \int_x \epsilon_{(1)} \cdot \epsilon_{(2)}. \tag{4.19}$$

It is easy to see that this decoherence induced interaction is irrelevant on the $1d$ defect. As a result, the scaling behavior of the decohered state is identical to that without decoherence.[6] For instance, the subsystem Renyi entropy scales as

$$S_A^{(2)} = \kappa l + \frac{1}{8}\ln l + O(1), \tag{4.20}$$

where κ is a scheme-dependent non-universal factor which can not be determined in the low energy field theory. It should be noted that we are currently dealing with a mixed state ρ in the presence of decoherence, thus such a non-universal contribution from the configurational entropy is expected to appear.

(2) In the scenario of decoherence in a $\mathbb{Z}_2$ odd basis, such as a dephasing in the Z direction, the Keldysh effective action preserves only a weak $\mathbb{Z}_2$ symmetry. At $t = t_f$, the UV symmetries of the boundary for two replicas are $\mathbb{Z}_2 \times \mathbb{Z}_2^{(p)}$ and the time reversal $\mathbb{Z}_2^T$. To construct an IR effective action, it is necessary to identify all local interactions that are consistent with this symmetry. The dominant contribution arises from

$$S_D^{IR} = -i\gamma_D \int_x \sigma_{(1)} \cdot \sigma_{(2)}, \tag{4.21}$$

where the notation stems from the identification of fields at the boundary, $\sigma_+^{(1)}(t_f) = \sigma_-^{(2)}(t_f) := \sigma_{(1)}$ and $\sigma_-^{(1)}(t_f) = \sigma_+^{(2)}(t_f) := \sigma_{(2)}$. Meanwhile, at IR the quantum jump

[6] Again, by assuming the emergence of the Kramers-Wannier duality as an approximate symmetry, an exactly marginal contribution to the decoherence action given by $S_D^{IR} \sim -i\gamma_D'[\epsilon_{(1)} + \epsilon_{(2)}]$ is not included. However, if the quantum jump operator L significantly breaks the Kramers-Wannier duality, this term should be taken into account. Incorporating this term induces a continuous variation in the scaling behavior of correlation functions and the Renyi entropy as the decoherence rate γ_D' varies. However, it has no impact on these quantities in the $n \to 1^+$ limit where γ_D' vanishes. As a result, the von Neumann entanglement entropy remains as $S_A = \kappa_1 l + \frac{1}{6}\ln l + O(1)$ where l is the subsystem size.

operator should be identified with the most relevant local operator that is $\mathbb{Z}_2$ odd, $L \sim \sigma$. As in the measurement scenario in Eq. (4.17), this interaction is relevant and flows to strong coupling at long distances. The non-negativity constraint in Eq. (4.2) at high-energy scales[7], as well as the physical expectation that decoherence pushes the density matrix towards its diagonal elements, suggest that the strength of decoherence γ_D should be positive and increase monotonically as we flow towards lower energy scales.

Notably, despite the similarity between the expression for decoherence in Eq. (4.21) and that for measurement, the Renyi entropy displays rather different features in the two scenarios. As illustrated in Fig. 4.2, while measurement induces the same boundary state inside and outside the subsystem A, the decoherence action S_D leads to distinct boundary states in these regions. Here, A refers to the subsystem for which the entropy is being computed.

Let us elucidate this point for the 2nd Renyi entropy. Inside the subsystem A, upon closing the time contour we have the boundary condition in Eq. (4.12), which yields the interaction term in Eq. (4.21) at low energies, identical to the one derived in the measurement scenario in Eq. (4.17). Consequently, inside A, the four halves of the two copies of Ising CFT are cut open at the line defect, with spins on the edge being parallel to each other. In contrast, when closing the time contour outside the subsystem A, the resulting S_D^{IR} vanishes. This is due to the fact that closing the time contour within each replica itself leads to $\sigma_+^{(\alpha)}(t_f) = \sigma_+^{(\alpha)}(t_f)$ at the line defect for both replicas, and the conservation of probability causes S_D^{IR} to vanish identically. Therefore, outside A, the defect flows to a boundary state as if no defect were present.

What is the consequence of this observation on the subsystem entropy? Consider an Ising CFT on a complex plane with a line defect. Upon folding the system at the defect line, the defect of the Ising CFT maps to the boundary of a critical Ashkin-Teller model [64] on a semi-infinite plane. The decoherence induced interaction inside the subsystem A leads to a fixed boundary condition where the spins on either side of the defect are locked into a ferromagnetically aligned state, while outside A, the boundary state of the Ashkin-Teller model corresponds to a trivial defect in the Ising CFT. The corresponding

[7]The UV correspondence of the interaction in Eq.(4.21) becomes clear upon substitution of $L \sim \sigma$ into Eq.(4.2), with the coefficient γ_D relating to the non-negative microscopic dissipation rate.

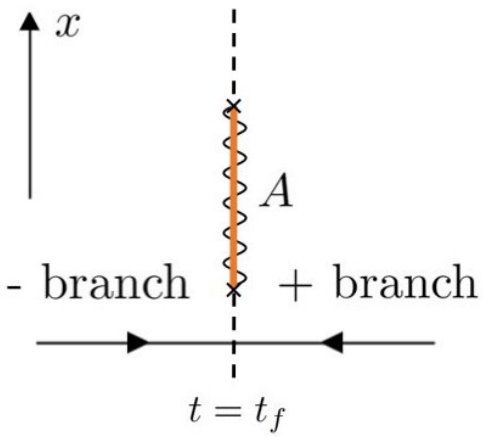

Figure 4.2: Illustration of the boundary condition at $t = t_f$ for the case of decoherence. The orange line indicates the region where S_D is present (inter-replica gluing), while the dashed line denotes a trivial defect (intra-replica gluing). It is noteworthy that the boundary conditions are different inside and outside subsystem A, where the entanglement entropy is evaluated.

boundary condition changing operator at endpoints of A in the Ashkin-Teller boundary CFT has a dimension of $\Delta = 1/32$ [126, 125]. Therefore, the 2nd Renyi entropy of the decohered state is expressed as

$$S_A^{(2)} = \kappa' l + \frac{1}{8}\ln l + O(1), \tag{4.22}$$

where the $1/8$ factor corresponds to $2 \times 2\Delta$ as we calculate the 2nd Renyi entropy using two copies of Ashkin-Teller boundary CFT. Upon taking the limit $n \to 1^+$, we find that the scaling of the von Neumann entanglement entropy follows an expression $S_A = \kappa_1' l + \frac{1}{16}\ln l + O(1)$.

The defect g-function, as defined in previous works [26, 27, 3] by $\ln g = (1-d/d\ln L)\ln Z_2(L)$ with L being the linear system size, can be calculated accordingly. Physically, g represents the overlap between the ground state of the Hamiltonian with periodic boundary condition and the boundary state. With symmet- ric decoherence, the irrelevance of the defect coupling leads to two decoupled trivial line defects in the Ising CFT, resulting in $g = 1$.[8] Conversely, in the case of decoherence in an $\mathbb{Z}_2$ odd basis, as previously described, the boundary state $|\uparrow\uparrow\uparrow\uparrow\rangle + |\downarrow\downarrow\downarrow\downarrow\rangle$ has four copies of ferromagnetically aligned Ising fixed boundary conditions. The g-function is obtained by taking the product of g for the four Ising layers, with an additional factor of 2 accounting for the multiplicity of $\uparrow$ and $\downarrow$. Thus, we have $g = 2 \times (1/\sqrt{2})^4 = 1/2$. Further breaking of the weak $\mathbb{Z}_2$ symmetry, such as decoherence in a direction slightly deviating from the Z axis, would result in the removal of this degeneracy, resulting in $g = 1/4$. Our results are consistent with those observed in a recent study [184]. Therefore, we have

> A $(1+1)d$ Ising CFT under decoherence over a finite period of time can be mapped to the boundary CFT of the critical Ashkin-Teller model, enabling us to analyze the entanglement characteristics in a precise manner.

This concludes our discussion on a finite time perturbation in $1d$.

[8] Even in cases where the Kramers-Wannier duality does not emerge and the contribution specified in Footnote. 6 is included, the exact marginality of this term ensures that g retains its original value, i.e., $g = 1$.

4.2.2 Finite time perturbations: two dimensions

Now we investigate the impact of an $O(1)$ time perturbation on a $(2+1)d$ system, specifically by considering the $(2+1)d$ Ising critical point as a case study. Throughout this subsection we focus on the two-replica formalism.

We begin with local measurements performed in a symmetric basis, where the associated local measurement operator is Z_2 even, and the action S_M induced by the measurement preserves a $\mathbb{Z}_2^2 \times \mathbb{Z}_2^{(p)}$ symmetry and the time reversal invariance due to Hermiticity. Note that in the case of $(2+1)d$ Ising model, the Kramers-Wannier duality is absent, resulting in the leading contribution to S_M^{IR} being given by

$$S_M^{IR} = -i\gamma_M(\epsilon_{(1)} + \epsilon_{(2)}). \tag{4.23}$$

where now the coupling is present on a $(2+0)d$ defect in the $(2+1)d$ space-time. Utilizing $\Delta_\epsilon = 1.41$ in $(2+1)d$ Ising CFT [150], we establish that this coupling is relevant[9]. Depending on the sign of the coupling constant γ_M, without further fine tuning, there can be two possible scenarios:

1. In the scenario where $\gamma_M > 0$, space-time of the system is cut open at the time slice $t = t_f$. the boundary at the cut is pushed to the ordinary boundary condition of a $(2+1)d$ critical Ising model, while the full symmetry of the UV theory is preserved in the IR. This scenario is expected to occur when the measurement is conducted, for example, in the local X basis.

2. For $\gamma_M < 0$, the coupling term again cuts the system at $t = t_f$, resulting in four open boundaries labeled as $(1,+)$, $(1,-)$; $(2,+)$, $(2,-)$, corresponding to the replica indices and the branch labels, respectively. The first and last two boundaries flow separately towards the extraordinary boundary universality class, leading to the spontaneous breaking of the $\mathbb{Z}_2^2$ symmetry of the original UV boundary condition. A breaking of the $\mathbb{Z}_2^{(p)}$ replica permutation takes place when the spin orientations of the two pairs are not the same. This scenario is expected to occur when the measurement is performed in the local Z_iZ_j basis.

[9] Since this term is relevant as opposed to marginal, its impact cannot be disregarded even in the $n \to 1^+$ limit.

When the measurement is in a $\mathbb{Z}_2$ odd basis, S_M at high energies preserves a $\mathbb{Z}_2 \times \mathbb{Z}_2^{(p)}$ symmetry. Recall that the $\mathbb{Z}_2$ arises from the weak spin flip symmetry that acts adjointly on both sides of the density matrix. At low energies, the dominant contribution to S_M^{IR} is again given by Eq. (4.17), with the local measurement operator identified with the Ising spin σ at long distances. Since $\Delta_\sigma = 0.52$ in $(2+1)d$, S_D^{IR} is relevant on the plane defect. As each replica can be viewed as a symmetry breaking field for the other, this coupling is expected to cut each replica into two halves. The four open boundaries at the plane defect are at the normal fixed point [19, 13, 25], with ferromagnetic alignment of spins on these boundaries, as $\Gamma > 0$. This causes the $\mathbb{Z}_2$ spin flip symmetry to be spontaneously broken at the plane defect. The trajectory-averaged correlation functions can be calculated accordingly. For example, we expect the connected correlation function

$$\overline{\langle Z(0)Z(x)\rangle} - \overline{\langle Z(0)\rangle\langle Z(x)\rangle} \sim O(1) \text{ const}, \tag{4.24}$$

where Z is the spin Z operator (or a generic $\mathbb{Z}_2$ odd operator). This long range order reveals the spontaneous $\mathbb{Z}_2$ symmetry breaking in the trajectory ensemble after measurement.

In the presence of decoherence, the effect on critical systems can be analyzed in a similar manner. In the case of decoherence occurring in a symmetric basis, the resultant S_D^{IR} is characterized by a $\mathbb{Z}_2^2 \times \mathbb{Z}_2^{(p)}$ symmetry of the UV boundary condition. The leading contribution to S_D^{IR} is given by $S_D^{IR} = -i\gamma_D(\epsilon_{(1)} + \epsilon_{(2)})$, which is relevant on a $(2+0)d$ defect in $(2+1)d$ spacetime. Long-wavelength behaviours are analyzed in the same manner as those below Eq. (4.23).

In the case of decoherence occurring in a local $\mathbb{Z}_2$ odd basis, the boundary condition at $t = t_f$ has a $\mathbb{Z}_2 \times \mathbb{Z}_2^{(p)}$ symmetry at UV. In a two-replica scheme, the leading contribution of the decoherence action is again given by Eq. (4.21), which drives the defect plane $t = t_f$ to a normal fixed point for both replicas. The $\mathbb{Z}_2$ spin flip symmetry is broken spontaneously, which is manifested by a non-zero long-range order:

$$\mathrm{tr}[\rho(t_f)Z(0)\rho(t_f)Z(x)]/\mathrm{tr}[\rho(t_f)^2] \sim \text{const}. \tag{4.25}$$

Additionally, given the expectation that decoherence tends to suppress the off-diagonal elements of the density matrix, and the correspondence between the coupling γ_D and the microscopic dissipation rate at high energies, it is reasonable to assume that γ_D remains

positive in the IR, and consequently the $\mathbb{Z}_2^{(p)}$ symmetry is preserved. Intriguingly, akin to the $1d$ case, when calculating subsystem Renyi entropy, distinct time contour closings at the plane defect lead to distinct boundary states inside and outside the subsystem A. Consequently, we have a boundary condition changing line defect at the edge of A. A comprehensive study of this line defect remains an interesting unresolved issue for future investigations.

4.2.3 The stationary state: one dimension

In this subsection, we investigate an alternative physical scenario, specifically a critical Hamiltonian subjected to a perturbation (measurement or decoherence) for a duration of $O(L)$ time comparable to the system size, resulting in the system achieving a stationary state. To exemplify this scenario, we utilize the critical Ising model in $(1+1)d$ and examine the entanglement characteristics of the stationary state.

We begin with a continuous weak measurement in a local $\mathbb{Z}_2$ symmetric basis, for example, in the X direction. The n-replica measurement action at the UV energy scales in Eq. (4.10) preserves a $(\mathbb{Z}_2^{\otimes n} \rtimes S_n) \times (\mathbb{Z}_2^{\otimes n} \rtimes S_n)$ symmetry in the bulk space-time. The most general IR effective action allowed by the UV internal symmetry can be expressed as

$$\begin{aligned} S_M^{IR} = &- i \int_{x,t} \sum_{\alpha \neq \beta} [\gamma_1 \epsilon_+^{(\alpha)} \cdot \epsilon_+^{(\beta)} + \gamma_1^* \epsilon_-^{(\alpha)} \cdot \epsilon_-^{(\beta)}] \\ &- i \int_{x,t} \gamma_2 \sum_{\alpha,\beta} \epsilon_+^{(\alpha)} \cdot \epsilon_-^{(\beta)}, \end{aligned} \tag{4.26}$$

where γ_2 is real due to the $\mathbb{Z}_2^T$ symmetry[10]. Notably, this is a marginal interaction in $(1+1)d$ Ising CFT. Here, we determine the long-distance behavior through a perturbative RG.

Using Jordan-Wigner transformation [141], we map the Ising model to a free Majorana

[10] In this subsection we ignore the term linear in ϵ by assuming the preservation of the Kramers-Wannier duality. If this assumption is relaxed, a term $S_M^{IR} = -i \int_{x,t} \sum_\alpha [\gamma_1 \epsilon_+^{(\alpha)} + \gamma_1^* \epsilon_-^{(\alpha)}]$ needs to be taken into account, which is relevant and results in an area law entangled phase.

fermion and obtain the full low energy effective theory,

$$\begin{aligned} S^{IR} &= \int_{x,t} \sum_{\alpha} \bar{\chi}_\alpha i\partial\chi_\alpha - \bar{\psi}_\alpha i\partial\psi_\alpha + S_M^{IR}, \\ S_M^{IR} &= -i\int_{x,t} \sum_{\alpha\neq\beta} (\gamma_1 \bar{\chi}_\alpha\chi_\alpha\bar{\chi}_\beta\chi_\beta + \gamma_1^* \bar{\psi}_\alpha\psi_\alpha\bar{\psi}_\beta\psi_\beta) \\ &\quad -i\int_{x,t} \gamma_2 \sum_{\alpha,\beta} \bar{\chi}_\alpha\chi_\alpha\bar{\psi}_\beta\psi_\beta, \end{aligned} \tag{4.27}$$

in which χ and ψ correspond to Majorana fermions on the forward and backward branches, respectively. The energy field ϵ is mapped to the Majorana mass [145]. The beta function at the one-loop level is given by[11]

$$\begin{aligned} \frac{d\gamma_1}{d\ln\mu} &= -\frac{4(n-2)i}{2\pi}\gamma_1^2 + \frac{ni}{2\pi}\gamma_2^2, \\ \frac{d\gamma_2}{d\ln\mu} &= \frac{4(n-1)i}{2\pi}\gamma_1^*\gamma_2 - \frac{4(n-1)i}{2\pi}\gamma_1\gamma_2, \end{aligned} \tag{4.28}$$

where μ denotes a cutoff scale.

Our primary focus is on the $n \to 1$ regime, where we can gain insight into the scaling behavior of the von Neumann entanglement entropy. We assume that γ_1 and γ_2 are real and positive at high energies, as they can be identified with the microscopic measurement rate at the UV scale. In the $n \to 1$ limit, γ_1 rapidly flows to its fixed point value $\gamma_1^{\text{fp}} \sim -i\gamma_2/2$, as depicted in Fig. 4.3. On the other hand, the value of γ_2 drifts slowly according to

$$\frac{d\gamma_2}{d\ln\mu}|_{\gamma_1=\gamma_1^{\text{fp}}} = -\frac{4(n-1)}{2\pi}\gamma_2^2. \tag{4.29}$$

Therefore, γ_2 is a marginally relevant perturbation. Physically, we anticipate that the system flows to an Ising disordered/ordered phase (depending on the basis of the measurements) at the longest wavelength, with a vanishing drifting velocity in the replica limit $n \to 1^+$.[12]

[11] The propagator of χ on the forward branch has an $i\eta$ prescription opposite to that of ψ in Keldysh field theory. This is crucial when performing the Wick rotation.

[12] We can physically understand this by noting that when $n = 1$, the γ_1 term disappears, and the γ_2 term reduces to an exactly marginal deformation $\sim \epsilon_1\epsilon_2$ of the Ashkin-Teller model.

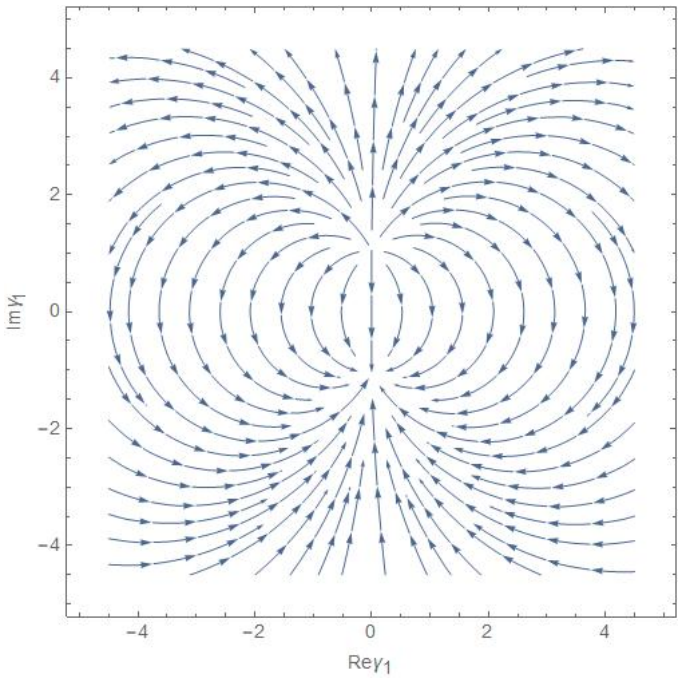

Figure 4.3: RG flow of the parameter γ_1 in the complex plane. In the limit of $n \to 1^+$, the flow of γ_2 is much slower than that of γ_1. Hence, when discussing the flow of γ_1, we can treat γ_2 as a constant. The plot shows the RG flow for $n = 1.05$ and $\gamma_2 = 2$.

This observation suggests intriguing scaling behaviors of the trajectory-averaged entanglement entropy. Specifically, the RG flow in Eq.(4.29) implies that, for n sufficiently close to 1, a correlation length much larger than any subsystem size l can always be generated. Therefore, if a critical Ising Hamiltonian is placed in an environment with $\mathbb{Z}_2$ symmetric measurements at a small measurement rate, after an extensive period of time the von Neumann entanglement entropy of a subsystem should still exhibit a logarithmic scaling with respect to l for very large subsystems. Alternatively, if a product state with zero entanglement is initially prepared and the system is subsequently evolved according to the combined dynamics described in Eq. (4.27), the entanglement entropy of a subsystem is expected to show a logarithmic growth over time, eventually reaching a size-dependent value for sufficiently large time. The effective central charge, which governs the logarithmic growth of entanglement, may vary continuously with the measurement rate γ_2 at microscopic scales. Indeed, this phenomenon was recently observed in a numerical study [160].

In the case of measurements conducted in a $\mathbb{Z}_2$ odd basis, for instance, the local Z basis, at high energies the n-replica measurement action in Eq. (4.10) preserves a $\mathbb{Z}_2 \times S_n \times S_n$ symmetry and a $\mathbb{Z}_2^T$ time reversal. The leading contribution at the low energies is

$$\begin{aligned} S_M^{IR} = &- i \int_{x,t} \sum_{\alpha \neq \beta} \{ [\gamma_1 \sigma_+^{(\alpha)} \cdot \sigma_+^{(\beta)} + \gamma_1^* \sigma_-^{(\alpha)} \cdot \sigma_-^{(\beta)}] \\ &+ \sum_{\alpha,\beta} \gamma_2 \sigma_+^{(\alpha)} \cdot \sigma_-^{(\beta)} \}. \end{aligned} \tag{4.30}$$

This is a relevant perturbation that would drive the state to an area law entangled phase where the $\mathbb{Z}_2$ spin flip symmetry is spontaneously broken in a ferromagnetic manner[13].

For a critical Ising chain subject to weak measurements in a local $\mathbb{Z}_2$ symmetric basis, it is anticipated that the logarithmic scaling of the von Neumann entanglement

[13] In light of the tendency for measurement to project the density matrix onto its diagonal and the correspondence at high energies between the coupling γ_2 and the microscopic measurement rate, it is reasonable to hypothesize that γ_2 retains its positivity along the RG flow. This, in turn, implies that the magnetizations of different replicas are ferromagnetically aligned, preserving the $S_n \times S_n$ replica permutation symmetry at low energies.

entropy can still be observed for large subsystems in the stationary state (provided that the Kramers-Wannier duality is present). On the other hand, when measurements are conducted in a $\mathbb{Z}_2$ odd basis, the stationary state is in a phase characterized by spontaneous breaking of the $\mathbb{Z}_2$ spin flip symmetry and an area law entanglement entropy.

Consideration can also be given to the characteristics of a quantum system with a critical Hamiltonian that undergoes decoherence over an extensive period of time. When the decoherence preserves the strong $\mathbb{Z}_2^+ \times \mathbb{Z}_2^+$ symmetry, the n-replica Lindblad action exhibits a $(\mathbb{Z}_2 \times \mathbb{Z}_2)^{\otimes n} \rtimes S_n$ symmetry and is time reversal invariant. The IR effective action may include all local interactions that are allowed by this symmetry. Among these couplings, the dominant contribution is given by

$$\begin{aligned} S_D^{IR} = &-i \int_{x,t} \sum_{\alpha \neq \beta} [\gamma_1 \epsilon_+^{(\alpha)} \cdot \epsilon_+^{(\beta)} + \gamma_1^* \epsilon_-^{(\alpha)} \cdot \epsilon_-^{(\beta)}] \\ &- i \int_{x,t} [\gamma_2 \sum_{\alpha \neq \beta} \epsilon_+^{(\alpha)} \cdot \epsilon_-^{(\beta)} + \gamma_3 \sum_{\alpha} \epsilon_+^{(\alpha)} \cdot \epsilon_-^{(\alpha)}], \end{aligned} \tag{4.31}$$

where γ_2 and γ_3 are real and positive parameters at high energies. By applying a Jordan-Wigner duality, it can be demonstrated that the one-loop beta function for the coupling constants is as follows:

$$\begin{aligned} \frac{d\gamma_1}{d\ln\mu} =& -\frac{4(n-2)i}{2\pi}\gamma_1^2 + \frac{(n-2)i}{2\pi}\gamma_2^2 + \frac{2i}{2\pi}\gamma_2\gamma_3, \\ \frac{d\gamma_2}{d\ln\mu} =& \frac{4(n-2)i}{2\pi}\gamma_1^*\gamma_2 - \frac{4(n-2)i}{2\pi}\gamma_1\gamma_2 \\ &+ \frac{4i}{2\pi}\gamma_1^*\gamma_3 - \frac{4i}{2\pi}\gamma_1\gamma_3, \\ \frac{d\gamma_3}{d\ln\mu} =& \frac{4(n-1)i}{2\pi}\gamma_1^*\gamma_2 - \frac{4(n-1)i}{2\pi}\gamma_1\gamma_2. \end{aligned} \tag{4.32}$$

In the replica limit, the values of γ_1 and γ_2 quickly approach their fixed point values, with $\gamma_1^{\text{fp}} \sim -i\gamma_3/2$ and $\gamma_2^{\text{fp}} \sim \gamma_3$, while the slow parameter γ_3 flows according to

$$\frac{d\gamma_3}{d\ln\mu}\Big|_{\gamma_1=\gamma_1^{\text{fp}}}^{\gamma_2=\gamma_2^{\text{fp}}} = -\frac{4(n-1)}{2\pi}\gamma_3^2. \tag{4.33}$$

The analysis of the scaling behaviour of the von Neumann entanglement entropy is therefore the same as in the measurement scenario discussed below Eq. (4.29).

When considering decoherence that only preserves the weak $\mathbb{Z}_2$ symmetry, such as dephasing in the Z direction, the n-replica Lindblad action in Eq. (4.2) exhibits a $\mathbb{Z}_2^{\otimes n} \rtimes S_n$ symmetry at high energies. The leading contribution to the quantum jump operator L at low energies is $L \propto \sigma$. Based on this symmetry, the dominant contribution to the IR effective theory can be expressed as

$$S_D = -i\gamma_D \int_{x,t} \sum_{\alpha} \sigma_+^{(\alpha)} \cdot \sigma_-^{(\alpha)}. \tag{4.34}$$

At the UV scale, the coupling constant γ_D can be identified as the dissipation rate, and thus it should be positive due to non-negativity. The decoherence action is relevant and leads to the spontaneous breaking of the $\mathbb{Z}_2^{\otimes n}$ symmetry, resulting in an area law entanglement after subtracting the volume law piece. Additionally, the S_n replica permutation symmetry may also be broken if the magnetizations in different replicas have opposite signs.

For a critical Ising chain subject to local decoherence in a $\mathbb{Z}_2$ symmetric basis, it is anticipated that the subleading logarithmic scaling of the von Neumann entanglement entropy will persist for large subsystems in the stationary state, as long as the Kramers-Wannier duality is present. On the other hand, with decoherence in a $\mathbb{Z}_2$ odd basis, the stationary state is in a phase characterized by spontaneous breaking of the spin flip and replica permutation symmetries, as well as an area law entanglement (after subtracting the leading volume law piece arising from the mixedness of the state).

4.3 Discussions

In this Chapter, we utilized a replicated Keldysh effective field theory to investigate the effects of measurements and decoherence on critical systems. Specifically, we examined both finite-time measurements/decoherence and the possible stationary state properties. Our results suggest that scalings of correlation functions of local operators that are linear in

the density matrix remain unaffected by measurement and decoherence over a finite period of time. To analyze higher moments in the density matrix, we carefully distinguished the symmetry of an n-replica theory in various situations, both in the bulk and on the boundary. The low energy effective theory can be derived based on this symmetry, and the fundamental consistency conditions of the Keldysh path integral. We then applied this framework to the critical Ising model in one and two spatial dimensions, and low-energy behaviors under different perturbations, such as IR symmetry breaking patterns and correlation functions, were discussed. In one spatial dimension, we also explicitly calculated certain entanglement characteristics and discussed their connection to recent numerical studies.

We end with some open directions:

1. One relevant issue is to define and classify topological phases in open quantum systems, such as the Symmetry-Protected Topological (SPT) phases [**?**], using a Keldysh effective field theory, and to investigate the implications of this non-trivial topology on various observables. A concrete example of driven-dissipative Chern insulator has been discussed in a remarkable study [158]. A natural conjecture is, when a unique pure stationary state with a non-zero dissipative gap is present in the open quantum dynamics, one can define an SPT phase for this stationary state. Furthermore, it is expected that the classification of these phases will match that of the recently proposed Average Symmetry-Protected Topological phases [115]. I will develop the theory of such phases in more detail in the next step of my research.

2. Another open question is how to define and characterize topological orders for ensembles and mixed states [11, 48], or in non-unitary dynamics. This raises two fundamental questions: (1) how to define and determine the stability of conventional ground-state topological orders under local measurements and decoherence, and (2) can there exist topologically ordered states in the stationary state of non-equilibrium dynamics? Is it possible for there to be open system/non-unitary topological orders that lack a ground-state counterpart? These questions pertain to the two distinct timescales addressed in this Chapter, and a comprehensive investigation of this matter is reserved for future work.

Chapter 5

Conclusion and Future Directions

In this thesis I studied the interplay between symmetry and topology in mixed ensembles. In the first part of this thesis, including Chapter. 2 and 3, I introduced the concept of average symmetry-protected topological (ASPT) phases in disordered ensembles with average symmetries and investigate their physical implications. We developed a systematic framework, based on the physical picture of defect decoration and the mathematical tool of spectral sequence, to classify and characterize ASPT phases, in both decohered and disordered systems. We have also studied average symmetry-enriched topological (ASET) phases in disordered systems. Our main results are:

- We emphasized the subtle differences between ASPT phases in decohered and disordered systems, which leads to different classifications of ASPT in the two scenarios. Nevertheless, they can both be classified and characterized under the same framework of spectral sequence (decorated defects).
- We discovered a plethora of ASPT phases that are intrinsically mixed, in the sense that they can only appear in mixed state systems (decohered or disordered) with part of the symmetry being average. In other words, these states cannot be viewed as clean SPT states deformed by decoherence or disorder. Some of these states can, however, be viewed as intrinsically gapless pure SPT deformed by decoherence or disorder. We discussed many examples, in both bosonic and fermionic systems.

- We established that if the bulk is in a non-trivial ASPT phase, the boundary state is highly likely to exhibit long-range quantum entanglement, with a probability approaching 1 as the system size increases (in the thermodynamical limit). This generalization extends the concept of t' Hooft anomaly to average symmetries, resulting in powerful constraints on the infrared dynamics of specific lattice systems.

- We developed a systematic theory of ASET phases in disordered $(2+1)d$ bosonic systems. Compared to clean SET phases, disordered ASET with average (and exact) symmetries have some distinct features: (1) While an average symmetry can still permute different anyons, its fractional representation on the anyons cannot be robustly defined, unless the fractionalization pattern involves some 't Hooft anomaly. (2) An average symmetry and an exact symmetry can jointly have fractional representation on the anyons. (3)The $\mathcal{H}^3$ obstructions of symmetry-enrichment patterns are lifted when the relevant symmetries become average. This leads to intrinsically disordered ASET phases without clean limits. The ground states of such ASET phases contain localized anyons, which leads to gapless (yet still localized) excitation spectral.

In the second part of the thesis (Chapter. 4), a replicated Keldysh effective field theory has been developed to investigate the effects of measurements and decoherence on critical systems. Specifically, we examined both finite-time measurements/decoherence and the possible stationary state properties. The long distance properties of both scenarios are described by an effective field theory, which can be derived solely based on symmetry considerations and the fundamental consistency conditions of the Keldysh path integral. We then applied this framework to the critical Ising model in one and two spatial dimensions, and discussed the connection between our results and recent numerical studies.

Many possible future directions have been mentioned in previous chapters. Let me end with some further open questions:

- *Boundary physics*: In this thesis I mostly focused on the systematic bulk classification and characterization of ASPT phases, with a few examples of bulk-boundary correspondence, including (1+1)d $\mathbb{Z}_2 \times \mathbb{Z}_2^{\text{ave}}$ ASPT phase and the surface ASET of a (3+1)d ASPT phase. In [115] and Chapter. 2, it was shown that the boundary of an

ASPT state has average 't Hooft anomaly, which leads to long range quantum entanglement. It will be useful to understand more systematically how average 't Hooft anomalies constrain the behavior of the boundary states (for example, the form of correlation functions), especially for the intrinsically mixed/disordered ASPTs which have no clean limit to begin with.

- *Topological order in mixed states*: I have limited myself to topological order in disorder ensemble, where the notion of SRE ensembles can be naturally extended to LRE ensembles. Defining the notion of topological order for general mixed state is an important question. In fact, a large family of examples can be obtained by "classically" gauging average symmetry and "quantum-mechanically" gauging exact symmetry in ASPT phases. This is an open problem I'm working on.

- *Phase transitions*: Quantum phase transitions of intrinsically mixed ASPT or ASET will necessarily involve decoherence or disorders in important manners. This makes the study of such (necessarily non-unitary) quantum phase transitions both challenging and exciting.

- *Physical realizations*: an important task is to realize some ASPT or ASET phases, especially the intrinsically mixed ones, in experimental platforms such as NISQ simulators or disordered solid-state systems. On this front, simple preparation protocols such as those outlined in Sec. 3.2 are particularly promising.

References

[1] David Aasen, Parsa Bonderson, and Christina Knapp. Torsorial actions on G-crossed braided tensor categories. July 2021.

[2] Ian Affleck, Tom Kennedy, Elliott H Lieb, and Hal Tasaki. Valence bond ground states in isotropic quantum antiferromagnets. *Communications in Mathematical Physics*, 115(3):477–528, 1988.

[3] Ian Affleck and Andreas WW Ludwig. Universal noninteger "ground-state degeneracy"in critical quantum systems. *Physical Review Letters*, 67(2):161, 1991.

[4] Victor V Albert. Lindbladians with multiple steady states: theory and applications. *arXiv preprint arXiv:1802.00010*, 2018.

[5] Victor V. Albert and Liang Jiang. Symmetries and conserved quantities in lindblad master equations. *Phys. Rev. A*, 89:022118, Feb 2014.

[6] Alexander Altland and Ben D Simons. *Condensed matter field theory*. Cambridge university press, 2010.

[7] Frank Arute, Kunal Arya, Ryan Babbush, Dave Bacon, Joseph C. Bardin, Rami Barends, Rupak Biswas, Sergio Boixo, Fernando G. S. L. Brandao, David A. Buell, Brian Burkett, Yu Chen, Zijun Chen, Ben Chiaro, Roberto Collins, William Courtney, Andrew Dunsworth, Edward Farhi, Brooks Foxen, Austin Fowler, Craig Gidney, Marissa Giustina, Rob Graff, Keith Guerin, Steve Habegger, Matthew P. Harrigan, Michael J. Hartmann, Alan Ho, Markus Hoffmann, Trent Huang, Travis S.

Humble, Sergei V. Isakov, Evan Jeffrey, Zhang Jiang, Dvir Kafri, Kostyantyn Kechedzhi, Julian Kelly, Paul V. Klimov, Sergey Knysh, Alexander Korotkov, Fedor Kostritsa, David Landhuis, Mike Lindmark, Erik Lucero, Dmitry Lyakh, Salvatore Mandrà, Jarrod R. McClean, Matthew McEwen, Anthony Megrant, Xiao Mi, Kristel Michielsen, Masoud Mohseni, Josh Mutus, Ofer Naaman, Matthew Neeley, Charles Neill, Murphy Yuezhen Niu, Eric Ostby, Andre Petukhov, John C. Platt, Chris Quintana, Eleanor G. Rieffel, Pedram Roushan, Nicholas C. Rubin, Daniel Sank, Kevin J. Satzinger, Vadim Smelyanskiy, Kevin J. Sung, Matthew D. Trevithick, Amit Vainsencher, Benjamin Villalonga, Theodore White, Z. Jamie Yao, Ping Yeh, Adam Zalcman, Hartmut Neven, and John M. Martinis. Quantum supremacy using a programmable superconducting processor. , 574(7779):505–510, October 2019.

[8] Michael F Atiyah, Vijay K Patodi, and Isadore M Singer. Spectral asymmetry and riemannian geometry. i. In *Mathematical Proceedings of the Cambridge Philosophical Society*, volume 77, pages 43–69. Cambridge University Press, 1975.

[9] Yimu Bao, Soonwon Choi, and Ehud Altman. Theory of the phase transition in random unitary circuits with measurements. *prb*, 101(10):104301, March 2020.

[10] Yimu Bao, Soonwon Choi, and Ehud Altman. Symmetry enriched phases of quantum circuits. *Annals of Physics*, 435:168618, December 2021.

[11] Yimu Bao, Ruihua Fan, Ashvin Vishwanath, and Ehud Altman. Mixed-state topological order and the errorfield double formulation of decoherence-induced transitions. *arXiv preprint arXiv:2301.05687*, 2023.

[12] Maissam Barkeshli, Parsa Bonderson, Meng Cheng, and Zhenghan Wang. Symmetry fractionalization, defects, and gauging of topological phases. *Physical Review B*, 100(11):115147, 2019.

[13] AJ Bray and MA Moore. Critical behaviour of semi-infinite systems. *Journal of Physics A: Mathematical and General*, 10(11):1927, 1977.

[14] E Brehm and Ilka Brunner. Entanglement entropy through conformal interfaces in the 2d ising model. *Journal of High Energy Physics*, 2015(9):1–26, 2015.

[15] Todd A. Brun. A simple model of quantum trajectories. *American Journal of Physics*, 70(7):719–737, July 2002.

[16] M. Buchhold, Y. Minoguchi, A. Altland, and S. Diehl. Effective Theory for the Measurement-Induced Phase Transition of Dirac Fermions. *Physical Review X*, 11(4):041004, October 2021.

[17] Daniel Bulmash and Maissam Barkeshli. Anomaly cascade in $(2 + 1)$-dimensional fermionic topological phases. *Phys. Rev. B*, 105:155126, Apr 2022.

[18] Daniel Bulmash and Maissam Barkeshli. Fermionic symmetry fractionalization in $(2 + 1)$ dimensions. *Phys. Rev. B*, 105:125114, Mar 2022.

[19] TW Burkhardt and JL Cardy. Surface critical behaviour and local operators with boundary-induced critical profiles. *Journal of Physics A: Mathematical and General*, 20(4):L233, 1987.

[20] F. J. Burnell, Xie Chen, Lukasz Fidkowski, and Ashvin Vishwanath. Exactly soluble model of a three-dimensional symmetry-protected topological phase of bosons with surface topological order. *prb*, 90(24):245122, December 2014.

[21] Berislav Buča and Tomaž Prosen. A note on symmetry reductions of the Lindblad equation: transport in constrained open spin chains. *New Journal of Physics*, 14(7):073007, July 2012.

[22] Berislav Buča and Tomaž Prosen. A note on symmetry reductions of the Lindblad equation: transport in constrained open spin chains. *New Journal of Physics*, 14(7):073007, July 2012.

[23] Pasquale Calabrese and John Cardy. Evolution of entanglement entropy in one-dimensional systems. *Journal of Statistical Mechanics: Theory and Experiment*, 2005(4):04010, April 2005.

[24] Pasquale Calabrese and John Cardy. Entanglement entropy and conformal field theory. *Journal of Physics A Mathematical General*, 42(50):504005, December 2009.

[25] John Cardy. *Scaling and renormalization in statistical physics*, volume 5. Cambridge university press, 1996.

[26] John L Cardy. Effect of boundary conditions on the operator content of two-dimensional conformally invariant theories. *Nuclear Physics B*, 275(2):200–218, 1986.

[27] John L Cardy. Boundary conditions, fusion rules and the verlinde formula. *Nuclear Physics B*, 324(3):581–596, 1989.

[28] Amos Chan, Rahul M. Nandkishore, Michael Pretko, and Graeme Smith. Unitary-projective entanglement dynamics. *prb*, 99(22):224307, June 2019.

[29] Xie Chen, Fiona J Burnell, Ashvin Vishwanath, and Lukasz Fidkowski. Anomalous symmetry fractionalization and surface topological order. *Physical Review X*, 5(4):041013, 2015.

[30] Xie Chen, Zheng-Cheng Gu, Zheng-Xin Liu, and Xiao-Gang Wen. Symmetry-protected topological orders in interacting bosonic systems. *Science*, 338(6114):1604–1606, 2012.

[31] Xie Chen, Zheng-Cheng Gu, Zheng-Xin Liu, and Xiao-Gang Wen. Symmetry protected topological orders and the group cohomology of their symmetry group. *prb*, 87(15):155114, April 2013.

[32] Xie Chen, Zheng-Cheng Gu, and Xiao-Gang Wen. Local unitary transformation, long-range quantum entanglement, wave function renormalization, and topological order. *prb*, 82(15):155138, October 2010.

[33] Xie Chen, Zheng-Cheng Gu, and Xiao-Gang Wen. Complete classification of one-dimensional gapped quantum phases in interacting spin systems. *prb*, 84(23):235128, December 2011.

[34] Xie Chen, Yuan-Ming Lu, and Ashvin Vishwanath. Symmetry-protected topological phases from decorated domain walls. *Nature Communications*, 5:3507, March 2014.

[35] Meng Cheng and Chenjie Wang. Rotation symmetry-protected topological phases of fermions. *Physical Review B*, 105(19):195154, 2022.

[36] Meng Cheng and Dominic J. Williamson. Relative anomaly in (1 + 1)d rational conformal field theory. *Physical Review Research*, 2(4):043044, oct 2020.

[37] Meng Cheng, Michael Zaletel, Maissam Barkeshli, Ashvin Vishwanath, and Parsa Bonderson. Translational Symmetry and Microscopic Constraints on Symmetry-Enriched Topological Phases: A View from the Surface. *Physical Review X*, 6(4):041068, December 2016.

[38] Ching-Kai Chiu, Jeffrey C. Y. Teo, Andreas P. Schnyder, and Shinsei Ryu. Classification of topological quantum matter with symmetries. *Reviews of Modern Physics*, 88(3):035005, July 2016.

[39] Gil Young Cho, Chang-Tse Hsieh, and Shinsei Ryu. Anomaly manifestation of Lieb-Schultz-Mattis theorem and topological phases. *prb*, 96(19):195105, November 2017.

[40] Andrea Coser and David Perez-Garcia. Classification of phases for mixed states via fast dissipative evolution. *arXiv e-prints*, page arXiv:1810.05092, October 2018.

[41] Chandan Dasgupta and Shang-keng Ma. Low-temperature properties of the random heisenberg antiferromagnetic chain. *Physical review b*, 22(3):1305, 1980.

[42] Caroline de Groot, Alex Turzillo, and Norbert Schuch. Symmetry Protected Topological Order in Open Quantum Systems. *arXiv e-prints*, page arXiv:2112.04483, December 2021.

[43] Caroline de Groot, Alex Turzillo, and Norbert Schuch. Symmetry Protected Topological Order in Open Quantum Systems. *Quantum*, 6:856, November 2022.

[44] Viktor Eisler and Ingo Peschel. Solution of the fermionic entanglement problem with interface defects. *arXiv e-prints*, page arXiv:1005.2144, May 2010.

[45] Alexander Elgart and Abel Klein. Localization in the random XXZ quantum spin chain. *arXiv e-prints*, page arXiv:2210.14873, October 2022.

[46] Dominic V. Else and Ryan Thorngren. Crystalline topological phases as defect networks. *prb*, 99(11):115116, March 2019.

[47] Dominic V. Else, Ryan Thorngren, and T. Senthil. Non-Fermi Liquids as Ersatz Fermi Liquids: General Constraints on Compressible Metals. *Physical Review X*, 11(2):021005, April 2021.

[48] Ruihua Fan, Yimu Bao, Ehud Altman, and Ashvin Vishwanath. Diagnostics of mixed-state topological order and breakdown of quantum memory. *arXiv preprint arXiv:2301.05689*, 2023.

[49] Lukasz Fidkowski and Alexei Kitaev. Topological phases of fermions in one dimension. *prb*, 83(7):075103, February 2011.

[50] Lukasz Fidkowski and Ashvin Vishwanath. Realizing anomalous anyonic symmetries at the surfaces of three-dimensional gauge theories. *Physical Review B*, 96(4):045131, jul 2017.

[51] Daniel S Fisher. Random antiferromagnetic quantum spin chains. *Physical review b*, 50(6):3799, 1994.

[52] Peter J Forrester. Log-gases and random matrices (lms-34). In *Log-Gases and Random Matrices (LMS-34)*. Princeton University Press, 2010.

[53] Daniel S. Freed. Short-range entanglement and invertible field theories. *arXiv e-prints*, page arXiv:1406.7278, June 2014.

[54] Daniel S. Freed and Michael J. Hopkins. Reflection positivity and invertible topological phases. *arXiv e-prints*, page arXiv:1604.06527, April 2016.

[55] Liang Fu. Topological Crystalline Insulators. *prl*, 106(10):106802, March 2011.

[56] Liang Fu and C. L. Kane. Topology, Delocalization via Average Symmetry and the Symplectic Anderson Transition. *prl*, 109(24):246605, December 2012.

[57] Liang Fu, C. L. Kane, and E. J. Mele. Topological Insulators in Three Dimensions. *prl*, 98(10):106803, March 2007.

[58] Yohei Fuji, Frank Pollmann, and Masaki Oshikawa. Distinct Trivial Phases Protected by a Point-Group Symmetry in Quantum Spin Chains. *prl*, 114(17):177204, May 2015.

[59] I. C. Fulga, B. van Heck, J. M. Edge, and A. R. Akhmerov. Statistical Topological Insulators. *arXiv e-prints*, page arXiv:1212.6191, December 2012.

[60] Davide Gaiotto and Theo Johnson-Freyd. Symmetry protected topological phases and generalized cohomology. *Journal of High Energy Physics*, 2019(5):7, May 2019.

[61] Davide Gaiotto and Anton Kapustin. Spin TQFTs and fermionic phases of matter. *International Journal of Modern Physics A*, 31:1645044–184, October 2016.

[62] Iñaki García-Etxebarria and Miguel Montero. Dai-Freed anomalies in particle physics. *Journal of High Energy Physics*, 2019(8):3, August 2019.

[63] Samuel J Garratt, Zack Weinstein, and Ehud Altman. Measurements conspire nonlocally to restructure critical quantum states. *arXiv preprint arXiv:2207.09476*, 2022.

[64] Paul Ginsparg. Applied conformal field theory. *arXiv preprint hep-th/9108028*, 1988.

[65] Nicolas Gisin and Ian C Percival. The quantum-state diffusion model applied to open systems. *Journal of Physics A: Mathematical and General*, 25(21):5677, 1992.

[66] Vittorio Gorini, Andrzej Kossakowski, and Ennackal Chandy George Sudarshan. Completely positive dynamical semigroups of n-level systems. *Journal of Mathematical Physics*, 17(5):821–825, 1976.

[67] Michael J. Gullans and David A. Huse. Dynamical Purification Phase Transition Induced by Quantum Measurements. *Physical Review X*, 10(4):041020, October 2020.

[68] Meng Guo, Pavel Putrov, and Juven Wang. Time reversal, SU(N) Yang-Mills and cobordisms: Interacting topological superconductors/insulators and quantum spin liquids in 3 + 1 D. *Annals of Physics*, 394:244–293, July 2018.

[69] Jeongwan Haah, Matthew B Hastings, Robin Kothari, and Guang Hao Low. Quantum algorithm for simulating real time evolution of lattice hamiltonians. *SIAM Journal on Computing*, (0):FOCS18–250, 2021.

[70] F Duncan M Haldane. Nonlinear field theory of large-spin heisenberg antiferromagnets: semiclassically quantized solitons of the one-dimensional easy-axis néel state. *Physical review letters*, 50(15):1153, 1983.

[71] Bertrand I Halperin. Quantized hall conductance, current-carrying edge states, and the existence of extended states in a two-dimensional disordered potential. *Physical Review B*, 25(4):2185, 1982.

[72] M. Z. Hasan and C. L. Kane. Colloquium: Topological insulators. *Reviews of Modern Physics*, 82(4):3045–3067, October 2010.

[73] Itamar Hason, Zohar Komargodski, and Ryan Thorngren. Anomaly matching in the symmetry broken phase: Domain walls, CPT, and the Smith isomorphism. *SciPost Physics*, 8(4):062, April 2020.

[74] M. B. Hastings. Lieb-Schultz-Mattis in higher dimensions. *prb*, 69(10):104431, Mar 2004.

[75] M. B. Hastings. Lieb-Schultz-Mattis in higher dimensions. *prb*, 69(10):104431, March 2004.

[76] M. B. Hastings and Xiao-Gang Wen. Quasiadiabatic continuation of quantum states: The stability of topological ground-state degeneracy and emergent gauge invariance. *prb*, 72(4):045141, July 2005.

[77] Matthew B. Hastings. Topological Order at Nonzero Temperature. *prl*, 107(21):210501, November 2011.

[78] Johannes Hauschild and Frank Pollmann. Efficient numerical simulations with tensor networks: Tensor network python (tenpy). *SciPost Physics Lecture Notes*, page 005, 2018.

[79] Timothy H. Hsieh, Hsin Lin, Junwei Liu, Wenhui Duan, Arun Bansil, and Liang Fu. Topological crystalline insulators in the SnTe material class. *Nature Communications*, 3:982, July 2012.

[80] Sheng-Jie Huang, Hao Song, Yi-Ping Huang, and Michael Hermele. Building crystalline topological phases from lower-dimensional states. *prb*, 96(20):205106, November 2017.

[81] Yoseph Imry and Shang-keng Ma. Random-field instability of the ordered state of continuous symmetry. *Phys. Rev. Lett.*, 35:1399–1401, Nov 1975.

[82] Hiroki Isobe and Liang Fu. Theory of interacting topological crystalline insulators. *prb*, 92(8):081304, August 2015.

[83] Kurt Jacobs and Daniel Steck. A straightforward introduction to continuous quantum measurement. *Contemporary Physics*, 47(5):279–303, September 2006.

[84] Chao-Ming Jian, Bela Bauer, Anna Keselman, and Andreas WW Ludwig. Criticality and entanglement in nonunitary quantum circuits and tensor networks of noninteracting fermions. *Physical Review B*, 106(13):134206, 2022.

[85] Chao-Ming Jian, Yi-Zhuang You, Romain Vasseur, and Andreas W. W. Ludwig. Measurement-induced criticality in random quantum circuits. *prb*, 101(10):104302, March 2020.

[86] Alex Kamenev. *Field theory of non-equilibrium systems*. Cambridge University Press, 2023.

[87] Alex Kamenev and Alex Levchenko. Keldysh technique and non-linear σ-model: basic principles and applications. *Advances in Physics*, 58(3):197–319, May 2009.

[88] C. L. Kane and E. J. Mele. Z_2 Topological Order and the Quantum Spin Hall Effect. *prl*, 95(14):146802, September 2005.

[89] Anton Kapustin. Bosonic topological insulators and paramagnets: a view from cobordisms. *arXiv preprint arXiv:1404.6659*, 2014.

[90] Anton Kapustin. Symmetry protected topological phases, anomalies, and cobordisms: beyond group cohomology. *arXiv preprint arXiv:1403.1467*, 2014.

[91] Anton Kapustin, Ryan Thorngren, Alex Turzillo, and Zitao Wang. Fermionic symmetry protected topological phases and cobordisms. *Journal of High Energy Physics*, 2015:52, December 2015.

[92] Itamar Kimchi, Yang-Zhi Chou, Rahul M. Nandkishore, and Leo Radzihovsky. Anomalous localization at the boundary of an interacting topological insulator. *prb*, 101(3):035131, January 2020.

[93] Itamar Kimchi, Adam Nahum, and T. Senthil. Valence Bonds in Random Quantum Magnets: Theory and Application to $YbMgGaO_4$. *Physical Review X*, 8(3):031028, July 2018.

[94] A. Yu. Kitaev. Fault-tolerant quantum computation by anyons. *Annals of Physics*, 303(1):2–30, jan 2003.

[95] Alexei Kitaev. Anyons in an exactly solved model and beyond. *Annals of Physics*, 321(1):2–111, January 2006.

[96] Alexei Kitaev. Toward topological classification of phases with short-range entanglement. In *Topological Insulators and Superconductors Workshop*. Kavli Institute for Theoretical Physics, University of California, 2011.

[97] K v Klitzing, Gerhard Dorda, and Michael Pepper. New method for high-accuracy determination of the fine-structure constant based on quantized hall resistance. *Physical review letters*, 45(6):494, 1980.

[98] Zohar Komargodski and David Simmons-Duffin. The random-bond Ising model in 2.01 and 3 dimensions. *Journal of Physics A Mathematical General*, 50(15):154001, April 2017.

[99] Liang Kong and Xiao-Gang Wen. Braided fusion categories, gravitational anomalies, and the mathematical framework for topological orders in any dimensions. *arXiv preprint arXiv:1405.5858*, 2014.

[100] Markus König, Steffen Wiedmann, Christoph Brüne, Andreas Roth, Hartmut Buhmann, Laurens W. Molenkamp, Xiao-Liang Qi, and Shou-Cheng Zhang. Quantum Spin Hall Insulator State in HgTe Quantum Wells. *Science*, 318(5851):766, November 2007.

[101] Markus König, Steffen Wiedmann, Christoph Brüne, Andreas Roth, Hartmut Buhmann, Laurens W. Molenkamp, Xiao-Liang Qi, and Shou-Cheng Zhang. Quantum Spin Hall Insulator State in HgTe Quantum Wells. *Science*, 318(5851):766, November 2007.

[102] B. Ladewig, S. Diehl, and M. Buchhold. Monitored open fermion dynamics: Exploring the interplay of measurement, decoherence, and free Hamiltonian evolution. *Physical Review Research*, 4(3):033001, July 2022.

[103] L. D. Landau and E. M. Lifshitz. *Statistical Physics, Part 1*, volume 5 of *Course of Theoretical Physics*. Butterworth-Heinemann, Oxford, 1980.

[104] Robert B Laughlin. Quantized hall conductivity in two dimensions. *Physical Review B*, 23(10):5632, 1981.

[105] Derek KK Lee and JT Chalker. Unified model for two localization problems: Electron states in spin-degenerate landau levels and in a random magnetic field. *Physical review letters*, 72(10):1510, 1994.

[106] Jong Yeon Lee, Chao-Ming Jian, and Cenke Xu. Quantum criticality under decoherence or weak measurement. *arXiv preprint arXiv:2301.05238*, 2023.

[107] Jong Yeon Lee, Yi-Zhuang You, and Cenke Xu. Symmetry protected topological phases under decoherence. *arXiv preprint arXiv:2210.16323*, 2022.

[108] P. A. Lee and A. Douglas Stone. Universal conductance fluctuations in metals. *Phys. Rev. Lett.*, 55:1622–1625, Oct 1985.

[109] Michael Levin and Zheng-Cheng Gu. Braiding statistics approach to symmetry-protected topological phases. *prb*, 86(11):115109, September 2012.

[110] Yaodong Li, Xiao Chen, and Matthew P. A. Fisher. Quantum Zeno effect and the many-body entanglement transition. *prb*, 98(20):205136, November 2018.

[111] Elliott Lieb, Theodore Schultz, and Daniel Mattis. Two soluble models of an antiferromagnetic chain. *Annals of Physics*, 16(3):407–466, 1961.

[112] Simon Lieu, Ron Belyansky, Jeremy T. Young, Rex Lundgren, Victor V. Albert, and Alexey V. Gorshkov. Symmetry breaking and error correction in open quantum systems. *Phys. Rev. Lett.*, 125:240405, Dec 2020.

[113] Cheng-Ju Lin, Weicheng Ye, Yijian Zou, Shengqi Sang, and Timothy H. Hsieh. Probing sign structure using measurement-induced entanglement. *Quantum*, 7:910, February 2023.

[114] Ruochen Ma. Exploring critical systems under measurements and decoherence via keldysh field theory. *arXiv preprint arXiv:2304.08277*, 2023.

[115] Ruochen Ma and Chong Wang. Average symmetry-protected topological phases. *arXiv preprint arXiv:2209.02723*, 2022.

[116] Ruochen Ma, Jian-Hao Zhang, Zhen Bi, Meng Cheng, and Chong Wang. Topological Phases with Average Symmetries: the Decohered, the Disordered, and the Intrinsic. *arXiv e-prints*, page arXiv:2305.16399, May 2023.

[117] Shang-keng Ma, Chandan Dasgupta, and Chin-kun Hu. Random antiferromagnetic chain. *Physical review letters*, 43(19):1434, 1979.

[118] Naren Manjunath, Vladimir Calvera, and Maissam Barkeshli. Nonperturbative constraints from symmetry and chirality on majorana zero modes and defect quantum numbers in (2+1) dimensions. *Phys. Rev. B*, 107:165126, Apr 2023.

[119] John McGreevy. Generalized symmetries in condensed matter. *Annual Review of Condensed Matter Physics*, 14:57–82, 2023.

[120] A. Milsted, L. Seabra, I. C. Fulga, C. W. J. Beenakker, and E. Cobanera. Statistical translation invariance protects a topological insulator from interactions. *prb*, 92(8):085139, August 2015.

[121] Roger S. K. Mong, Jens H. Bardarson, and Joel E. Moore. Quantum Transport and Two-Parameter Scaling at the Surface of a Weak Topological Insulator. *prl*, 108(7):076804, February 2012.

[122] David F. Mross, Yuval Oreg, Ady Stern, Gilad Margalit, and Moty Heiblum. Theory of Disorder-Induced Half-Integer Thermal Hall Conductance. *prl*, 121(2):026801, July 2018.

[123] Tobias J. Osborne. Simulating adiabatic evolution of gapped spin systems. *pra*, 75(3):032321, March 2007.

[124] Masaki Oshikawa. Commensurability, Excitation Gap, and Topology in Quantum Many-Particle Systems on a Periodic Lattice. *prl*, 84(7):1535–1538, February 2000.

[125] Masaki Oshikawa and Ian Affleck. Defect Lines in the Ising Model and Boundary States on Orbifolds. *prl*, 77(13):2604–2607, September 1996.

[126] Masaki Oshikawa and Ian Affleck. Boundary conformal field theory approach to the critical two-dimensional Ising model with a defect line. *Nuclear Physics B*, 495(3):533–582, February 1997.

[127] P. M. Ostrovsky, I. V. Gornyi, and A. D. Mirlin. Theory of anomalous quantum Hall effects in graphene. *prb*, 77(19):195430, May 2008.

[128] Ingo Peschel and Viktor Eisler. Exact results for the entanglement across defects in critical chains. *Journal of Physics A Mathematical General*, 45(15):155301, April 2012.

[129] Hoi Chun Po, Haruki Watanabe, Chao-Ming Jian, and Michael P. Zaletel. Lattice Homotopy Constraints on Phases of Quantum Magnets. *prl*, 119(12):127202, September 2017.

[130] Frank Pollmann, Erez Berg, Ari M. Turner, and Masaki Oshikawa. Symmetry protection of topological phases in one-dimensional quantum spin systems. *prb*, 85(7):075125, February 2012.

[131] Frank Pollmann and Ari M. Turner. Detection of symmetry-protected topological phases in one dimension. *prb*, 86(12):125441, September 2012.

[132] Frank Pollmann, Ari M. Turner, Erez Berg, and Masaki Oshikawa. Entanglement spectrum of a topological phase in one dimension. *prb*, 81(6):064439, February 2010.

[133] John Preskill. Lecture notes for physics 229: Quantum information and computation. *California Institute of Technology*, 16(1):1–8, 1998.

[134] John Preskill. Quantum Computing in the NISQ era and beyond. *Quantum*, 2:79, August 2018.

[135] Xiao-Liang Qi, Taylor L. Hughes, and Shou-Cheng Zhang. Topological field theory of time-reversal invariant insulators. *prb*, 78(19):195424, November 2008.

[136] Xiao-Liang Qi and Shou-Cheng Zhang. Topological insulators and superconductors. *Reviews of Modern Physics*, 83(4):1057–1110, October 2011.

[137] Zohar Ringel, Yaacov E. Kraus, and Ady Stern. Strong side of weak topological insulators. *prb*, 86(4):045102, July 2012.

[138] Sam Roberts, Beni Yoshida, Aleksander Kubica, and Stephen D. Bartlett. Symmetry-protected topological order at nonzero temperature. *pra*, 96(2):022306, August 2017.

[139] G. Rosenberg and M. Franz. Witten effect in a crystalline topological insulator. *prb*, 82(3):035105, July 2010.

[140] Shinsei Ryu, Andreas P. Schnyder, Akira Furusaki, and Andreas W. W. Ludwig. Topological insulators and superconductors: tenfold way and dimensional hierarchy. *New Journal of Physics*, 12(6):065010, June 2010.

[141] Subir Sachdev. Quantum phase transitions. *Physics world*, 12(4):33, 1999.

[142] Andreas P. Schnyder, Shinsei Ryu, Akira Furusaki, and Andreas W. W. Ludwig. Classification of topological insulators and superconductors in three spatial dimensions. *prb*, 78(19):195125, November 2008.

[143] Ulrich Schollwöck. The density-matrix renormalization group in the age of matrix product states. *Annals of Physics*, 326(1):96–192, January 2011.

[144] T. Senthil. Symmetry-Protected Topological Phases of Quantum Matter. *Annual Review of Condensed Matter Physics*, 6:299–324, March 2015.

[145] T. Senthil, Dam Thanh Son, Chong Wang, and Cenke Xu. Duality between (2 + 1) d quantum critical points. *physrep*, 827:1–48, September 2019.

[146] Hassan Shapourian, Ken Shiozaki, and Shinsei Ryu. Many-Body Topological Invariants for Fermionic Symmetry-Protected Topological Phases. *prl*, 118(21):216402, May 2017.

[147] Ken Shiozaki and Shinsei Ryu. Matrix product states and equivariant topological field theories for bosonic symmetry-protected topological phases in (1+1) dimensions. *Journal of High Energy Physics*, 2017(4):100, April 2017.

[148] Ken Shiozaki, Hassan Shapourian, Kiyonori Gomi, and Shinsei Ryu. Many-body topological invariants for fermionic short-range entangled topological phases protected by antiunitary symmetries. *prb*, 98(3):035151, July 2018.

[149] L. M. Sieberer, M. Buchhold, and S. Diehl. Keldysh field theory for driven open quantum systems. *Reports on Progress in Physics*, 79(9):096001, September 2016.

[150] David Simmons-Duffin. The lightcone bootstrap and the spectrum of the 3d Ising CFT. *Journal of High Energy Physics*, 2017(3):86, March 2017.

[151] Brian Skinner, Jonathan Ruhman, and Adam Nahum. Measurement-Induced Phase Transitions in the Dynamics of Entanglement. *Physical Review X*, 9(3):031009, July 2019.

[152] W. Son, L. Amico, R. Fazio, A. Hamma, S. Pascazio, and V. Vedral. Quantum phase transition between cluster and antiferromagnetic states. *EPL (Europhysics Letters)*, 95(5):50001, September 2011.

[153] Hao Song, Sheng-Jie Huang, Liang Fu, and Michael Hermele. Topological Phases Protected by Point Group Symmetry. *Physical Review X*, 7(1):011020, January 2017.

[154] Zhida Song, Chen Fang, and Yang Qi. Real-space recipes for general topological crystalline states. *Nature Communications*, 11(1):4197, August 2020.

[155] Masuo Suzuki. Relationship among exactly soluble models of critical phenomena. i: 2d ising model, dimer problem and the generalized xy-model. *Progress of Theoretical Physics*, 46(5):1337–1359, 1971.

[156] Ryan Thorngren and Dominic V. Else. Gauging spatial symmetries and the classification of topological crystalline phases. *Phys. Rev. X*, 8:011040, Mar 2018.

[157] Ryan Thorngren, Ashvin Vishwanath, and Ruben Verresen. Intrinsically gapless topological phases. *Physical Review B*, 104(7):075132, 2021.

[158] F. Tonielli, J. C. Budich, A. Altland, and S. Diehl. Topological Field Theory Far from Equilibrium. *prl*, 124(24):240404, June 2020.

[159] Daniel C Tsui, Horst L Stormer, and Arthur C Gossard. Two-dimensional magnetotransport in the extreme quantum limit. *Physical Review Letters*, 48(22):1559, 1982.

[160] Xhek Turkeshi, Alberto Biella, Rosario Fazio, Marcello Dalmonte, and Marco Schiró. Measurement-induced entanglement transitions in the quantum Ising chain: From infinite to zero clicks. *prb*, 103(22):224210, June 2021.

[161] Ari M. Turner, Frank Pollmann, and Erez Berg. Topological phases of one-dimensional fermions: An entanglement point of view. *prb*, 83(7):075102, February 2011.

[162] Ruben Verresen, Ryan Thorngren, Nick G. Jones, and Frank Pollmann. Gapless Topological Phases and Symmetry-Enriched Quantum Criticality. *Physical Review X*, 11(4):041059, October 2021.

[163] Ashvin Vishwanath and T. Senthil. Physics of Three-Dimensional Bosonic Topological Insulators: Surface-Deconfined Criticality and Quantized Magnetoelectric Effect. *Physical Review X*, 3(1):011016, January 2013.

[164] Chong Wang, Adam Nahum, Max A Metlitski, Cenke Xu, and T Senthil. Deconfined quantum critical points: symmetries and dualities. *Physical Review X*, 7(3):031051, 2017.

[165] Chong Wang, Andrew C. Potter, and T. Senthil. Classification of Interacting Electronic Topological Insulators in Three Dimensions. *Science*, 343(6171):629–631, February 2014.

[166] Chong Wang and T. Senthil. Boson topological insulators: A window into highly entangled quantum phases. *prb*, 87(23):235122, June 2013.

[167] Chong Wang and T. Senthil. Interacting fermionic topological insulators/superconductors in three dimensions. *prb*, 89(19):195124, May 2014.

[168] Chong Wang and T. Senthil. Interacting fermionic topological insulators/superconductors in three dimensions. *prb*, 89(19):195124, May 2014.

[169] Juven C. Wang, Zheng-Cheng Gu, and Xiao-Gang Wen. Field-theory representation of gauge-gravity symmetry-protected topological invariants, group cohomology, and beyond. *Phys. Rev. Lett.*, 114:031601, Jan 2015.

[170] Q.-R. Wang and Z.-C. Gu. Towards a complete classification of symmetry-protected topological phases for interacting fermions in three dimensions and a general group supercohomology theory. *Phys. Rev. X*, 8:011055, 2018.

[171] Q.-R. Wang and Z.-C. Gu. Construction and classification of symmetry-protected topological phases in interacting fermion systems. *Phys. Rev. X*, 10(3):031055, 2020.

[172] Qing-Rui Wang, Shang-Qiang Ning, and Meng Cheng. Domain wall decorations, anomalies and spectral sequences in bosonic topological phases. *arXiv preprint arXiv:2104.13233*, 2021.

[173] Zack Weinstein, Rohith Sajith, Ehud Altman, and Samuel J Garratt. Nonlocality and entanglement in measured critical quantum ising chains. *arXiv preprint arXiv:2301.08268*, 2023.

[174] Steven R White. Density matrix formulation for quantum renormalization groups. *Physical review letters*, 69(19):2863, 1992.

[175] HM Wiseman and GJ Milburn. Interpretation of quantum jump and diffusion processes illustrated on the bloch sphere. *Physical Review A*, 47(3):1652, 1993.

[176] Edward Witten. Fermion path integrals and topological phases. *Reviews of Modern Physics*, 88(3):035001, July 2016.

[177] Zhou Yang, Dan Mao, and Chao-Ming Jian. Entanglement in one-dimensional critical state after measurements. *arXiv preprint arXiv:2301.08255*, 2023.

[178] Yuan Yao and Masaki Oshikawa. Generalized Boundary Condition Applied to Lieb-Schultz-Mattis-Type Ingappabilities and Many-Body Chern Numbers. *Physical Review X*, 10(3):031008, July 2020.

[179] Weicheng Ye, Meng Guo, Yin-Chen He, Chong Wang, and Liujun Zou. Topological characterization of lieb-schultz-mattis constraints and applications to symmetry-enriched quantum criticality. *SciPost Physics*, 13(3):066, 2022.

[180] Matthew Yu. Symmetries and anomalies of (1+1)d theories: 2-groups and symmetry fractionalization. *Journal of High Energy Physics*, 2021(8):61, August 2021.

[181] Michael P. Zaletel. Detecting two-dimensional symmetry-protected topological order in a ground-state wave function. *prb*, 90(23):235113, December 2014.

[182] Jian-Hao Zhang, Yang Qi, and Zhen Bi. Strange correlation function for average symmetry-protected topological phases. *arXiv preprint arXiv:2210.17485*, 2022.

[183] Jian-Hao Zhang, Shuo Yang, Yang Qi, and Zheng-Cheng Gu. Real-space construction of crystalline topological superconductors and insulators in 2d interacting fermionic systems. *Phys. Rev. Research*, 4:033081, Jul 2022.

[184] Yijian Zou, Shengqi Sang, and Timothy H Hsieh. Channeling quantum criticality. *arXiv preprint arXiv:2301.07141*, 2023.

APPENDICES

Appendix A

Appendices for Chapter. 2

A.1 Atiyah-Hirzebruch spectral sequence for Class AII

In order to define a fermionic theory in symmetry class AII, one should equip the space-time manifold with a $\text{pin}^{\tilde{c}}_{+}$ structure. In $(d+1)$-dimension, the structure group fits in the short exact sequence:

$$1 \longrightarrow U(1) \longrightarrow \text{pin}^{\tilde{c}}_{+} \longrightarrow O(d+1) \longrightarrow 1, \tag{A.1}$$

with the reflection element in $O(d+1)$ squares to 1 in Euclidean signature and acts on $U(1)$ by complex conjugation. For our purpose, we calculate the cobordism $\Omega^{\bullet}_{\text{pin}^{\tilde{c}}_{+}}$ using an AHSS with E_2 page given by $E_2^{p,q} = H^p(B\mathbb{Z}_2; \Omega^q_{\text{spin}^c}(\text{pt}))$, with the coefficient group twisted appropriately by $\mathbb{Z}_2$. For example, the IQH root state and the E_8 root state are both time reversal odd, so $\mathbb{Z}_2$ acts on their corresponding elements in $\Omega^{\bullet}_{\text{spin}^c}$ non-trivially. On the other hand, $\mathbb{Z}_2$ acts on the $U(1)$ charge trivially. The E_2 page in low degree is

given by

$$\begin{array}{c|cccccc}
2U(1)^{\mathcal{T}} & 2(-1)^{\mathbb{Z}_2} & & 2(-1)^{\mathbb{Z}_2 t^2} & & 2(-1)^{\mathbb{Z}_2 t^4} & \\
0 & & & & & & \\
U(1) & U(1) & (-1)^{\mathbb{Z}_2 t} & & (-1)^{\mathbb{Z}_2 t^3} & & (-1)^{\mathbb{Z}_2 t^5} \\
0 & & & & & & \\
U(1)^{\mathcal{T}} & (-1)^{\mathbb{Z}_2} & & (-1)^{\mathbb{Z}_2 t^2} & & (-1)^{\mathbb{Z}_2 t^4} & \\
\hline
 & 0 & 1 & 2 & 3 & 4 & 5\,,
\end{array} \tag{A.2}$$

in which $U(1)^{\mathcal{T}}$ indicates the coefficient twisted by time reversal. t is the generator of the cohomology ring $H^\bullet(B\mathbb{Z}_2;\mathbb{Z}_2) = \mathbb{Z}_2[t]$ with t in degree one. In this spectral sequence only the d_3 differential can possibly be non-trivial. Given[60, 180]

$$d_3 = (-1)^{(\mathrm{Sq}^2 + t\cdot \mathrm{Sq}^1 + t^2)} \circ \beta, \tag{A.3}$$

for $\mathcal{T}^2 = -1$ when acting on fermions, one can see that the d_3 differential vanishes for elements with total degrees up to 4. Here β is the Bockstein of the following sequence in cohomology:

$$1 \longrightarrow \mathbb{Z}_2 \xrightarrow{(-1)^x} U(1) \xrightarrow{x^2} U(1) \longrightarrow 1 \tag{A.4}$$

such that $\beta : H^n(B\mathbb{Z}_2; U(1)) \to H^{n+1}(B\mathbb{Z}_2;\mathbb{Z}_2)$. Physically, the vanishing of differential means the decorations we discussed in Sec. 2.5 are consistent. The calculation also agrees with the $\mathbb{Z}_2^3$ classification of class AII TIs in three spatial dimensions [165].

Appendix B

Appendices for Chapter. 3

B.1 On the definition of disordered ASPT

The definition of disordered average SPT has originally given in Ref. [115] is slightly more complicated than that given in Sec. 3.1.2. In particular, in Ref. [115] a short-range entangled ensemble requires any two ground states to be adiabatically connected, namely for any disorder realization I, I', it is required that $|\Psi_I\rangle = U_{II'}|\Psi_I\rangle$ for some finite-depth local unitary $U_{II'}$. Instead, in Sec. 3.1.2 we only demand that any ground state in the ensemble $|\Psi_I\rangle$ to be short-range entangled with correlation length $\xi_I < \xi_m$ for some finite maximal correlation length in the ensemble ξ_m. We now discuss to what extend our new definition is equivalent to the old one.

Consider a ground state in the ensemble $|\Psi_I\rangle$ in a large but finite system without boundary. As a short-range entangled state, it belongs to an invertible phase labeled by $\omega_I^{D+1} \in h^{D+1}(A)$, where $h^{D+1}(A)$ classifies invertible phases with exact symmetry A in D space dimensions. On a finite system, we could effectively compactify the space by viewing certain dimensions as points – for example, the entire system can be viewed as a point if we zoom out far enough. When the system is compactified this way to a $(D-p)$ dimensional space, it should be labeled as a $(D-p)$ invertible state labeled by $\omega_I^{D+p-1} \in h^{D-p+1}(A)$ (it should also depend on the compactification cycle but we will omit this information in the

notation). In general ω_I^{D+p-1} is not directly decided by the bulk state ω_I^{D+1}. In particular, when $p = D$ the system reduces to a point and the only nontrivial information left is the charge under A symmetry.

Now the condition in Ref. [115] is the statement that ω_I^{D-p+1} is identical for any disorder realization I, for all $0 \leq p \leq D$. We now show that the new condition in Sec. 3.1.2 automatically implies the old condition for $0 \leq p \leq D-1$: if for some $0 \leq p \leq D-1$, $\omega_I \neq \omega_I'$ for two disorder realizations H_I and $H_{I'}$, then we can choose a third disorder realization in the ensemble I'', which has $H_{I''} = H_I$ in some region R, and $H_{I''} = H_{I'}$ in the complement $\bar{R}$. Notice that the spatial independence of the disorder potential is crucial for this construction. The difference in ω in R and $\bar{R}$, for suitably chosen R, implies a long-range entangled boundary state on ∂R, which leads to a correlation length $\sim |\partial R|$. This leads to unbounded correlation length, and therefore violates the new condition in Sec. 3.1.2.

The above argument does not apply for $p = D$, since two regions with different A charges do not need to have nontrivial boundary state. However, our definition of exact symmetry in Sec. 3.1.2 requires that the exact charge to be identical for each disorder realization, so the $p = D$ condition is automatically satisfied.

B.2 A brief review of spectral sequence

This section provides a brief overview of the LHS spectral sequence of group cohomology, which is crucial for classifying the decohered ASPT phases. Furthermore, we extend our discussion to the Atiyah-Hirzebruch (AH) spectral sequence, which is particularly relevant for classifying the disordered ASPT phases.

A spectral sequence consists of an assembly of Abelian groups $E_r^{p,q}$ $(0 \leq r, p, q \in \mathbb{Z})$. For a fixed r, the collection of all $E_r^{p,q}$ are called E_r *page*. The differentials are defined as the endomorphism of the E_r page as:

$$\mathrm{d}_r : E_r^{p,q} \to E_r^{p+r,q-r+1}, \tag{B.1}$$

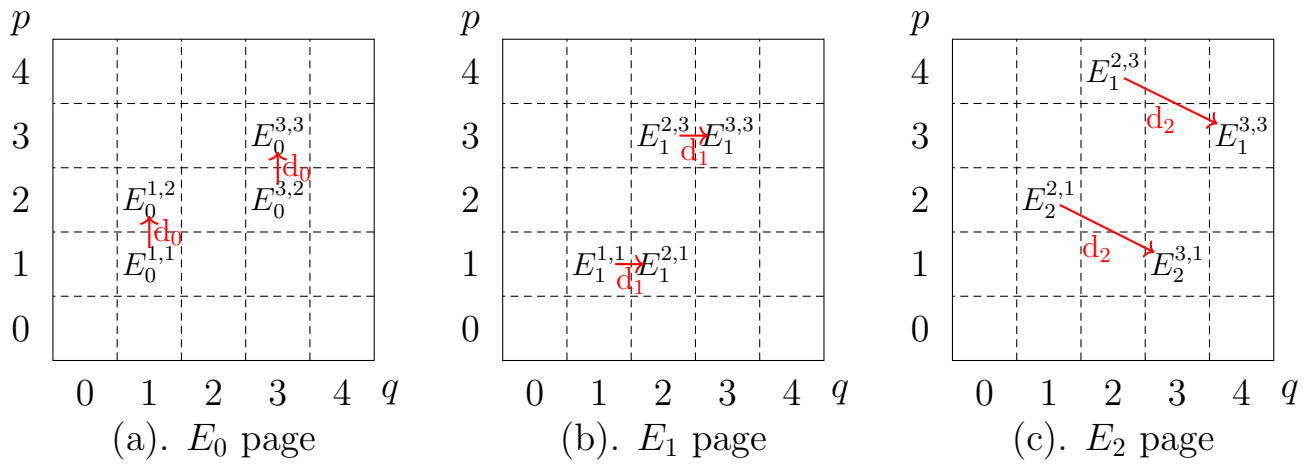

Figure B.1: LHS spectral sequence and differentials in E_0, E_1, and E_2 pages.

which should satisfy $\mathrm{d}_r^2 = 0$. Therefore, the E_r pages and the differentials d_r form a cochain complex, with the following isomorphism:

$$E_{r+1}^{p,q} \simeq \frac{\mathrm{Ker}(\mathrm{d}_r^{p,q})}{\mathrm{Im}(\mathrm{d}_r^{p-r,q+r-1})} = H_*(E_r, \mathrm{d}_r), \tag{B.2}$$

where $H_*(E_r, \mathrm{d}_r)$ is the homology group of the cochain complex $\{E_r, \mathrm{d}_r\}$.

For the LHS spectral sequence with the symmetry group given by Eq. (3.16), we denote the set of n-cochains, n-cocycles, and n-coboundaries of a group G_0 with coefficients in M by $\mathcal{C}^n[G_0, M]$, $\mathcal{Z}^n[G_0, M]$, and $\mathcal{B}^n[G_0, M]$, respectively.

The E_0 page of the LHS spectral sequence is defined as a group of cochains $E_0^{p,q} = \mathcal{C}^p\left(G, \mathcal{C}^q[A, M]\right)$, and the d_0 differential maps a cochain in $E_0^{p,q}$ to a cochain $E_0^{p,q+1}$ (see Fig. B.1(a) for illustration). The kernel of $\mathrm{d}_0^{p,q}$ is $\mathcal{C}^p\left(G, \mathcal{Z}^q[A, M]\right)$, while the image of $\mathrm{d}_0^{p,q-1}$ is just $\mathcal{C}^p\left(G, \mathcal{B}^q[A, M]\right)$. Hence the E_1 page is given according to Eq. (B.2) by

$$\begin{aligned} E_1^{p,q} &= \frac{\mathrm{Ker}(\mathrm{d}_0^{p,q})}{\mathrm{Im}(\mathrm{d}_0^{p,q-1})} = \frac{\mathcal{C}^p\left(G, \mathcal{Z}^q[A, M]\right)}{\mathcal{C}^p\left(G, \mathcal{B}^q[A, M]\right)} \\ &= \mathcal{C}^p\left(G, \mathcal{H}^q[A, M]\right). \end{aligned} \tag{B.3}$$

We recognize that E_1 page is a subgroup of E_0 page: $E_1 \subset E_0$. More precisely, if we label

the elements of $E_0^{p,q}$ by $w_0^{p,q}$, the elements of $E_1^{p,q}$ are the equivalence classes of elements in $E_0^{p,q}$ that satisfy the condition $\mathrm{d}_0^{p,q} w_0^{p,q} = 0$.

Subsequently, for the E_1 page $E_1 = \mathcal{C}^p\left(G, \mathcal{H}^q[A, M]\right)$, the differential d_1 maps a cochain in $\mathcal{C}^p\left(G, \mathcal{H}^q[A, M]\right)$ to a cochain in $\mathcal{C}^{p+1}\left(G, \mathcal{H}^q[A, M]\right)$ [see Fig. B.1(b)]. The kernel of $\mathrm{d}_1^{p,q}$ is cocycles in $\mathcal{Z}^p\left(G, \mathcal{H}^q[A, M]\right)$, and the image of $\mathrm{d}_1^{p-1,q}$ is coboundries in $\mathcal{B}^p\left(G, \mathcal{H}^q[A, M]\right)$. Then according to Eq. (B.2), the E_2 page is given by

$$\begin{aligned} E_2^{p,q} &= \frac{\mathrm{Ker}(\mathrm{d}_1^{p,q})}{\mathrm{Im}(\mathrm{d}_1^{p-1,q})} = \frac{\mathcal{Z}^p\left(G, \mathcal{H}^q[A, M]\right)}{\mathcal{B}^p\left(G, \mathcal{H}^q[A, M]\right)} \\ &= \mathcal{H}^p\left(G, \mathcal{H}^q[A, M]\right). \end{aligned} \tag{B.4}$$

And E_2 page is a subset of E_1 page,

$$E_2 \subset E_1 \subset E_0. \tag{B.5}$$

More precisely, elements of E_2 page are those elements in E_0 page that satisfy the conditions

$$\mathrm{d}_0 w_0 = 0, \quad \mathrm{d}_1 w_0 = 0. \tag{B.6}$$

Following the above paradigm, we can further define the arbitrary E_r page, satisfying the following condition:

$$E_r \subset E_{r-1} \subset \cdots \subset E_2 \subset E_1 \subset E_0. \tag{B.7}$$

The elements in E_r page should satisfy the following r conditions,

$$\mathrm{d}_q w_0 = 0, \quad 0 \leq q \leq r-1. \tag{B.8}$$

In particular, if there is a large enough integer r such that the condition $\mathrm{d}_r w_0 = 0$ is satisfied over the entire E_r page, then the E_{r+1} page is essentially identical to the E_r page: $E_{r+1} = E_r$, and all higher pages are the same. It is then said that the spectral sequence stabilizes at the E_r page. For the LHS spectral sequence, the E_∞ page is isomorphic to the group cohomology $\mathcal{H}^{p+q}[\tilde{G}, M]$ as a set. In this thesis, we set $M = U(1)$ for the classification of ASPT phases.

The generalization to the AH spectral sequence is straightforward: We can construct the E_r pages of the AH spectral sequence from LHS spectral sequence by substituting the term

$\mathcal{H}^q[A, U(1)]$ characterizing the classification of A-symmetric SPT phases in q-dimensional spacetime by the generalized cohomology group $h^q(A)$ characterizing the classification of A-symmetric invertible topological phases. For example, the E_2 page is defined as

$$E_2^{p,q} = \mathcal{H}^p[G, h^q(A)],\ p + q = d + 1. \tag{B.9}$$

Likewise, we can also define the differentials as Eq. (B.1), and the AH spectral sequence will converge to the generalized cohomology group $h^{d+1}(\tilde{G})$, i.e., E_∞ is isomorphic to $h^{d+1}(\tilde{G})$.

Physically, the difference between AH and LHS spectral sequences is that $\mathcal{H}^q[A, M]$ classifies the A-symmetric SPT phases in q-dimensional spacetime in the LHS spectral sequence, while $h^q(A)$ classifies the A-symmetric invertible topological phases in q-dimensional spacetime in the AH spectral sequence.

Appendix C

Appendices for Chapter. 4

C.1 Weak Measurements

This Appendix presents a derivation of the state evolution under weak measurements. For simplicity, I focus on a two-level system as a toy model. A generalization to the many body cases, Eq. (4.7) and Eq. (4.8), is straightforward. The derivation follows a methodology similar to that outlined in Ref. [15].

Consider a two dimensional Hilbert space, with basis states $|0\rangle$ and $|1\rangle$. The two basis states are eigenstates of a Hermitian operator O, which has eigenvalues of 0 and 1. A generalized measurement is a partition of unity by non-negative Hermitian operators:

$$\sum_a A_a^\dagger A_a = \mathbf{1}. \tag{C.1}$$

The probability of obtaining the outcome a in a generic state $|\Psi\rangle$ is given by $\langle\Psi|A_a^\dagger A_a|\Psi\rangle$.

In the two level system, projective measurements in the eigenbasis of O are implemented by

$$P_0 = \mathbf{1} - O, \quad P_1 = O, \tag{C.2}$$

which project the state onto either $|0\rangle$ or $|1\rangle$ depending on the measurement outcome. If we want a measurement that only alters the state $|\Psi\rangle$ slightly, i.e. a continuous measurement,

we can choose

$$A_\pm = \sqrt{\frac{1 \pm \Gamma}{2}} P_0 + \sqrt{\frac{1 \mp \Gamma}{2}} P_1, \tag{C.3}$$

with $\Gamma \in [0, 1]$ being the measurement strength. The expression is simply an interpolation between no measurement ($\Gamma = 0$) and projective measurement ($\Gamma = 1$). When $\Gamma \ll 1$, the post-measurement state $|\Psi'\rangle$ is only weakly altered:

$$|\Psi'\rangle = \begin{cases} A_+|\Psi\rangle/\sqrt{p_+}, & \text{if } + \text{ measured}, \\ A_-|\Psi\rangle/\sqrt{p_-}, & \text{if } - \text{ measured}, \end{cases} \tag{C.4}$$

with the probabilities $p_\pm = \frac{1}{2}[1 \pm \Gamma(1 - 2\langle O\rangle)]$. Here $\langle O\rangle = \langle\Psi|O|\Psi\rangle$ is the expectation value of O in the pre-measurement state. The change in the state density matrix, up to first order in Γ is given by

$$\delta\rho \approx -\frac{\Gamma}{2}[M, [M, \rho]] + \sqrt{\Gamma} W \{M, \rho\}, \tag{C.5}$$

where the measurement operator M is defined as $M =: O - \langle O\rangle$. $W = \pm 1$ for outcome $+$ and $-$, respectively. This equation immediately implies Eq. (4.7) and Eq. (4.8).

In the scenario where measurements are performed over an $O(L)$ time, it is important to handle the averaging over the trajectory ensemble with care, particularly when $n > 1$ replicas are involved. This is because the measurement action S_M explicitly depends on the expectation value of O within a specific outcome trajectory, i.e., $\langle O\rangle(t) = \mathrm{tr}[O\rho(t)]$, which arises from the definition of the measurement operator $M_t = O - \langle O\rangle(t)$. Therefore, to solve the time evolution of $\rho_n = \overline{\rho^{\otimes n}}$ for $n > 1$ (in this Chapter, we focused mostly on ρ_2), it is necessary to determine the evolution of ρ_{n+1} simultaneously [16]. To handle this, we employ a mean-field approximation to account for the measurement feedback on the time evolution. Specifically, the trajectory-averaged product is approximated as

$$\overline{\mathrm{tr}(\rho O) \cdot \rho \otimes \rho} \approx \mathrm{tr}(\rho_2 O) \cdot \rho_2, \tag{C.6}$$

which becomes more accurate as the measurement strength Γ decreases. This approximation is valid for the purpose of our study, which is to investigate the stability of the critical system against infinitesimal measurement. Accordingly, the trajectory-averaged

expectation value $\mathrm{tr}(\rho_2 O)$ is then replaced by the expectation value of O in the unperturbed ground state, which is absorbed by normal ordering of the CFT operators. As a result, all one-point functions in the CFT are set to 0.